

General Disclaimer

One or more of the Following Statements may affect this Document

- This document has been reproduced from the best copy furnished by the organizational source. It is being released in the interest of making available as much information as possible.
- This document may contain data, which exceeds the sheet parameters. It was furnished in this condition by the organizational source and is the best copy available.
- This document may contain tone-on-tone or color graphs, charts and/or pictures, which have been reproduced in black and white.
- This document is paginated as submitted by the original source.
- Portions of this document are not fully legible due to the historical nature of some of the material. However, it is the best reproduction available from the original submission.

CRES

REMOTE SENSING LABORATORY

151169

CR 151169

SNOW BACKSCATTER IN THE 1-8 GHz REGION

(NASA-CR-151169) SNOW BACKSCATTER IN THE
1-8 GHz REGION (Kansas Univ. Center for
Research, Inc.) 107 p HC A06/MF A01

N77-16198

CSCI 171

Unclass

G3/32 13269

RSL Technical Report
177-61

H. Stiles
F. Ulaby
B. Hanson
L. Dellwig

June, 1976

Principal Investigator: Fawwaz T. Ulaby



Supported by:
NATIONAL AERONAUTICS AND SPACE ADMINISTRATION
Lyndon B. Johnson Space Center
Houston, Texas 77058

NASA CONTRACT NAS 9-10261

THE UNIVERSITY OF KANSAS CENTER FOR RESEARCH, INC.

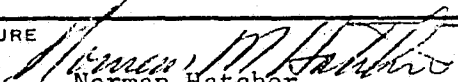
2291 Irving Hill Drive—Campus West Lawrence, Kansas 66045



MEMORANDUM

Lyndon B. Johnson Space Center

NASA

REFER TO: TF5/76-484	DATE January 3, 1977	INITIATOR TF5/NHatcher:dv:12/7/76:4505	ENCL
TO: Distribution		cc	
FROM: TF5/Monitor, Contract NAS 9-15003, Radar Measurements in Agricultural Applications		SIGNATURE  Norman Hatcher	
SUBJ: Review of University of Kansas Remote Sensing Laboratory Technical Reports 177-61, Snow Backscatter in the 1-8 GHz Region and 177-59, Radar Backscatter Properties of Milo and Soybeans.			

Enclosed for your information are copies of the subject reports. Dr. Ulaby of KU (University of Kansas) requested that these reports be forwarded to you.

Snow Studies

RSL TR 177-61 provides background information and prior experimental results regarding the penetration/backscatter characteristics of snow as functions of the various radar instrument parameters and snow conditions. The report then presents the results of a field experiment conducted by KU in Kansas during the early part of 1975 to further quantify the response of snow-covered, frozen and unfrozen, and non snow-covered grassy ground as a function of a wide range of instrument parameters. The instrument used for the experiment was the 1-8 GHz MAS (Microwave Active Spectrometer). These studies were conducted as a first step toward determining (a) how well soil moisture might be measured under covers of snow and ice, (b) how well snow/freeze/thaw boundaries might be delineated from radar data, and (c) the optimum instrument parameters for conducting such measurements.

Among the findings from the experiment, which was limited to snow thicknesses of 15 centimeters and below, are the following:

1. For a smooth snow surface, the backscatter coefficient drops rapidly with increasing incidence angle. This drop is more pronounced with increasing frequency.
2. On the average, there is very little difference in backscatter as a function of frequency. Crosspolarization is low at the low frequencies, typically about 20 dB down near 8 GHz. The magnitude of the difference between cross and like polarization generally increases with increasing incidence angle.
3. The radar return from grass-covered thawed ground is slightly higher (typically 1.5 dB) than from very moist ground frozen to a depth of about 1 centimeter.
4. The backscatter from a 15 cm cover of dry snow was higher by about 2 to 8 dB than from wet snow at 1.2 GHz throughout the incidence angle range of



THE UNIVERSITY OF KANSAS SPACE TECHNOLOGY CENTER

Raymond Nichols Hall

2291 Irving Hill Drive—Campus West Lawrence, Kansas 66045

Telephone:

SNOW BACKSCATTER IN THE 1-8 GHz REGION

RSL Technical Report

177-61

H. Stiles
F. Ulaby
B. Hanson
L. Dellwig

June, 1976

Principal Investigator: Fawwaz T. Ulaby

Supported by: National Aeronautics and Space Administration
Lyndon B. Johnson Space Center
Houston, Texas 77058

NASA Contract NAS 9-10261



TABLE OF CONTENTS

	<u>Page</u>
ABSTRACT.....	vi
1.0 INTRODUCTION.....	1
2.0 BACKGROUND	1
3.0 DIELECTRIC PROPERTIES	8
3.1 Dielectric Properties of Water and Ice	8
3.2 Dielectric Properties of Soils.....	13
3.3 Dielectric Properties of Snow.....	13
4.0 SYSTEM DESCRIPTION	21
5.0 DATA PRESENTATION	25
5.1 Ground Truth.....	25
5.1.1 General.....	25
5.1.2 Soil Moisture.....	25
5.1.3 Temperature.....	31
5.1.4 Snow.....	31
5.2 Angular Response	31
5.3 Polarization Response.....	31
5.4 Spectral Response.....	31
6.0 DATA ANALYSIS.....	42
6.1 Freeze-Thaw Effect.....	42
6.2 Snow Effect.....	42
7.0 CONCLUSIONS.....	51
APPENDIX A: Ground Truth Data	A-1 to A-18
APPENDIX B: Tabulated Scattering Coefficients.....	B-1 to B-16

LIST OF FIGURES

	<u>Page</u>
Figure 1. Comparison of radar derived thickness (cm) with actual thickness using short pulse radar. (Vickers [8])	3
Figure 2. Ice thickness measurements using an FM-CW radar. (Page [10])	3
Figure 3. σ^0 vs. θ for different categories of sea ice. (Parashar [11])	4
Figure 4. σ^0 vs. θ for different categories of sea ice. (Parashar [11])	5
Figure 5. σ^0 vs. ice thickness. (Parashar [11])	6
Figure 6. Effects of snow on gamma at Ku-band. (Cosgriff, et al. [7]).	7
Figure 7. A comparison of radar and gamma ray determinations of snow depth. (Vickers and Rose [14]).	7
Figure 8. Relative backscatter at nadir vs. snow depth. (Linlor [16]).	9
Figure 9. Brightness temperature vs. water equivalent dry snow, Crater Lake, Oregon, 22 March 1970. (Edgerton, et al. [17]).	10
Figure 10. Brightness temperature of various depths of snow on a metal plate. Note that the first 60 cm snow and the 51 cm snow packed points are for the same total snow mass. (Edgerton, et al. [17])	11
Figure 11. Dielectric properties of water.	12
Figure 12. Dielectric properties of ice. (Evans [20]).	14
Figure 13. Dielectric properties of soils. (Cihlar [21]).	15
Figure 14. Dielectric properties of dry snow. (Evans [20]).	16
Figure 15. Variation of loss tangent of snow with temperature. (Cumming [19]).	17

LIST OF FIGURES (CONTINUED)

	<u>Page</u>
Figure 16. Dielectric constant of foam rubber with varying wetnesses. (Linlor [24])	17
Figure 17. Dielectric properties of wet snow. (Evans [20])	19
Figure 18. Skin depth of wet snow.	20
Figure 19. MAS 1-8 system.	23
Figure 20a. Test plot configuration.	27
Figure 20b. Temperature probe locations.	27
Figure 21. Soil moistures for the near range (0° and 10°), 1975.	28
Figure 22. Soil moistures for the middle range (20° , 30° , 50°), 1975.	29
Figure 23. Soil moistures for the far range (70°), 1975.	30
Figure 24. Ground surface temperature, 1975.	32
Figure 25. Snow data, 1975.	33
Figure 26. Angular response of σ^0 of short grass.	34
Figure 27. Angular response of σ^0 of short grass with 15 cm dry powder snow cover.	35
Figure 28. Angular response of σ^0 of short grass with 0.5 cm ice over 6.5 cm snow cover.	36
Figure 29. Polarization response of σ^0 of short grass.	37
Figure 30. Polarization response of σ^0 of short grass with 15 cm dry powder snow cover.	38
Figure 31. Spectral response of σ^0 of short grass.	39
Figure 32. Spectral response of σ^0 of short grass with dry powder snow cover.	40
Figure 33. Spectral response of σ^0 of short grass with 0.6 cm ice over 10.8 snow cover.	41

LIST OF FIGURES (CONTINUED)

	<u>Page</u>
Figure 34. Spectral responses of σ^0 of frozen (to 1 cm) and thawed ground with short grass cover.	43
Figure 35. Angular responses of σ^0 of short grass and short grass with a 15 cm dry powder snow cover.	44
Figure 36. Angular responses of σ^0 of short grass and short grass with a 12 cm wet snow cover.	45
Figure 37a. Response of σ^0 to total snow water per unit area.	47
Figure 37b. Response of σ^0 to total snow water content per unit area.	48
Figure 37c. Response of σ^0 to total snow water content per unit area.	49
Figure 38. Correlation coefficient and sensitivity of σ^0 to total snow water content per unit area at 0° angle of incidence versus frequency, both with and without the 0.5 gm/cm ² snow water data set.	50
Figure 39a. Response of σ^0 to total snow water content per unit area.	52
Figure 39b. Response of σ^0 to total snow water content per unit area.	53
Figure 39c. Response of σ^0 to total snow water content per unit area.	54
Figure 40. Correlation coefficient and sensitivity of σ^0 to total snow water content per unit area for HH polarization vs. frequency.	55
Figure 41. Correlation coefficient and sensitivity of σ^0 to total snow water content per unit area for HV polarization vs. frequency.	56
Figure 42. Correlation coefficient and sensitivity of σ^0 to total snow water content per unit area for VV polarization vs. frequency.	57

LIST OF FIGURES (CONTINUED)

	<u>Page</u>
Figure 43. Correlation coefficient and sensitivity of σ^0 to total snow water content per unit area for HH polarization vs. angle of incidence.	58
Figure 44. Correlation coefficient and sensitivity of σ^0 to total snow water content per unit area for HV polarization vs. angle of incidence.	59
Figure 45. Correlation coefficient and sensitivity of σ^0 to total snow water content per unit area for VV polarization vs. angle of incidence.	60

ABSTRACT

The 1-8 GHz Microwave Active Spectrometer (MAS 1-8) system was used to measure the backscatter response of snow covered ground between 21 February and 23 April 1975. The scattering coefficient was measured for all linear polarization combinations at angles of incidence between nadir and 70°. Ground truth data consisted of soil moisture, soil temperature profile, snow depth, snow temperature profile, and snow water equivalent. The results of the experiment indicate that the radar sensitivity to snow water equivalent increases in magnitude with increasing frequency and is almost angle independent for angles of incidence higher than 30°, particularly at the higher frequencies. In the 50°-70° angular range and in the 6-8 GHz frequency range, the sensitivity is typically between -0.4 dB/.1 g/cm² and -0.5 dB/.1 g/cm² and the associated linear correlation coefficient has a magnitude of about 0.8.

1.0 INTRODUCTION

In some areas of the world, the major source of water for power, irrigation, and human consumption is from snowpack melt. Accurate measurement of the runoff is therefore very important for both flood control and proper conservation of this resource. The traditional method of snowpack data acquisition is the physical sampling of snow depth and density. The measurements are then related to runoff by one of several methods: historical normal, index method, water balance method, or hydrologic methods [1,2]. These methods have the disadvantage of using a limited number of discrete samples. Remote sensing has the potential to provide more accurate large-scale snowpack information, which can serve to improve the hydrologist's prediction of runoff.

The microwave backscatter coefficient, σ^0 , has been shown to be dependent on the moisture content of soils [3,4] and vegetation [5,6]. Also σ^0 is affected by snow cover [7]. These effects result from the range of dielectric properties of the target due mainly to water content. The relative dielectric constants of dry soils and dry snow in the microwave region are in general between 2 and 4. The relative dielectric constant of water, on the other hand, is more than an order of magnitude larger, its value being a function of temperature, frequency and mineral content. It is this disparity that makes backscattering measurements sensitive to variations in mixtures of water, soils, and snow.

This study is an investigation into the effects of snow on the microwave backscattering properties of the ground. A truck mounted radar spectrometer was used to obtain backscatter measurements across the 1-8 GHz frequency band for three linear polarization combinations at incidence angles between 0° and 70° (relative to nadir).

2.0 BACKGROUND

Previous measurements of microwave properties of ice and snow fall into two categories. The first category, measurements on ice over water, is

primarily concerned with profiling thickness. The second category, measurements of ice and snow over land, is more complex due in part to the problem of determining the dielectric properties of the snow.

Measurements by Vickers [8] using a short pulse (1ns) radar operating at 35 GHz indicated that ice thickness could be measured with a radar (Figure 1). The system operated on the basis of time delay from reflections at the air-ice and ice-water interfaces. The minimum thickness that could be measured was about 10 cm and the accuracy was \pm 2 cm. Measurements of ice thickness were taken by Page, et al. [9,10] using a 10 GHz FM-CW radar driving a wave analyzer and plotter. Range determination is based on the frequency difference resulting from the time delay in reflections between the ice boundaries. A modulation deviation of 1 GHz gave a minimum measurable thickness of about 10 cm with \pm 1 cm accuracy (Figure 2). Success of such experiments is dependent on the degree of smoothness at both the air-ice and the ice-water interfaces. Surface roughness tends to degrade the accuracy of the measurements.

Airborne scatterometer measurements over sea ice were conducted at 400 MHz and 13.3 GHz [11]. The purpose of the experiment was classification of ice types. Figures 3 and 4 show the angular response at the two frequencies. Figure 5 shows the response of σ^0 to thickness of the ice. These curves show that for ice greater than 1 foot thick at 13.3 GHz there is good sensitivity to changes in depth at all angles. For the lesser thicknesses, layering effects cause oscillations.

Parashar [11] was able to classify four types of sea ice with 86% success with six look angles at 13.3 GHz. It was also noted that the 400 MHz correct classification percentage was only about 62%. Other investigators [12,13] have also noted qualitative relationships between ice type and radar return on SLAR images. They observed that totally frozen lakes showed up darker than lakes with only a 2 meter ice cover and that different ice types could be mapped from radar imagery.

Some of the first measurements on snow covered earth were by Cosgriff, et al. [7] utilizing a truck mounted CW-Doppler scatterometer operating at 10, 15.5 and 35 GHz. They state that in general snow had the effect of lowering the backscatter from terrain as exemplified in Figure 6. Vickers

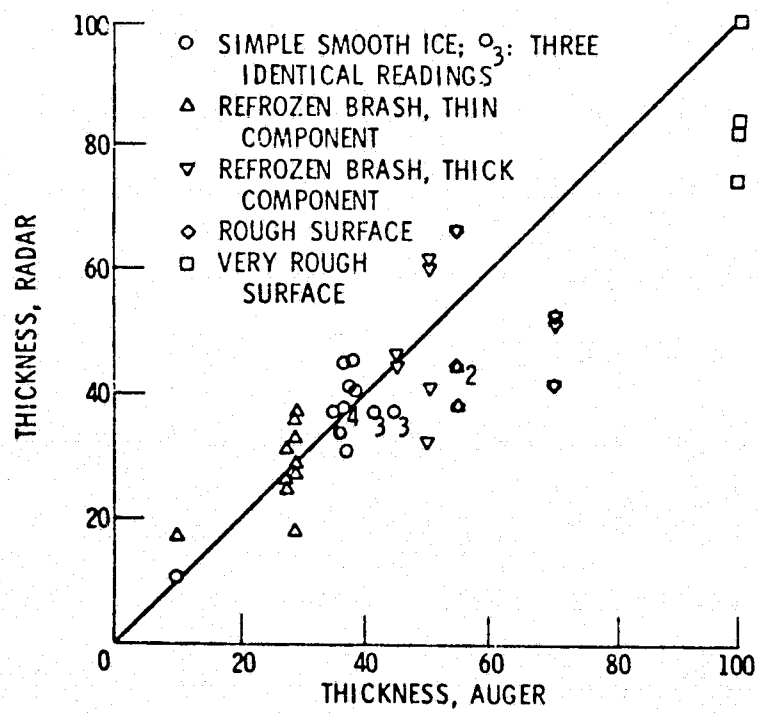


Figure 1. Comparison of radar derived thickness (cm) with actual thickness using short pulse radar. (Vickers [8])

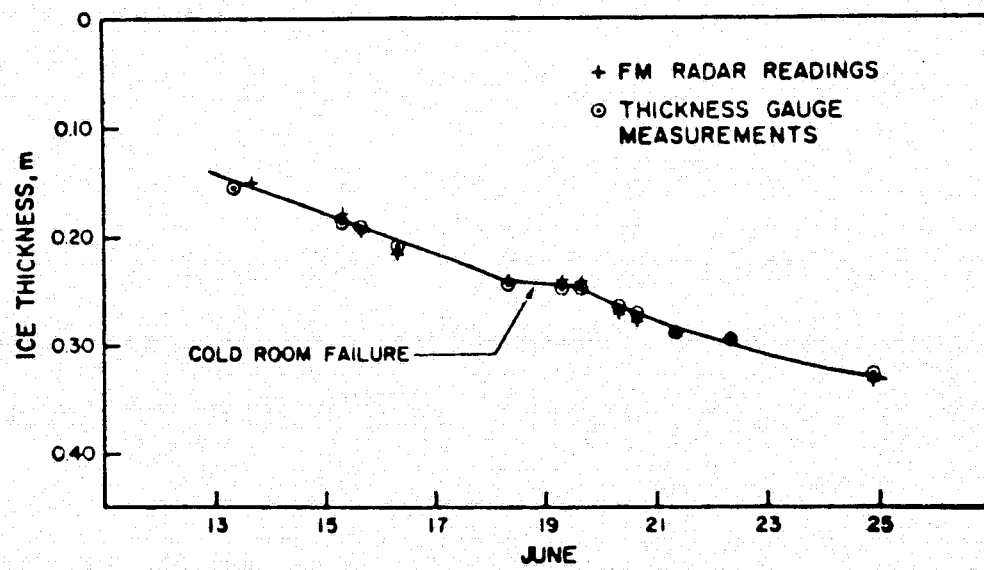


Figure 2. Ice thickness measurements using an FM-CW radar. (Page [10])

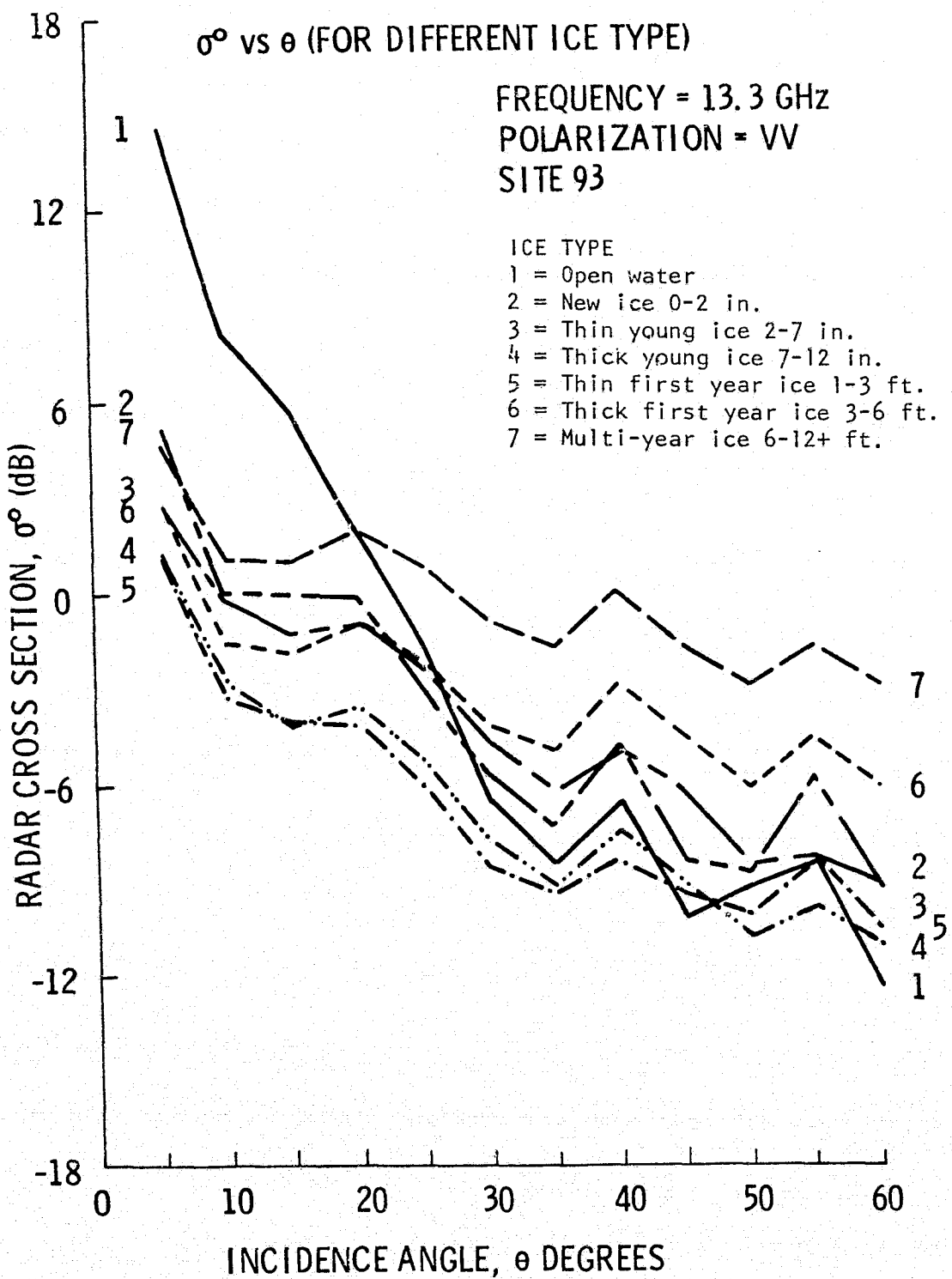


Figure 3. σ^0 vs. θ for different categories of sea ice. (Parashar [11])

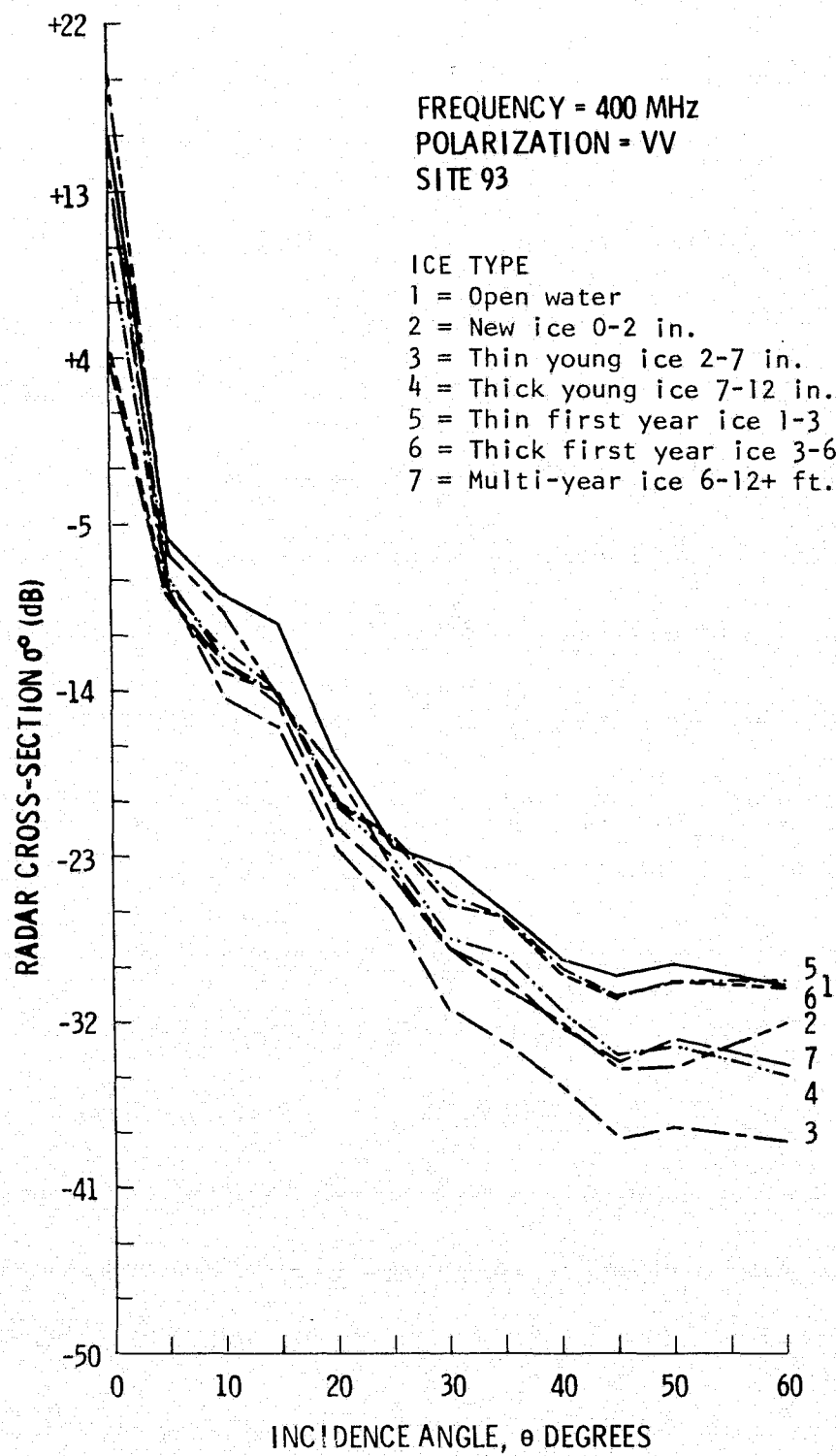


Figure 4. σ^0 vs. θ for different categories of sea ice. (Parashar [11])

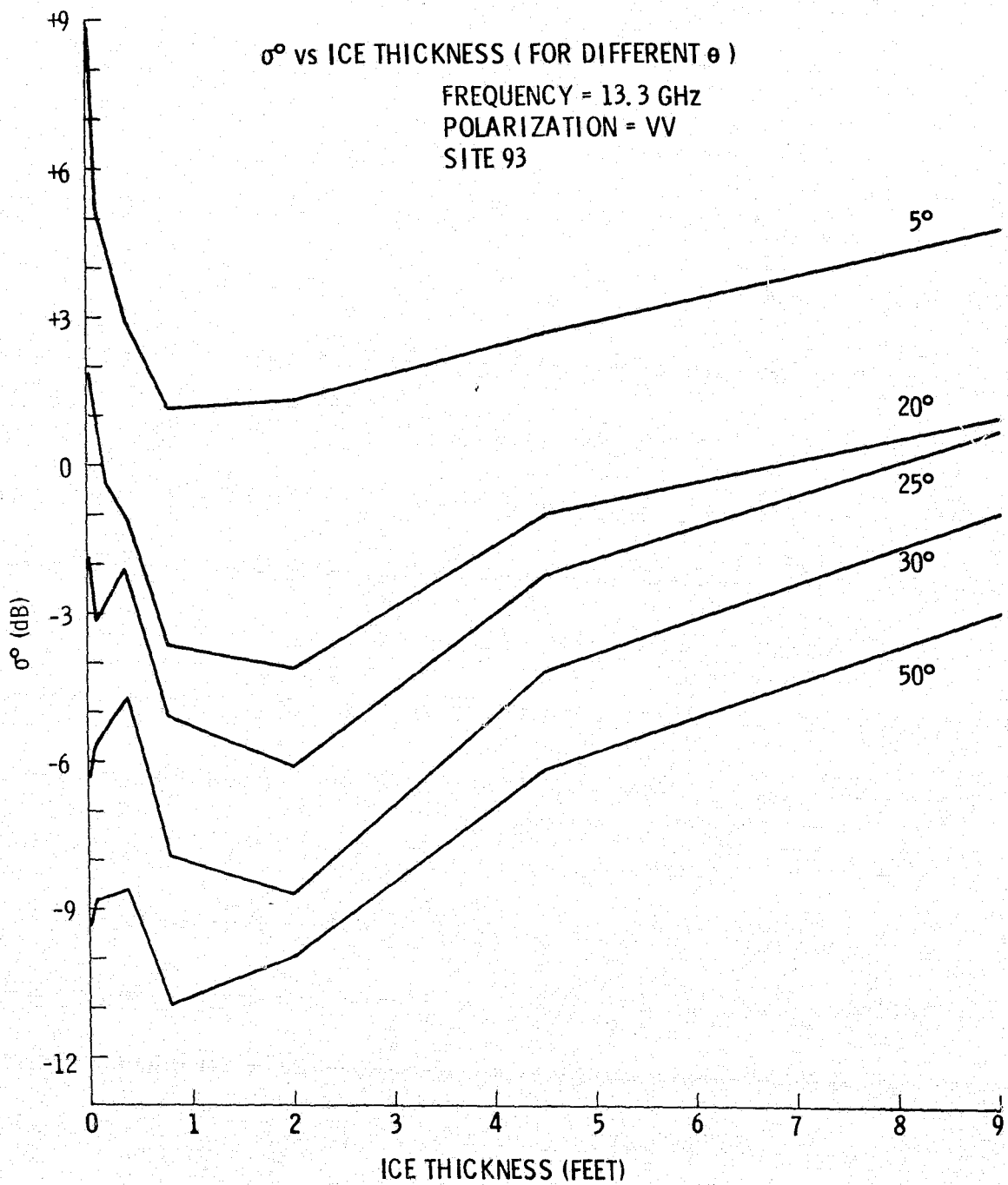


Figure 5. (Parashar [11])

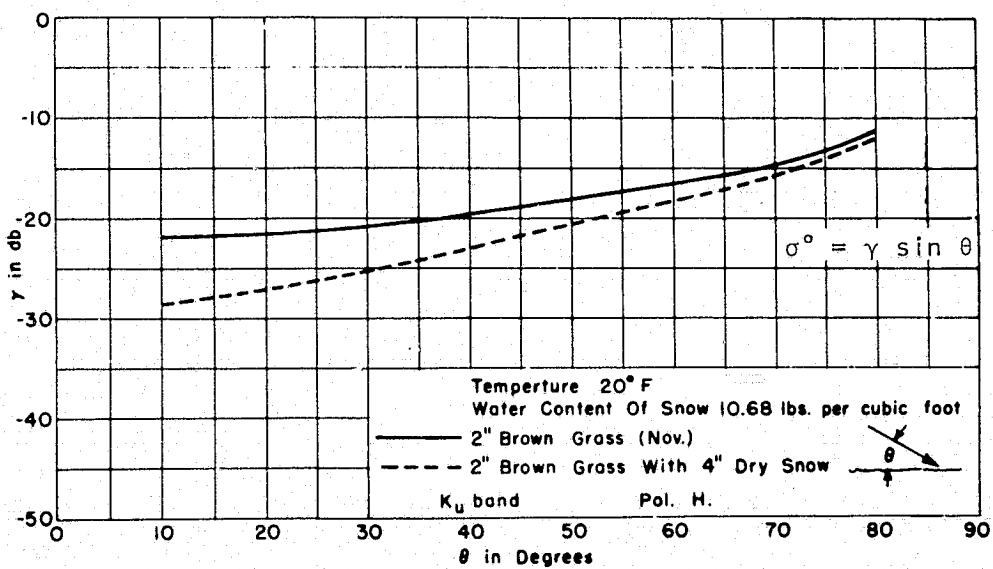


Figure 6. Effects of snow on gamma at Ku-band. (Cosgriff, et al. [7])

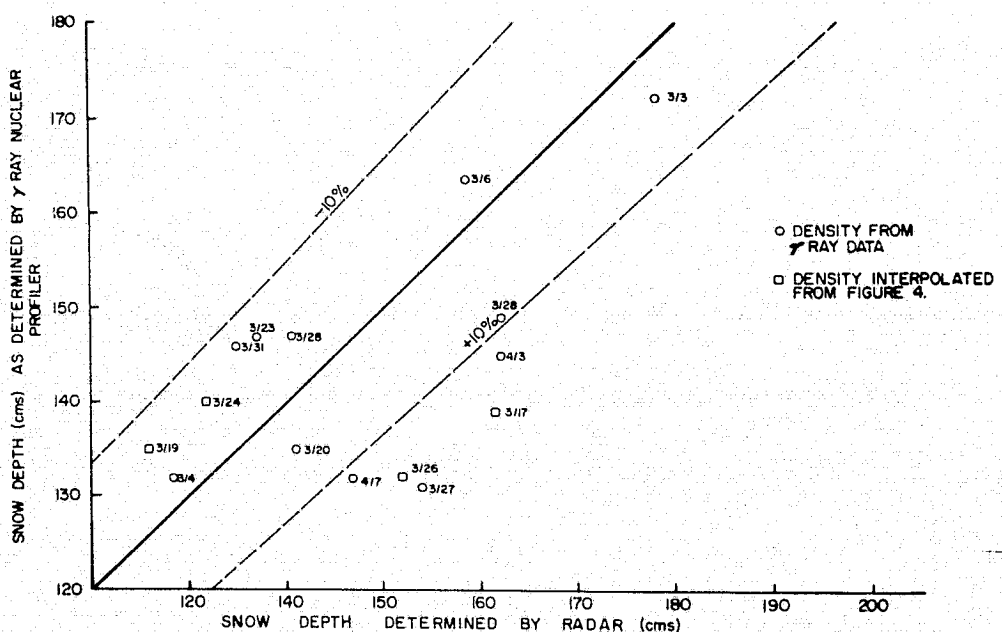


Figure 7. A comparison of radar and gamma ray determinations of snow depth. (Vickers and Rose [14])

and Rose [14] used a 2.7 GHz short pulse radar and a gamma ray profiler to investigate snowpack stratification (similar to Vicker's system [8] for ice thickness measurements). However, for depth determination (Figure 7), density data had to be known. Thus this method has the drawback of needing ground based calibration of either the snow density or depth in order to determine the other by remote sensing. They postulated that thickness measurements in the presence of free water could be made if the dynamic range of their system was increased. Waite and MacDonald [15] observed that on SLAR imagery at K-band new dry snow had little effect on the radar return from the underlying ground. High return was observed over some areas of old perennial snow. Presumably, this was due to volume scattering from inhomogeneities in the old snow. Cross polarization tended to bring out this effect more than like-polarization.

Linlor [16] used a CW radar to measure the relative backscatter at nadir from snow as a function of snow depth. Considerable variation with depth is shown (Figure 8) but no attempt was made at analysis of the response.

Microwave radiometers have also been used in remote sensing of snow and ice. Edgerton et al. [17] made radiometric measurements of snow at 1.42, 4.99, 13.4 and 37 GHz, determining a direct relationship between brightness temperature and water equivalent of dry snow (Figure 9). Furthermore, as total snow mass increased there was in general a decrease in brightness temperature. Figure 10 demonstrates that total snow mass was the main factor influencing the brightness temperature of snow. The snow mass for the 60 cm and 51 cm data points are identical and the brightness temperatures are also the same.

3.0 DIELECTRIC PROPERTIES

3.1 Dielectric Properties of Water and Ice

The relative dielectric constant of water varies as a function of frequency, temperature and concentration of impurities (Figure 11). It is important to note the significant variation of the real and imaginary parts with temperature and frequency. Impurities will cause an ionic conductivity loss term which will affect the imaginary part of the dielectric constant. The effect of impurities will be neglected since only fresh water is being investigated. The real part of the relative dielectric constant of ice has

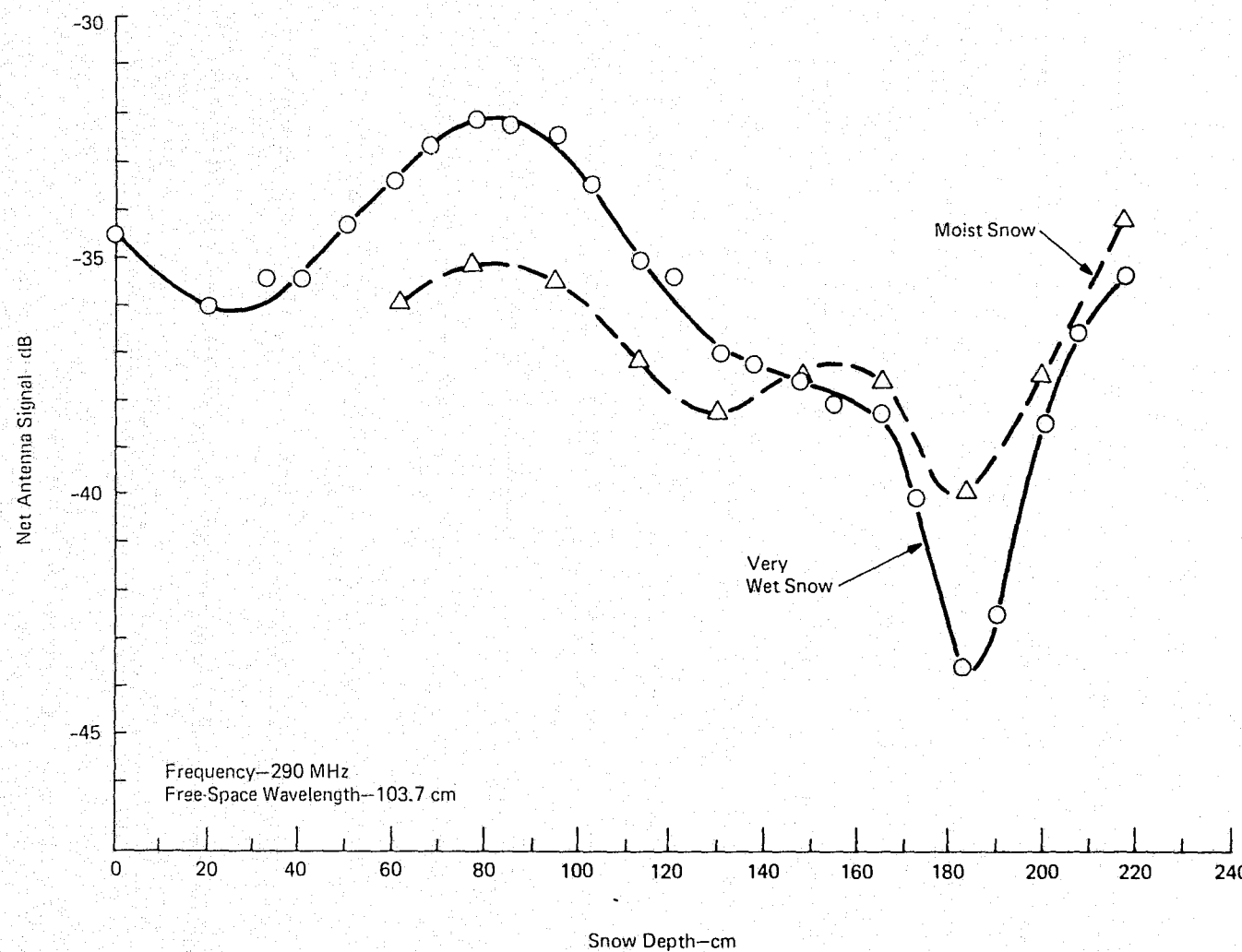


Figure 8. Relative backscatter at nadir vs. snow depth. (Linlor [16]).

$\theta = 45^\circ$
 $\lambda = \text{Wavelength}$
 $H = \text{Horizontal Polarization}$
 $V = \text{Vertical Polarization}$

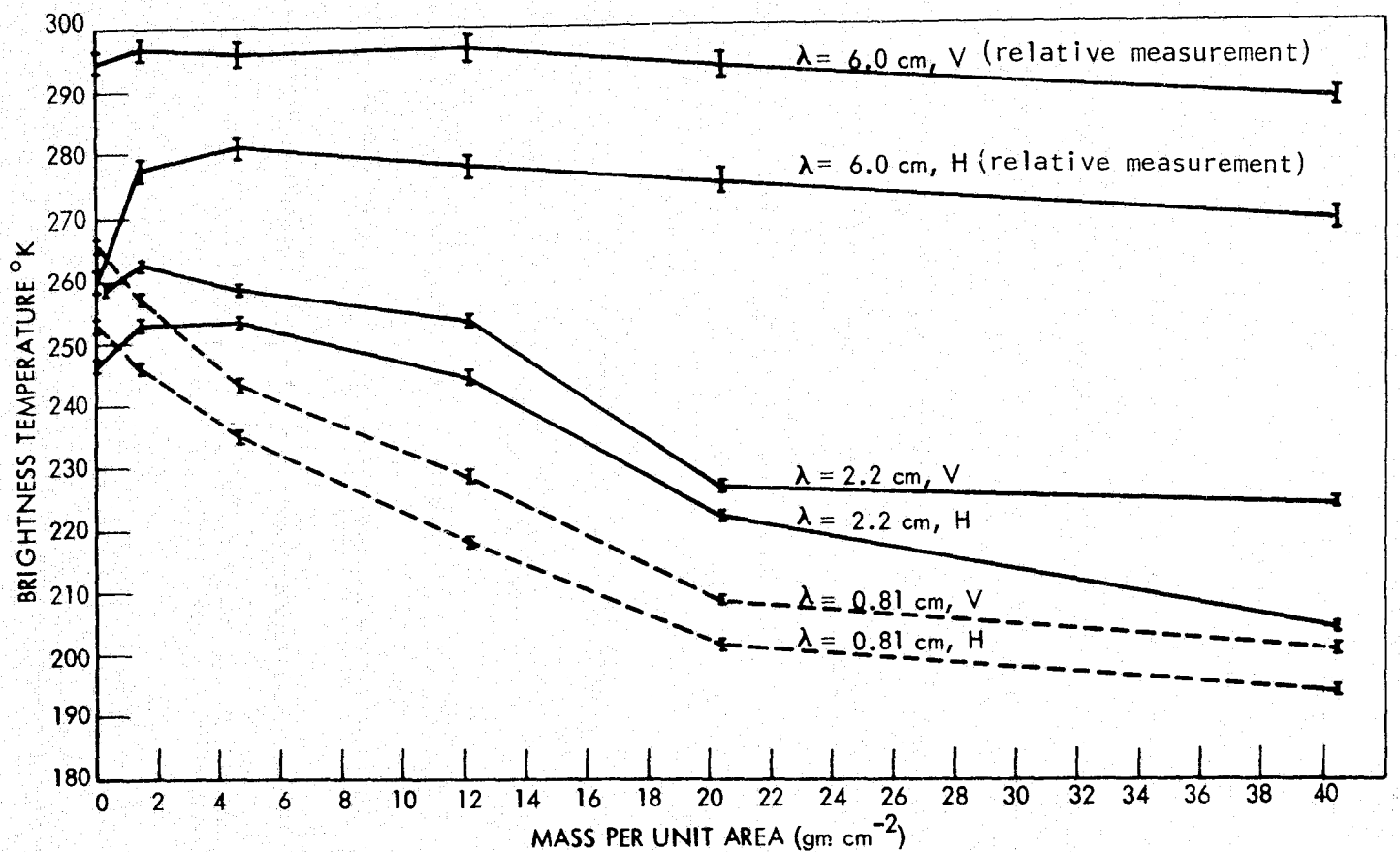


Figure 9. Brightness temperature vs. water equivalent dry snow, Crater Lake, Oregon, 22 March 1970.
(Edgerton, et al. [17])

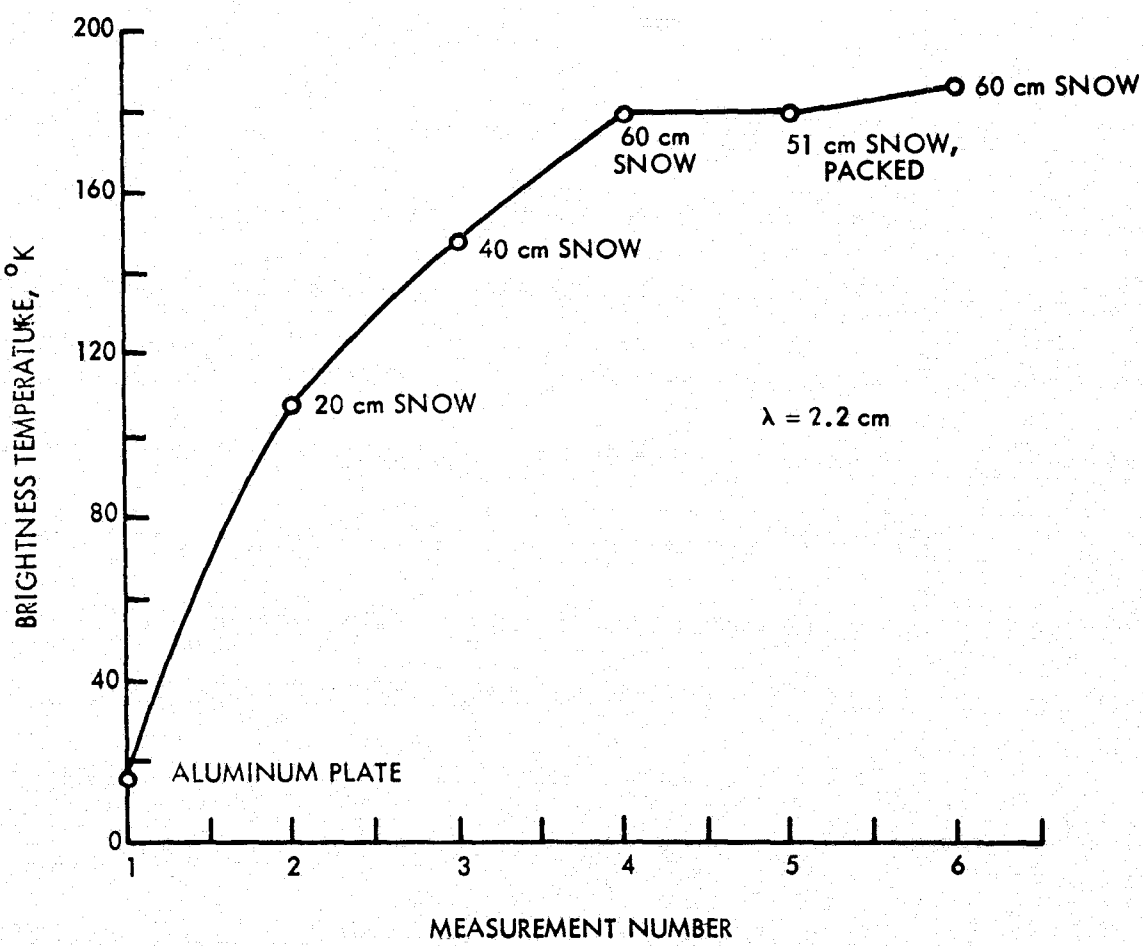


Figure 10. Brightness temperature of various depths of snow on a metal plate. Note that the first 60 cm snow and the 51 cm snow packed points are for the same total snow mass.

(Edgerton, et al. [17])

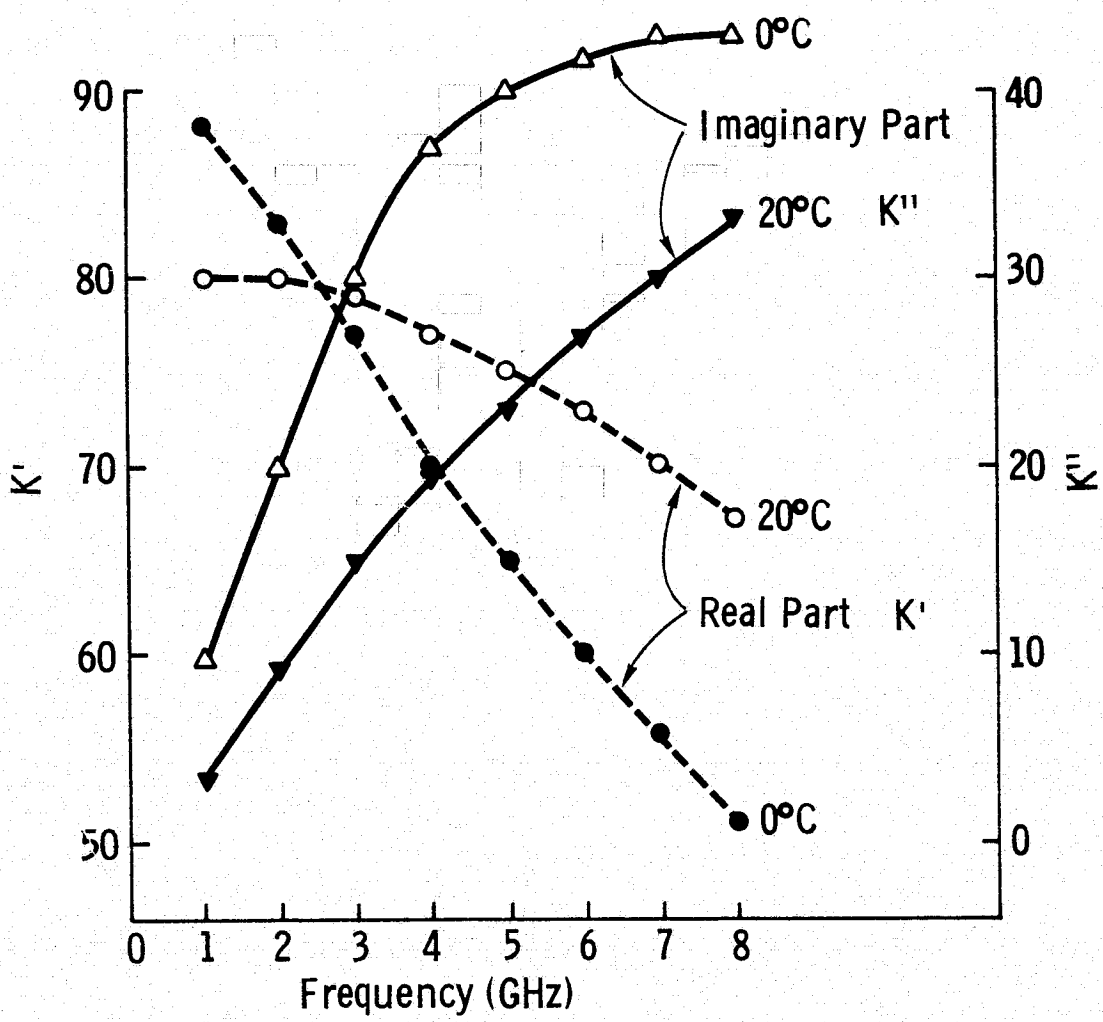


Figure 11. Dielectric Properties of Water.

been shown to be relatively independent of temperature by Cumming [19]. However, the imaginary part was shown to be temperature dependent. Evans [20, Figure 12] shows results from several experimental measurements of the real and imaginary parts of the relative dielectric constant. The frequency independence of the real part and dependence of the imaginary part over the microwave region are clearly shown.

3.2 Dielectric Properties of Soils

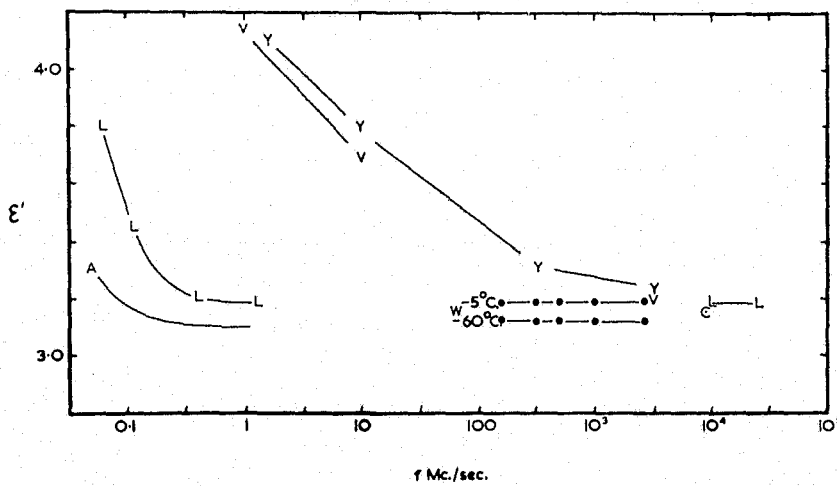
Cihlar and Ulaby [21] showed that the dominant factor influencing the dielectric properties of soils was the soil moisture content. Although there is some variation in the real and imaginary parts of the relative dielectric constant with soil type, the major effect is obviously the soil moisture (Figure 13). The effect of the relative dielectric constant of the soil is then reflected in the backscatter coefficient, σ^* , or the power reflection coefficient and the depth of penetration.

3.3 Dielectric Properties of Snow

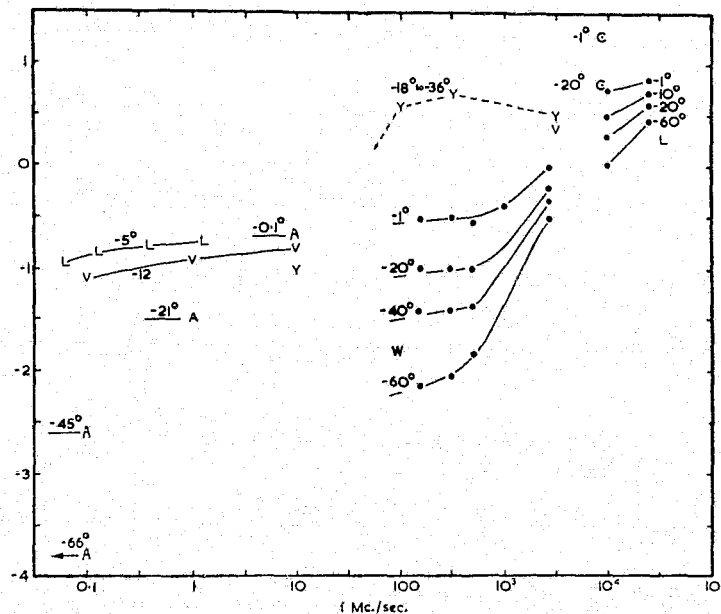
The dielectric properties of snow are much more difficult to quantify than those of the soil, water, or ice. The dielectric constant of dry snow may be related to the density of the snow by the Weiner theory for mixtures [22],

$$\frac{K_m - 1}{K_m + U} = \rho \left(\frac{K_1 - 1}{K_1 + U} \right) + (1 - \rho) \frac{K_2 - 1}{K_2 + U}$$

where K_m , K_1 and K_2 are the relative dielectric constants of dry snow, ice and air respectively, ρ is the volumetric portion of ice, and U is the parameter (the Formzahl) characterizing the structure of the mixture. The numerical values of the Formzahl can vary from 2 (for spherical particles) to infinity (for elongated particles). Values for freshly fallen snow are normally between 2 and 10 [20]. The relationship of dielectric constant and loss tangent of snow to snow density is shown in Figure 14 by Evans [20] for the data from several experimenters. Cumming [19] found that the real part of the dielectric constant was temperature independent; but, the loss tangent was sensitive to temperature as illustrated by Figure 15.



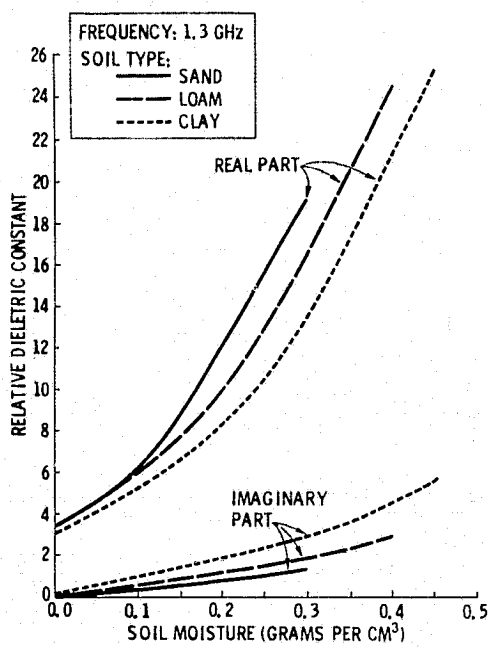
Relative permittivity of ice (ordinates) versus logarithm of radio-frequency (abscissae).



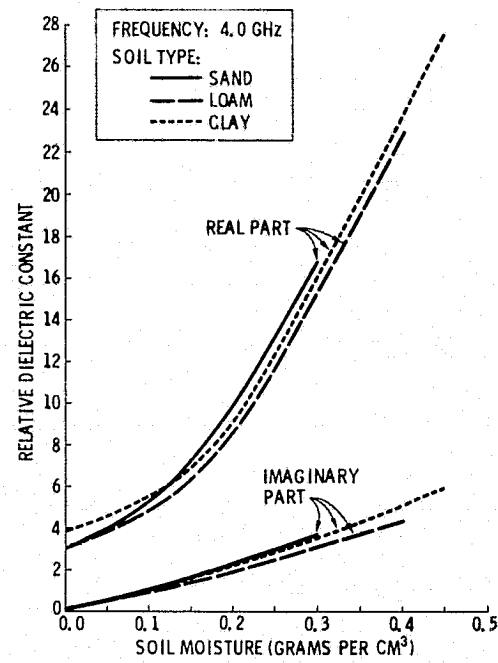
Loss tangent of ice versus radio frequency. The quantity plotted vertically is $\log_{10}(f \tan \delta)$ where f is the frequency in Mc.sec. On the high-frequency tail of a relaxation spectrum this quantity is constant: it has the further useful property that the attenuation of a radio wave (measured in db./m.) passing through the medium is directly proportional to $f \tan \delta$. Temperatures are marked in $^{\circ}\text{C}$.

- L: Lamb (1946) and Lamb and Turney (1949) -5°C at low frequencies, 0° to -190°C at high frequencies: distilled water.
- C: Cumming (1952) Distilled water, tap water, and melted snow (no observable difference).
- A: Auty and Cole (1952) Conductivity water, ice free from stress. Limiting values plotted arbitrarily at 1,000 times the relaxation frequency.
- V: Von Hippel (1954) Conductivity water, ice not available.
- Y: Yashino (1961) Antarctic ice core samples, not annealed, density 0.91g./cm.^3
- W: Westphal (private communication) Greenland ice, annealed, density 0.90g./cm.^3

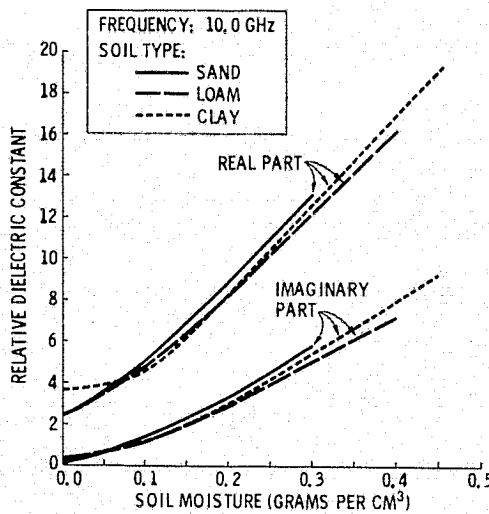
Figure 12. Dielectric properties of ice. (Evans [20])



Representative dielectric constant values as a function of volumetric water content for sand, loam, and clay at 1.3 GHz.



Representative dielectric constant values as a function of volumetric water content for sand, loam, and clay at 4.0 GHz.

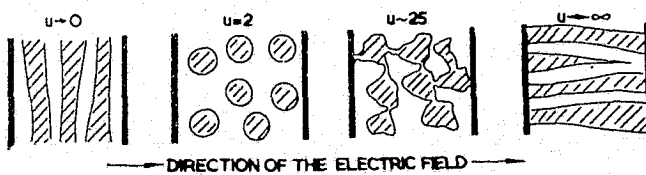
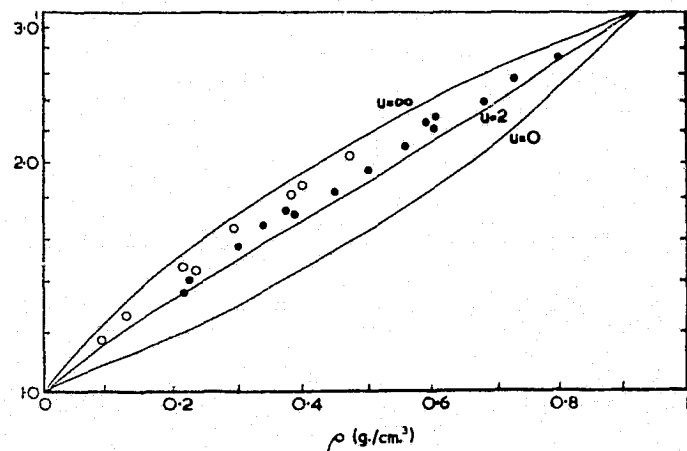


Representative dielectric constant values as a function of volumetric water content for sand, loam, and clay at 10.0 GHz.

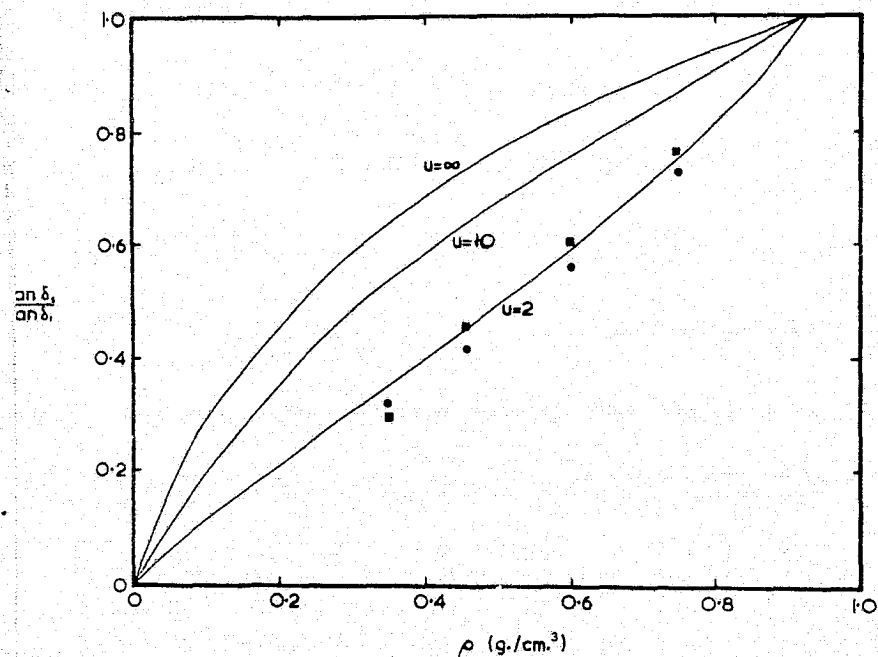
Figure 13. Dielectric properties of soils.

(Cihlar [21])

ORIGINAL PAGE IS
OF POOR QUALITY



Relative permittivity of snow (ordinates) vs. density (abscissae). The upper curves are computed as explained in section 1.2 for snow particles having the characteristic Formzahl values $u = 0, 2, 10$ and ∞ in Weiner's formula and taking the relative permittivity of solid ice to be 90 at low frequencies. The lower curves are for the limiting value of the permittivity at high frequencies, taken to be 3.2 for solid ice. Measured values: 0 due to Kuroiwa (1956) at frequencies less than 1 Mc.sec. and at 3 Mc./sec., • due to Cumming (1952) at 9.375 Mc./sec. The sketches beneath the graphs show how snow structure is related to the Formzahl.



Loss tangent of snow versus density (abscissae). The quantity plotted vertically is the ratio of the loss tangent of the ice/air mixture forming snow to that of the solid ice. Smooth curves are plotted for different values of the Formzahl in Weiner's formula assuming that $\tan \delta$ is much less than unity for the solid ice considered. Measured values are due to Cumming (1952) at 9,375 Mc./sec., • at 0°C., □ at -8°C.

Figure 14. Dielectric properties of dry snow. (Evans [20])

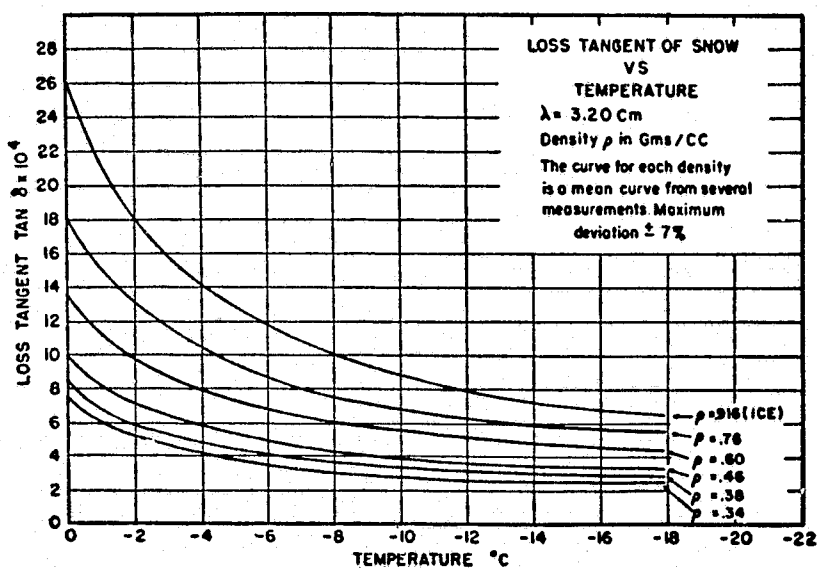


Figure 15. Variation of loss tangent of snow with temperature.
(Cumming [19])

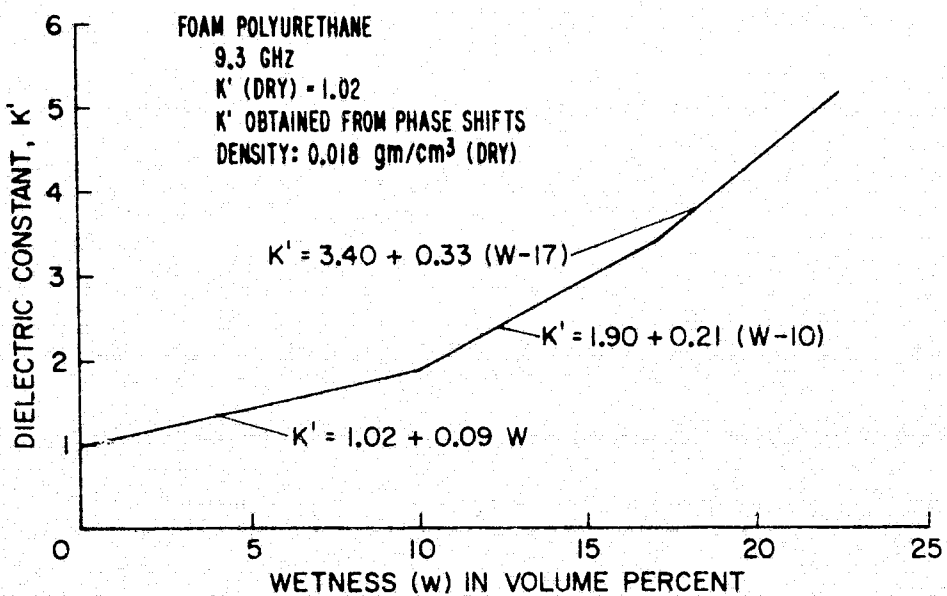


Figure 16. Dielectric constant of foam rubber with varying wetness.
(Linlor [24])

Free water greatly affects the dielectric constant in a manner similar to the effect in soils. The relative dielectric constant for snow containing free water is given by the following equation from Edgerton [17]

$$K_{\text{wet snow}} = \frac{K_{\text{water}} pU + K_{\text{snow}} (1 - p)}{pU + (1 - p)}$$

$$U = \frac{K_{\text{snow}} + f}{K_{\text{water}} + f}$$

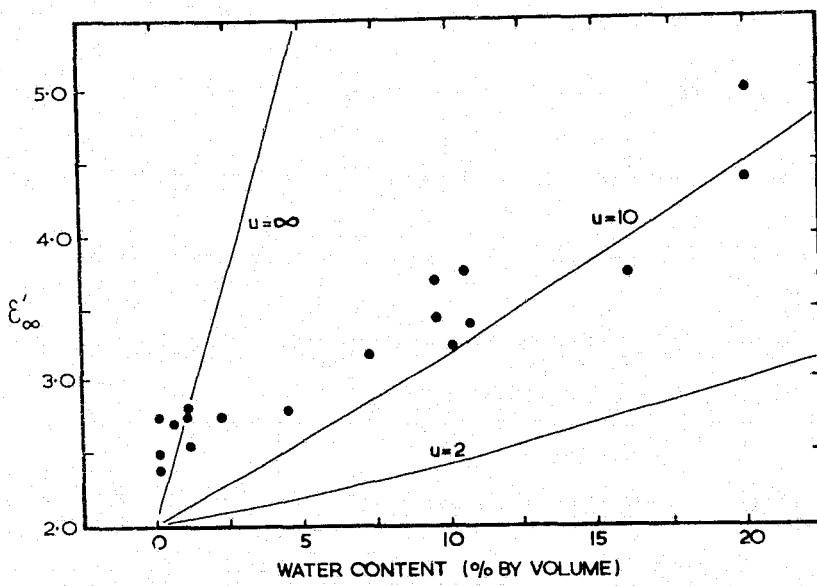
where p is the volume percentage of water and f is a form number describing the distribution of water in the snow. Ambach [23] in his development of a meter to measure free water using changes in capacitance chose 32 as a representative value. Since quantifying snow wetness is very difficult, Linlor et al. [24] performed experiments using foam rubber as the supporting medium. The effect of varying wetness is shown in Figure 16 along with some actual snow measurements: Figure 17 from Evans [20]. Figure 18 demonstrates the extreme sensitivity of the loss tangent to variations in the free water content of the snow.

For a lossy medium, the penetration of electromagnetic energy into that medium will be limited by attenuation. The attenuation coefficient for a medium is given by

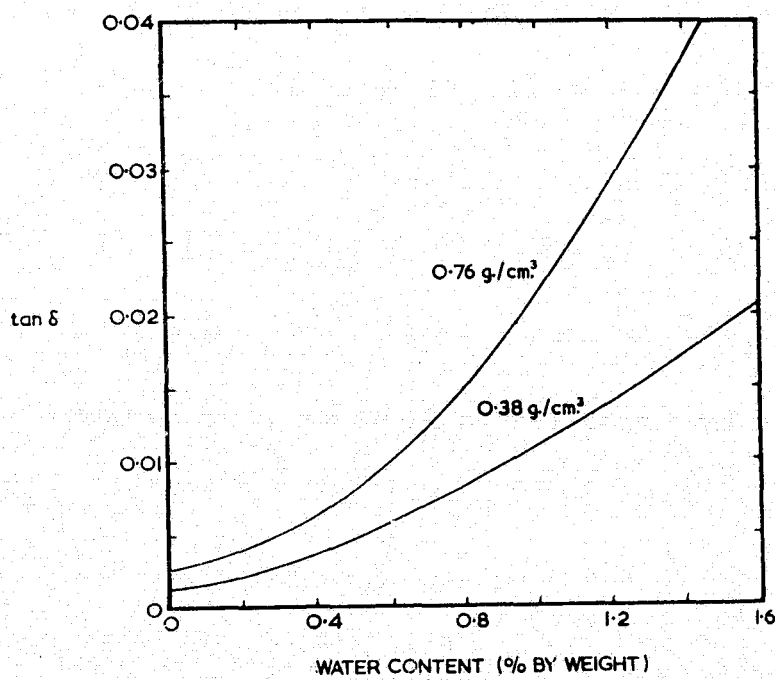
$$\alpha = \frac{2\pi}{\lambda} \sqrt{\frac{K'}{2} \left[\sqrt{1 + \left(\frac{K''}{K'} \right)^2} - 1 \right]}$$

where λ is wavelength and the complex relative dielectric constant is given by

$$K_c = K' - jK''$$



Permittivity of wet snow at high frequencies (ordinates) vs. volume percentage of liquid water (abscissae). The permittivity of the dry snow is assumed to be 2.0, corresponding to a specific gravity of approximately 0.5. The continuing lines are calculated from Weiner's mixing formula and the measured values are due to Kuroiwa (1956). There is a system error in his measurement of the free water content. Ambach (1963, p. 174-177) has given results for snow of much lower density.



Loss tangent of snow (ordinates) vs. free water content in per cent by weight (abscissae). Mean curves are shown for two snow samples of density 0.76 g./cm^3 and 0.38 g./cm^3 , temperature 0°C ., radio frequency 9,375 Mc./sec. (after Cumming, 1952).

Figure 17. Dielectric properties of set snow. (Evans [20])

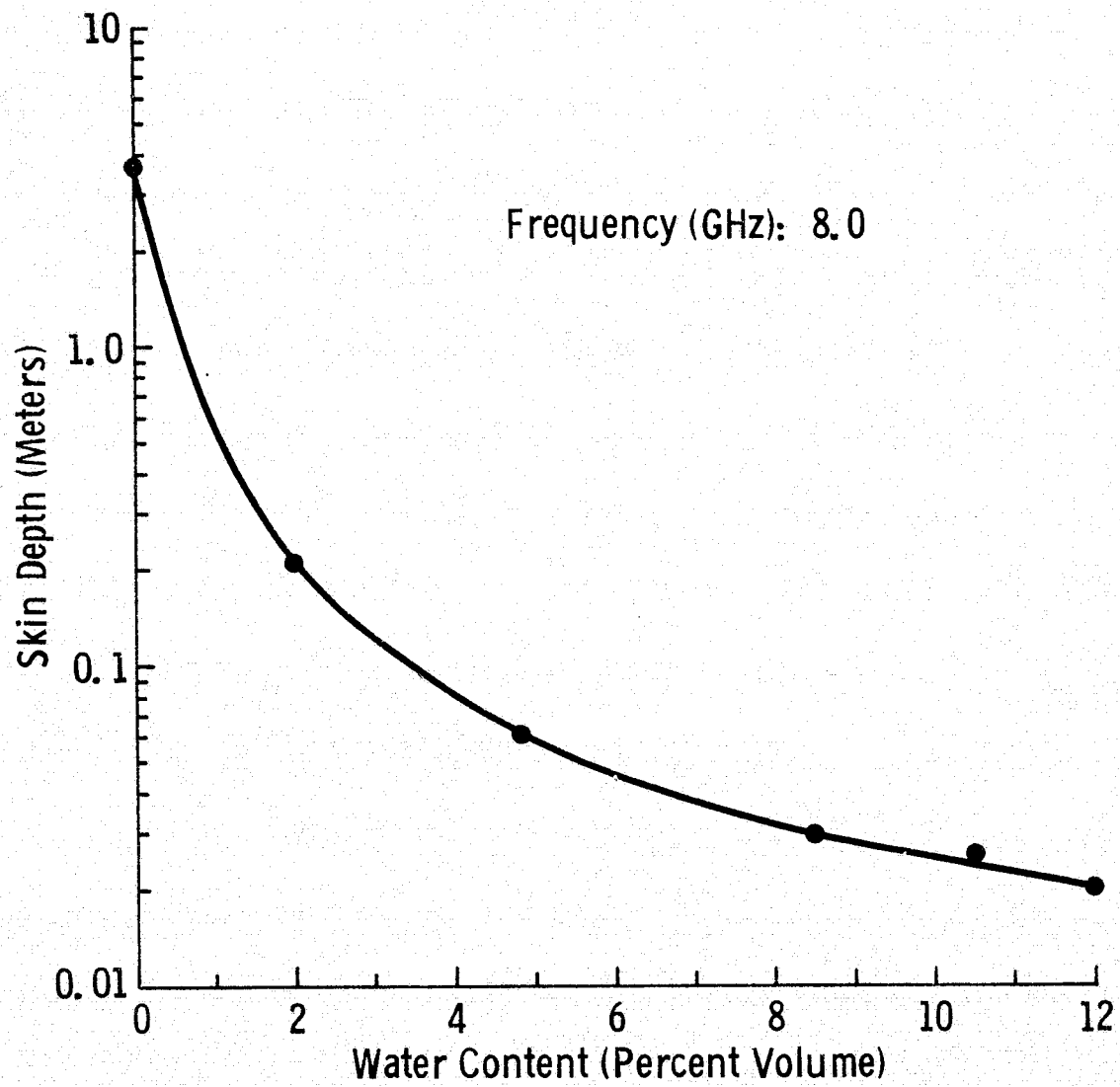


Figure 18. Skin Depth of Wet Snow.

For the case of dry snow or even for wet snow, experiments have shown that

$$K' \gg K''$$

With this condition, the attenuation coefficient may be approximated by

$$\alpha = \frac{\pi K''}{\lambda \sqrt{K'}}$$

The skin depth (D) is therefore

$$D = \frac{1}{\alpha} = \frac{\lambda K'}{\pi \sqrt{K''}} = \frac{\lambda}{\pi \sqrt{K'} \tan \delta}$$

where $\tan \delta$ is the loss tangent

$$\tan \delta = \frac{K''}{K'}$$

Skin depths calculated from dielectric constant data reported in the literature are presented in Table 1. Skin depth versus water content from Linlor's data [24] is shown in Figure 18.

4.0 SYSTEM DESCRIPTION

Radar backscatter data were acquired with the University of Kansas truck mounted 1-8 GHz Microwave Active Spectrometer (MAS 1-8). Figure 19 and Table 2 show the system and give system specifications. Radar backscatter data were acquired at eight frequencies in the 1-8 GHz range. The system operates in three polarization configurations: HH (horizontal transmit-horizontal receive), HV (horizontal transmit-vertical receive) and

Table 1: Skin Depths for Snow

Description	Frequency (GHz)	K'	K''	tan	Skin Depth	Source
Dry Snow	37	1.9	.05	---	7 cm	Edgerton [17]
Dry Snow	13.6	2.76	.03	---	38.8 cm	Edgerton [17]
Wet Snow	1.0	1.5	---	10^{-1}	78 cm	Linlor [16]
Wet Snow	8.0	1.5	---	10^{-1}	9.7 cm	Linlor [16]
Dry Snow	1.0	1.32	.0002	---	548 m	Evans [20]
Dry Snow	8.0	1.32	.0002	---	68 m	Evans [20]
Foam 8.5% H ₂ O	1.83	---	---	---	43 cm	Linlor [24]
Foam 8.5% H ₂ O	8.0	---	---	---	3 cm	Linlor [24]
Saturated Snow	10	---	---	---	.9 cm	Linlor [24]
Freshly Fallen Snow	3	1.2	---	.00029	100 m	Vickers [14]
Freshly Fallen Snow	10	1.26	---	.00042	20.2 m	Vickers [14]
Hard Packed Snow	3	1.50	---	.0009	28.9 m	Vickers [14]
Ice	3	3.2	---	.0009	19.8 m	Vickers [14]

ORIGINAL PAGE IS
OF POOR QUALITY

23



Figure 19. MAS 1-8 System.

Table 2: MAS 1-8 Specifications

Type:	FM-CW
Modulating waveform:	Triangular
Center frequencies:	1.2, 1.6, 2.25, 3.25, 4.25, 5.25, 6.25, 7.25 GHz
FM sweep: ΔF	400 MHz
Transmit power:	100 mW
IF: F_{IF}	49.5 KHz
IF bandwidth: ΔF_{IF}	11.5 KHz
Antennas:	
Height above ground:	19 m
Transmit antenna diameter:	1.22 m
Receive antenna diameter:	1.22 m
Feeds:	Dual polarized switchable 1-12 GHz log periodics
Effective system beamwidth:	12° at 1.2 GHz to 2° at 7.25 GHz
Incidence angle range:	0° (nadir)-80°
Polarization:	Horizontal transmit-horizontal receive (HH) Horizontal transmit-vertical receive (HV) Vertical transmit-vertical receive (VV)
Calibration:	
Internal	Coaxial delay line
External	Luneberg lens

VV (vertical transmit-vertical receive). Data can be acquired at any incidence angle from 0° to 80° (relative to nadir).

Signal fading is reduced by using both spatial and frequency averaging. Frequency averaging results from the 400 MHz bandwidth. Spatial averaging was accomplished by measuring the return from different locations on the test site. The number of frequency independent samples of return power is smallest near nadir; therefore for fading reduction, more spatial samples were acquired at the smaller angles. Assuming Rayleigh fading, knowledge of the number of independent measurements gives the confidence intervals on the measurements. Ninety percent confidence limits for 3 cm tall grass are shown in Table 3.

5.0 DATA PRESENTATION

5.1 Ground Truth

5.1.1 General

The test plot, 20 x 60 meters (Figure 20), was a flat area with Little Blue Stem grass cover. Ground data (Appendix A) were acquired in conjunction with the spectrometer measurements. Data consisted of soil moistures, soil temperatures, air temperature, snow depth, snow layering, snow temperatures, and snow water equivalent. Since the experiment was conducted during the winter dormancy period, the height and physical condition of the ground cover was essentially constant with the exception of the last few data sets.

5.1.2 Soil Moisture

During the radar data collection, soil samples were taken at three positions on the field so that spatial variations could be accounted for. These samples were taken from the 0-5 cm soil layer. Soil moistures for the near (0° - 10°), middle (20° - 50°), and far (70°) ranges are shown in Figures 21, 22 and 23. Soil samples were not taken between data sets 8 and 15. Calculated soil moistures greater than 50% are believed to be the result of standing water on the surface.

Table 3: 90% Confidence Limits

<u>Angle of Incidence</u>	<u>Number of Spatial Measurements</u>	<u>90% Confidence Limits</u>	
		<u>1.2 GHz</u>	<u>7.25 GHz</u>
0°	12	+1.8 -2.4	+1.8 -2.4
10°	12	+1.3 -1.6	+1.8 -2.4
20°	12	+ .9 -1.1	+1.8 -2.4
30°	12	+ .7 - .8	+1.5 -2.1
50°	8	+ .7 - .8	+1.5 -2.1
70°	8	+ .4 - .4	+ .9 -1.0

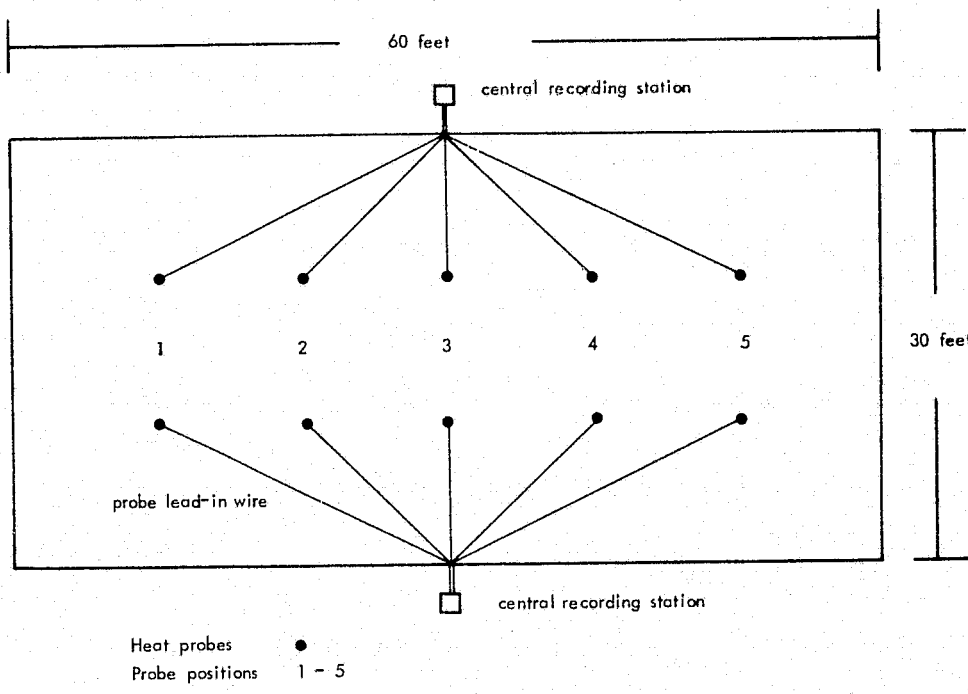


Figure 20a.

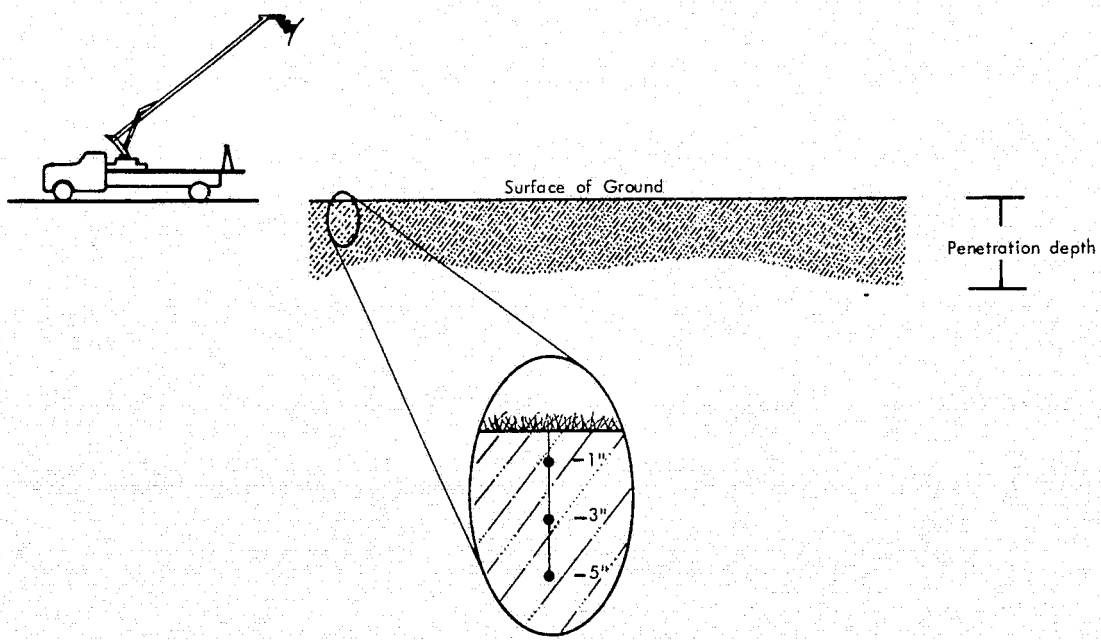


Figure 20b.

ORIGINAL PAGE IS
OF POOR QUALITY

Soil Moisture: Percent by Weight 0 - 5 cm
Angle of Incidence: Near Range (0° and 10°)

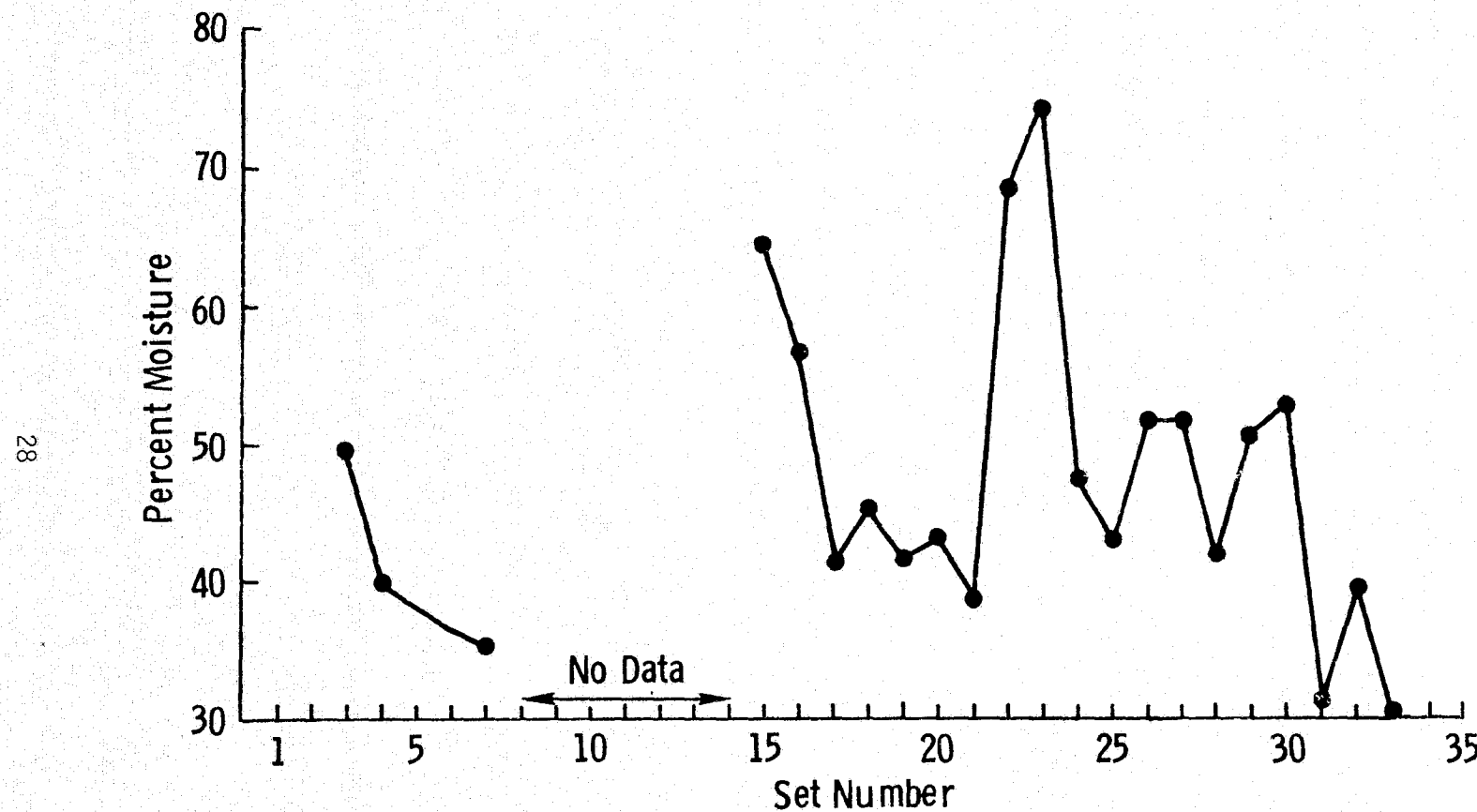


Figure 21. Soil Moistures for the Near Range (0° and 10°), 1975.

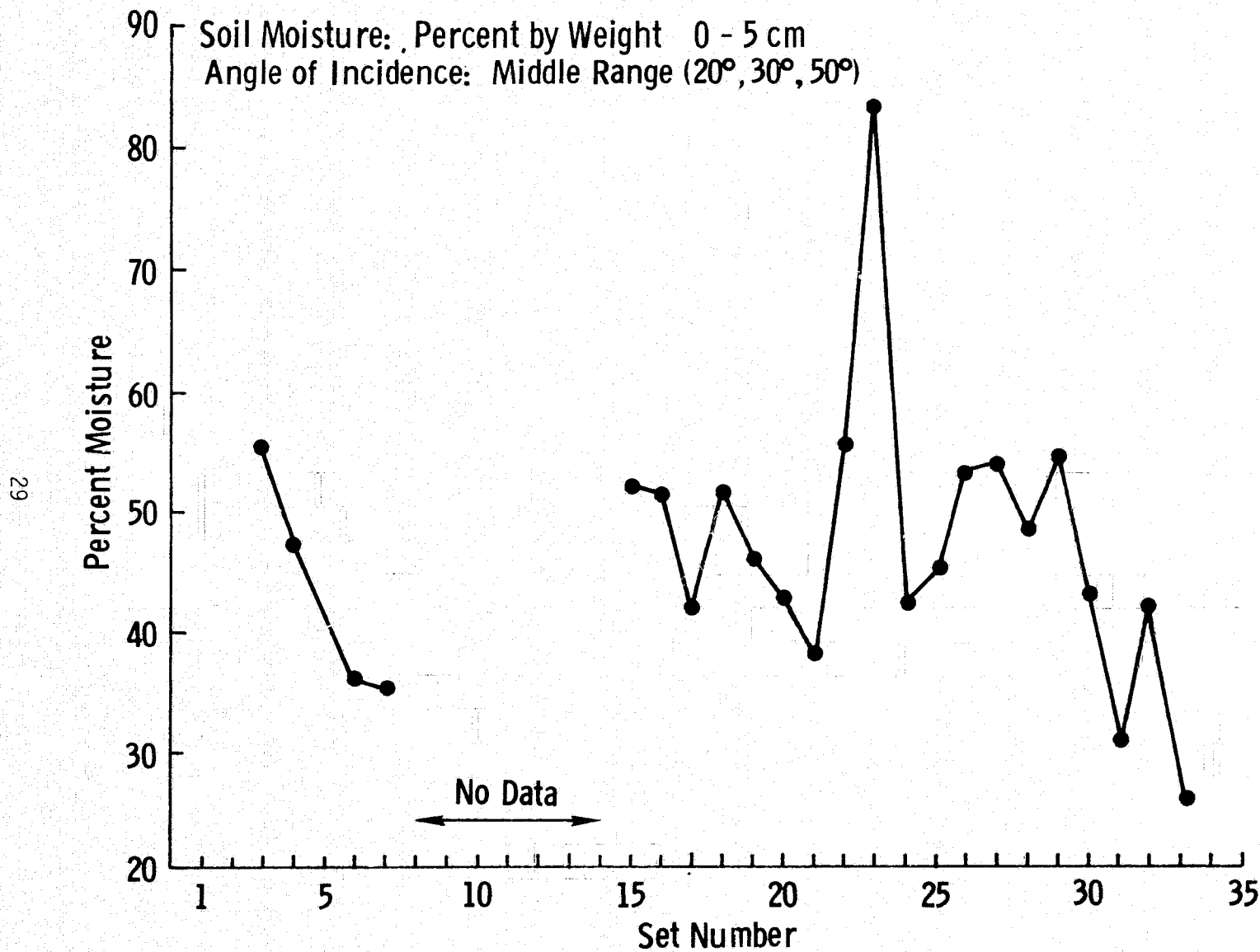


Figure 22. Soil Moistures for the Middle Range ($20^\circ, 30^\circ, 50^\circ$), 1975.

Soil Moisture: Percent by Weight 0 - 5 cm
Angle of Incidence: Far Range (70°)

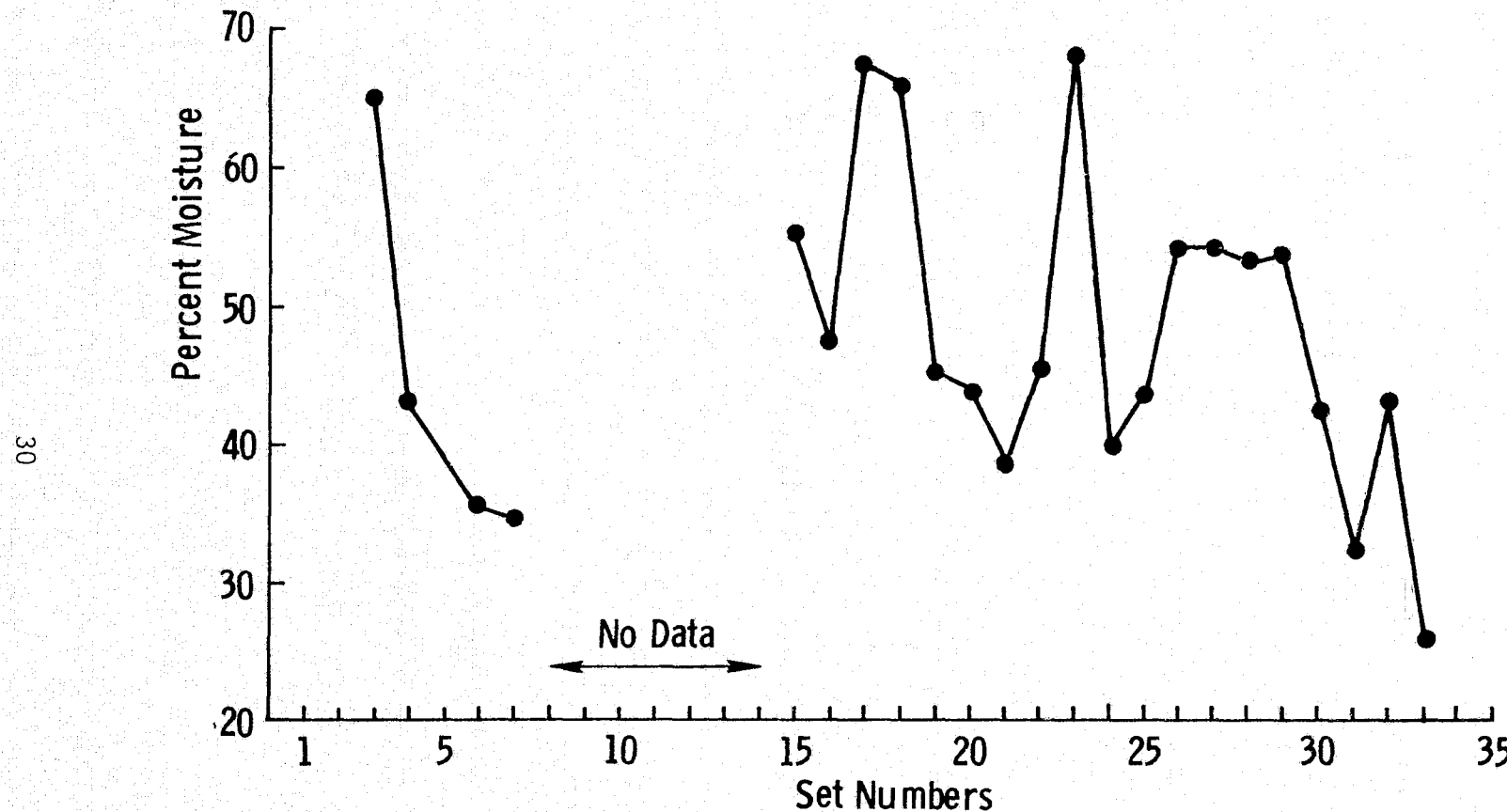


Figure 23. Soil Moistures for the Far Range (70°), 1975.

5.1.3 Temperature

Ground temperature was monitored at 10 locations on the test plot (Figure 20). The sensors were thermistor type thermometers buried at 1, 3 and 5 inch depths. Also, surface temperatures were taken (Figure 24). The recorder was a battery operated solid state device with multiple input capability and an accuracy of 1°C .

5.1.4 Snow

The data acquired on snow were depth, temperature, and water equivalent. Water equivalent is percent volume of water obtained from complete melting of a given volume of snow. If layers existed within the snow, thickness and water equivalents were recorded. Snow depth for the data sets with snow cover, and total snow water for a 1 cm^2 area are plotted in Figure 25.

5.2 Angular Response

Figures 26-28 show the scattering coefficient angular response for three of the data sets. Note that the responses show a smooth surface; σ^0 drops rapidly with increasing angle. For each data set, increasing frequency makes the surface look rougher as demonstrated by the slower decay from nadir.

5.3 Polarization Response

On the average, there is very little difference between horizontal and vertical polarization response (Figures 29 and 30). Cross polarization is very low for the low frequencies, normally about 20 dB down from HH at nadir, while at 7.25 GHz the difference is only about 10 dB. The magnitude of the difference between HV and the like polarized cases decreases with increasing incidence angle at 7.25 GHz.

5.4 Spectral Response

Figures 31-33 show scattering cross section spectral responses for three different ground conditions. Run 4 illustrated in Figure 31 is the spectral response of σ^0 with no snow cover. Run 6, illustrated in Figure 32, was measured with a light powder 15 cm snow cover. Notice the significant

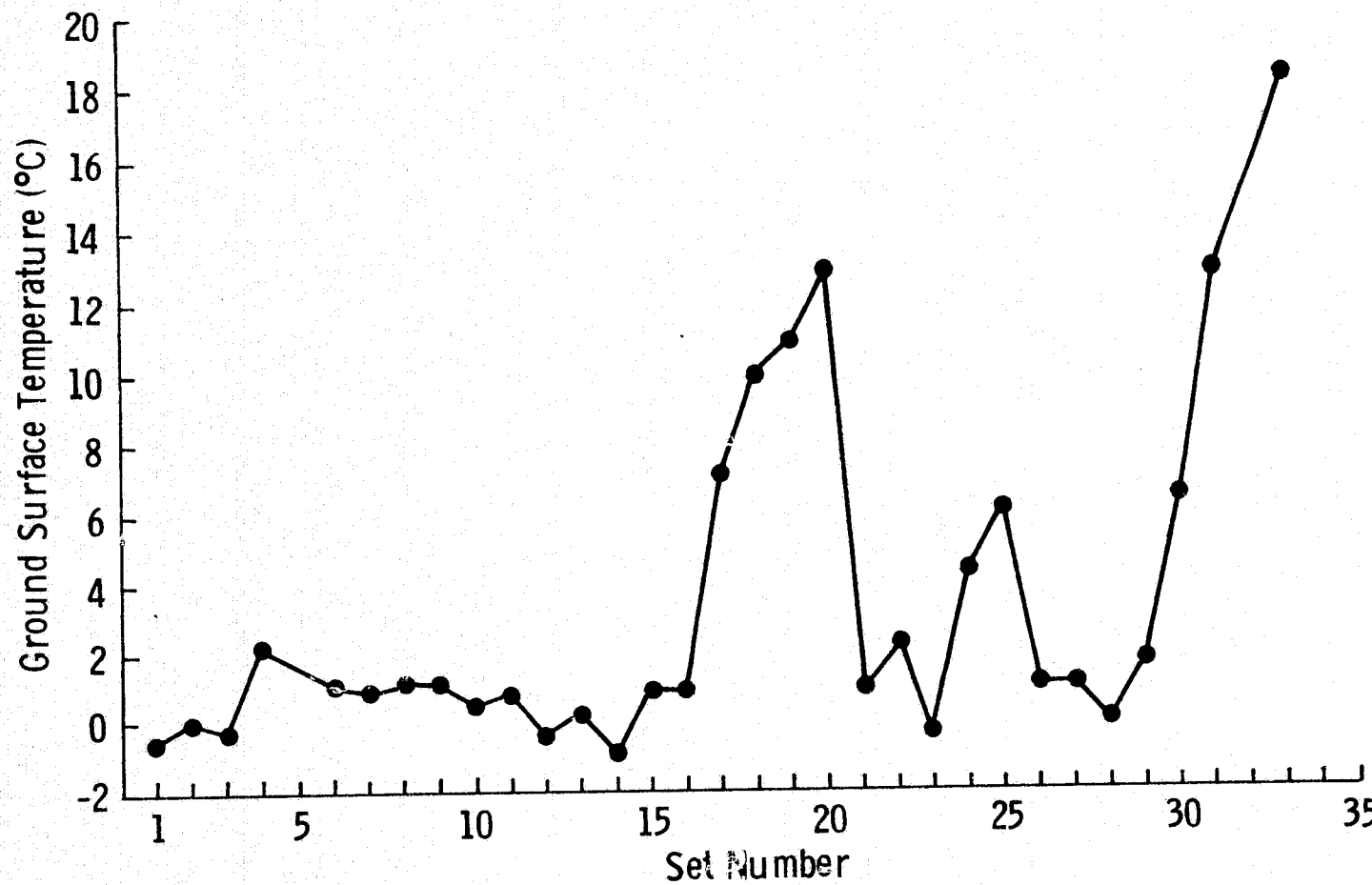


Figure 24. Ground Surface Temperature, 1975.

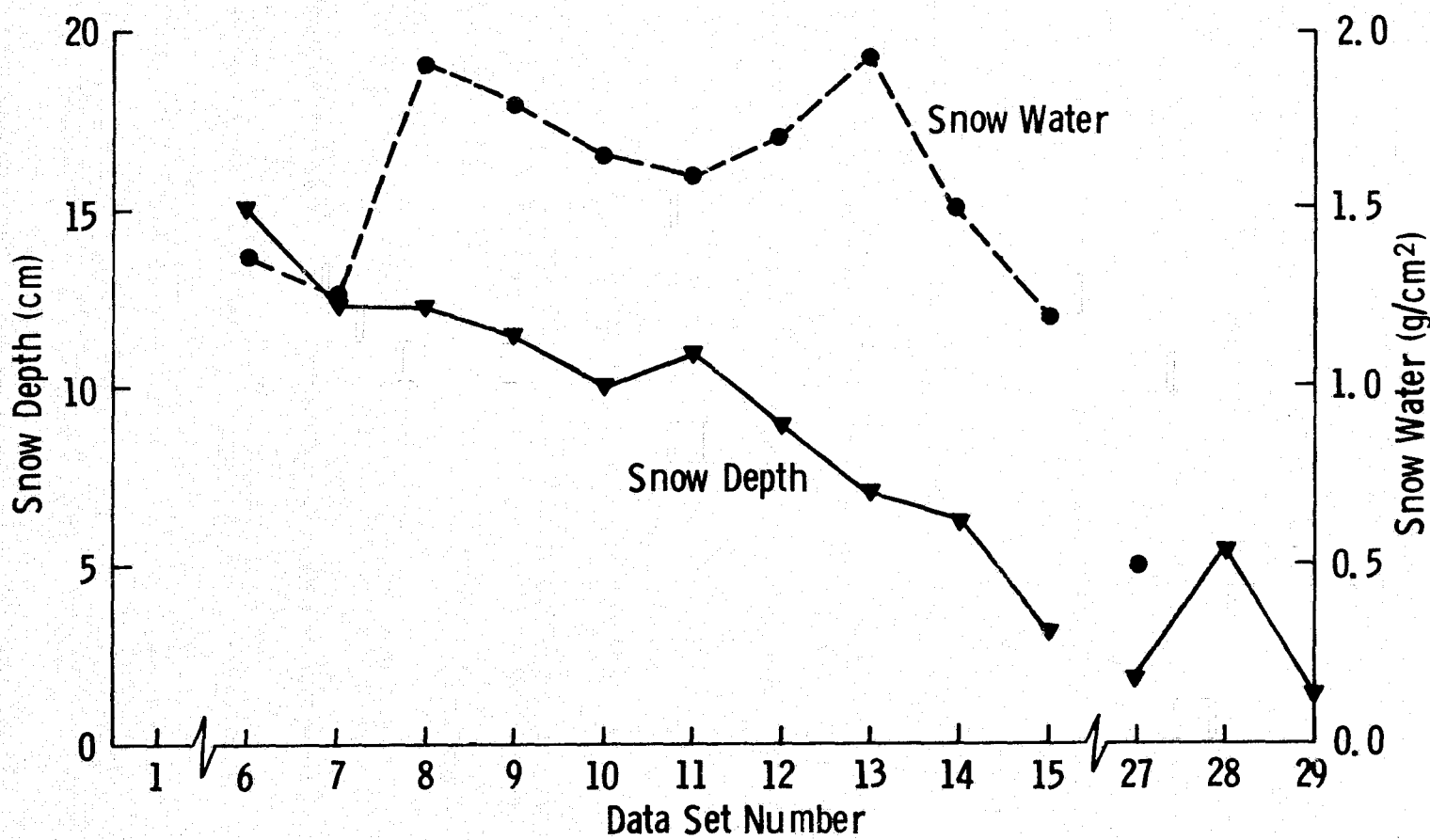


Figure 25. Snow Data, 1975.

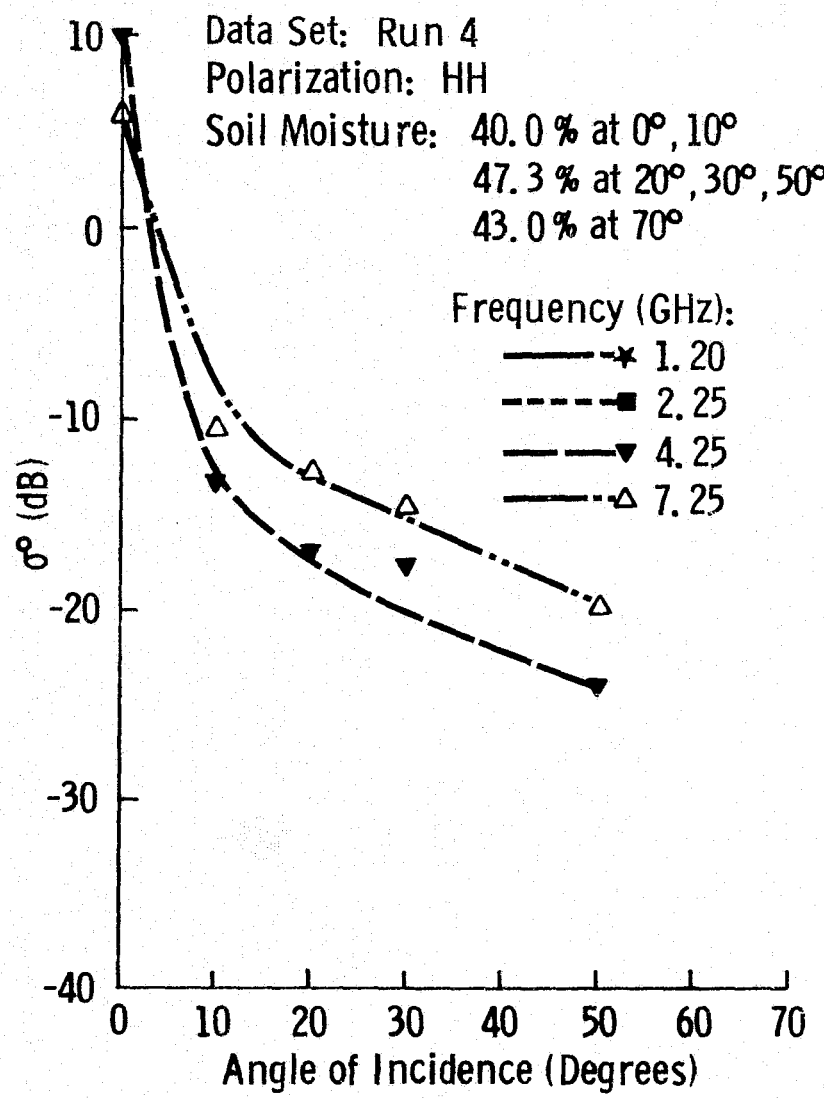
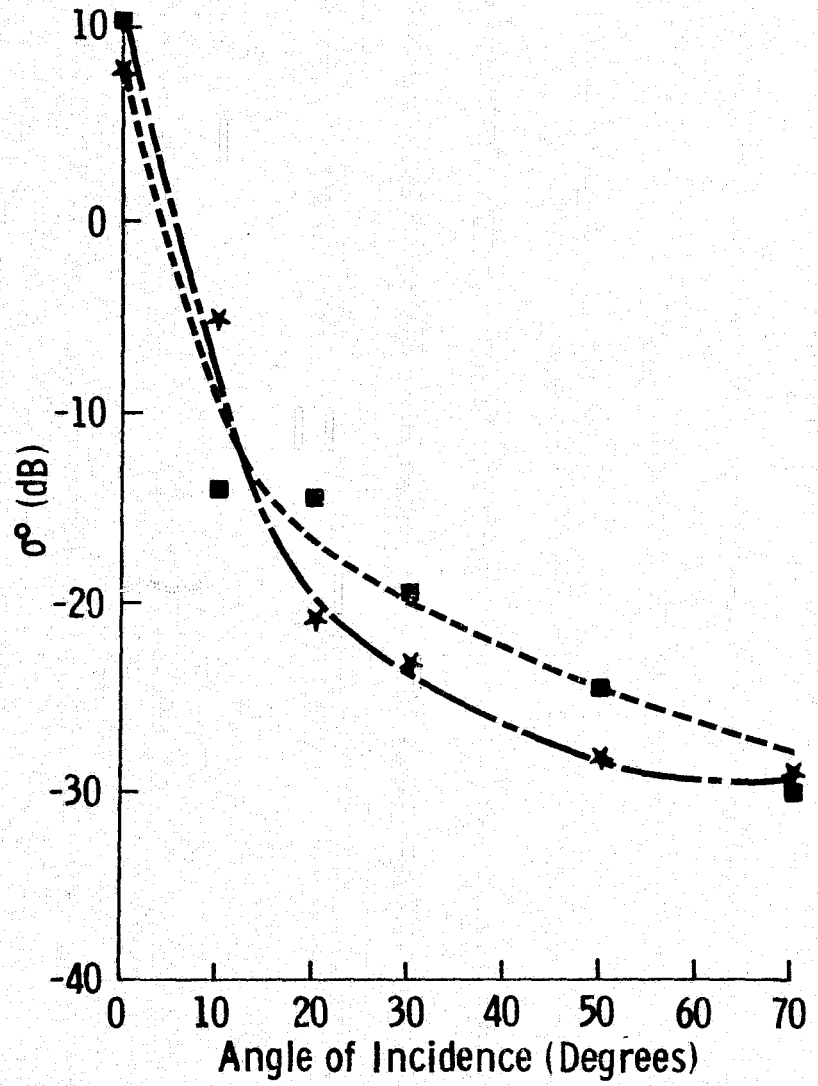


Figure 26. Angular Response of σ_0 of Short Grass.

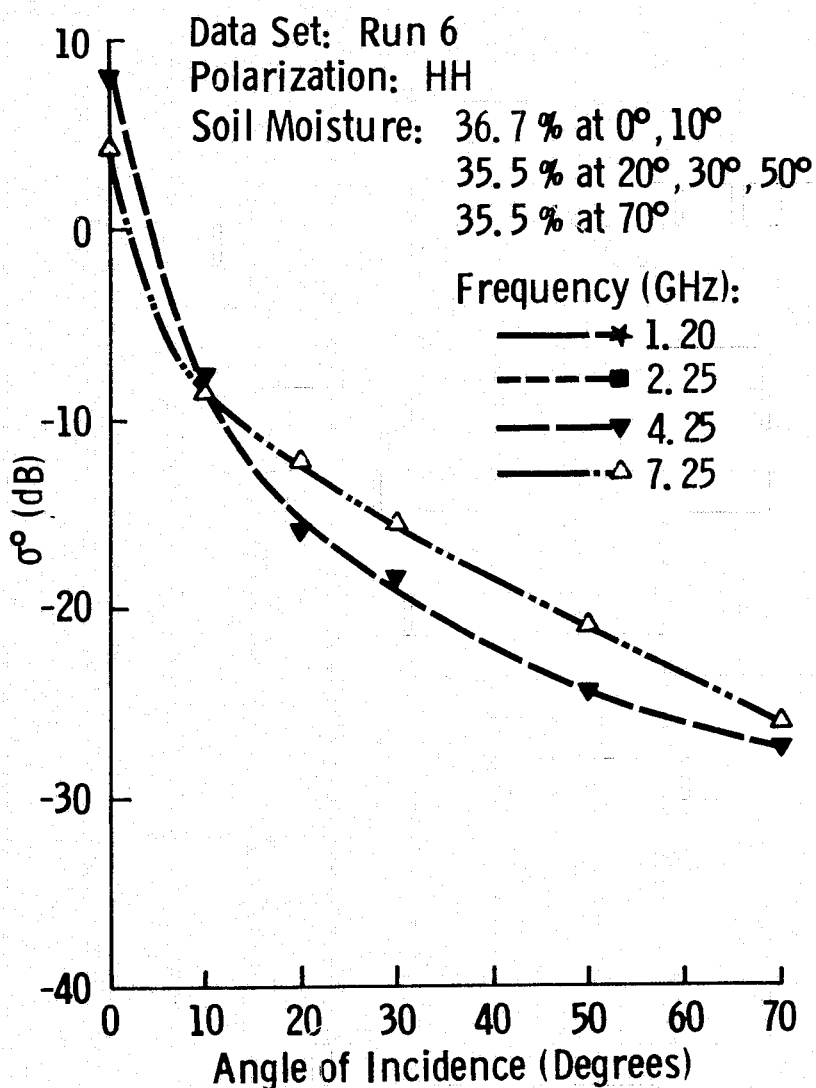
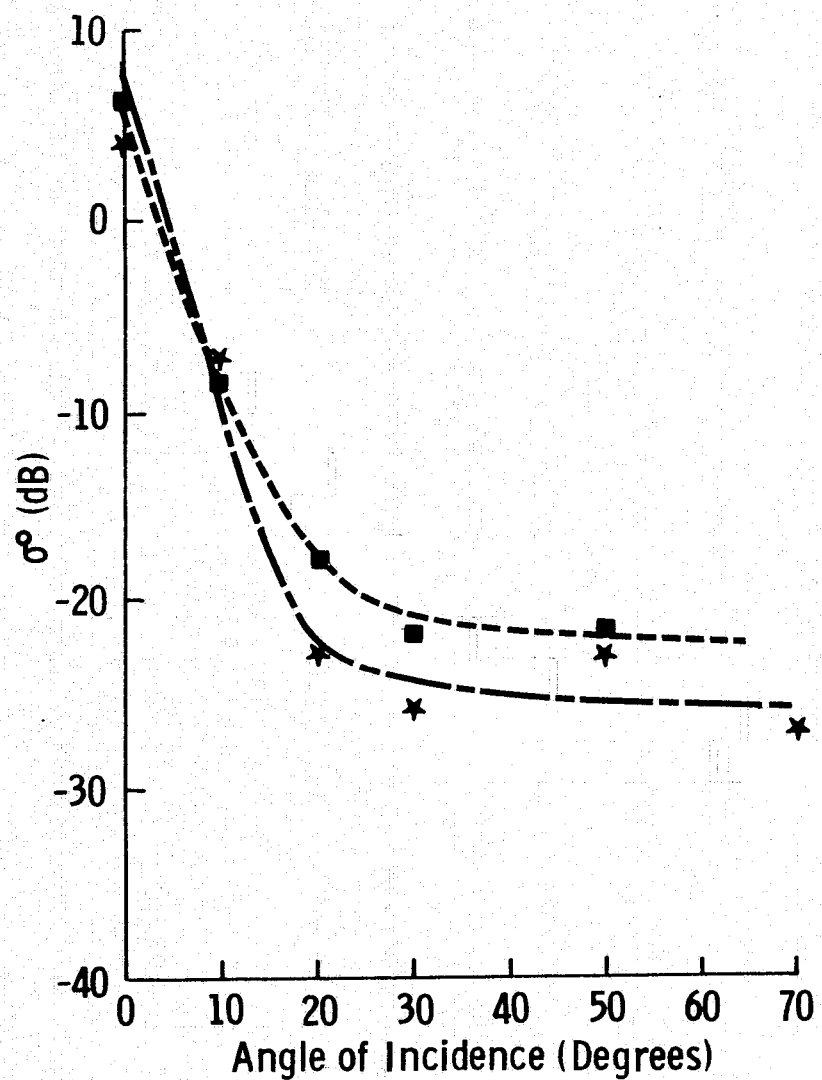


Figure 27. Angular Response of 0° of Short Grass with 15 cm Dry Powder Snow Cover.

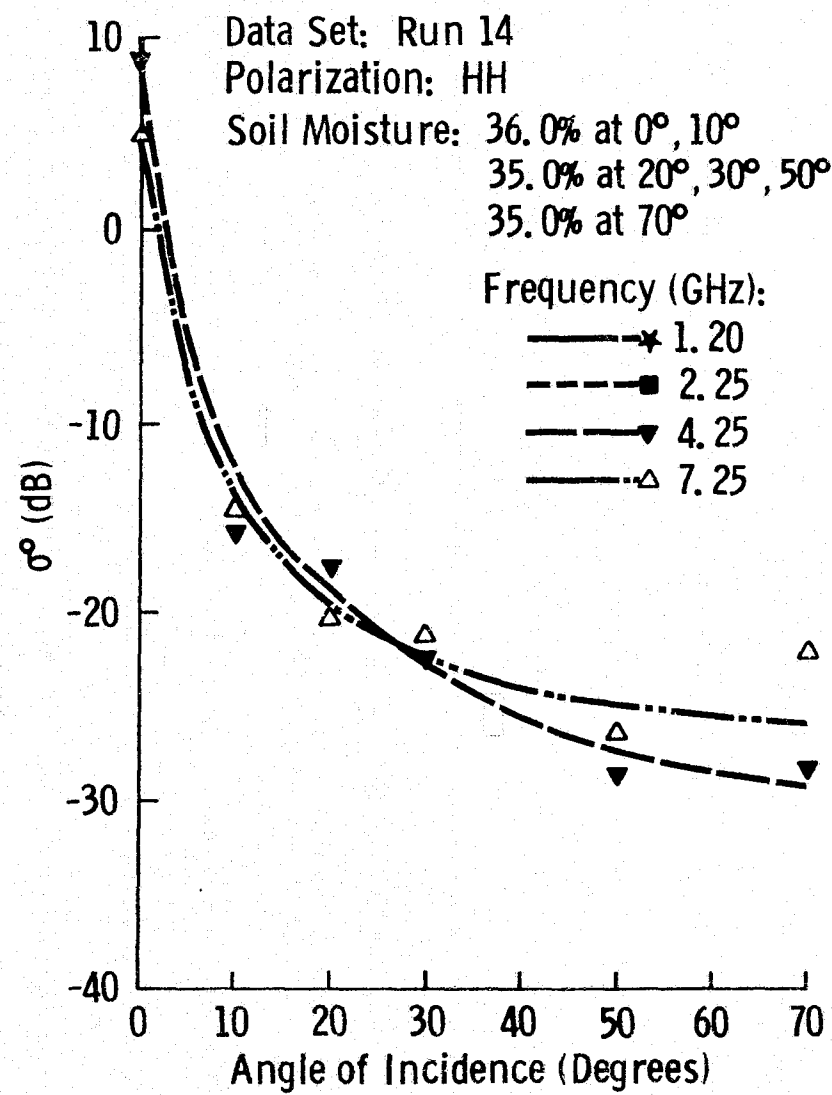
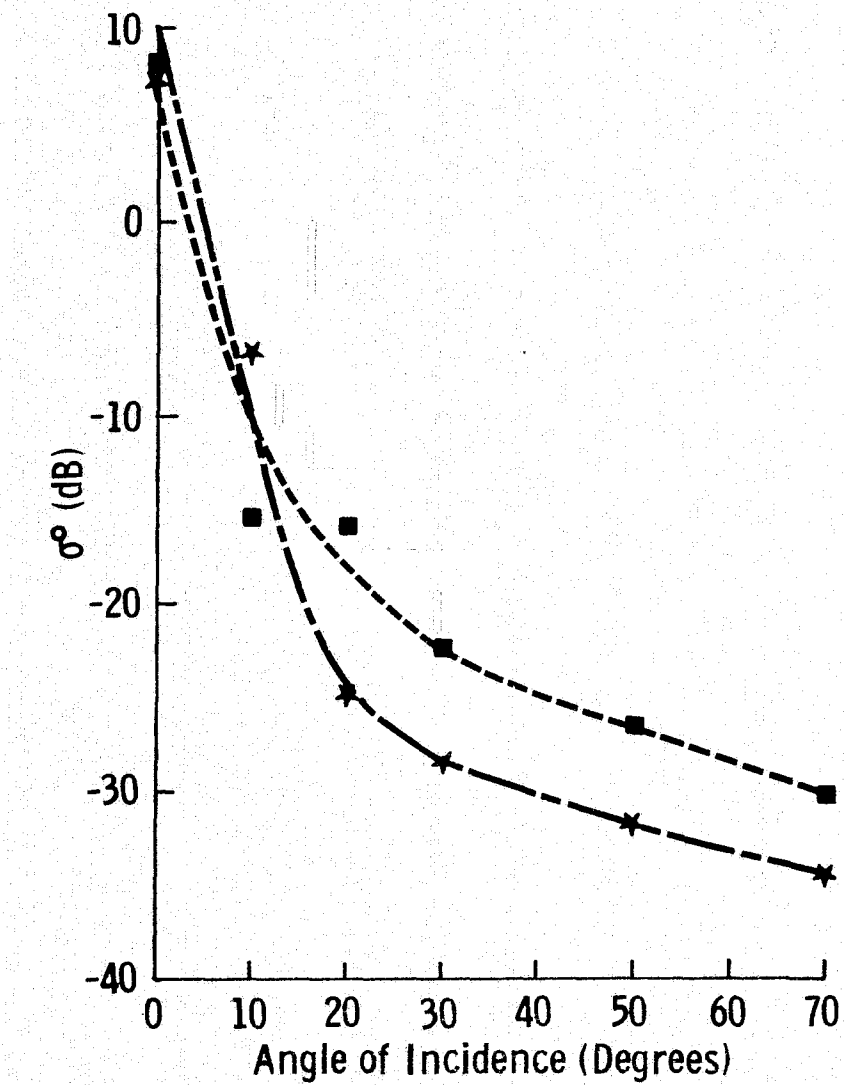


Figure 28. Angular Response of 0° of Short Grass with 0.5 cm Ice Over 6.5 cm Snow Cover.

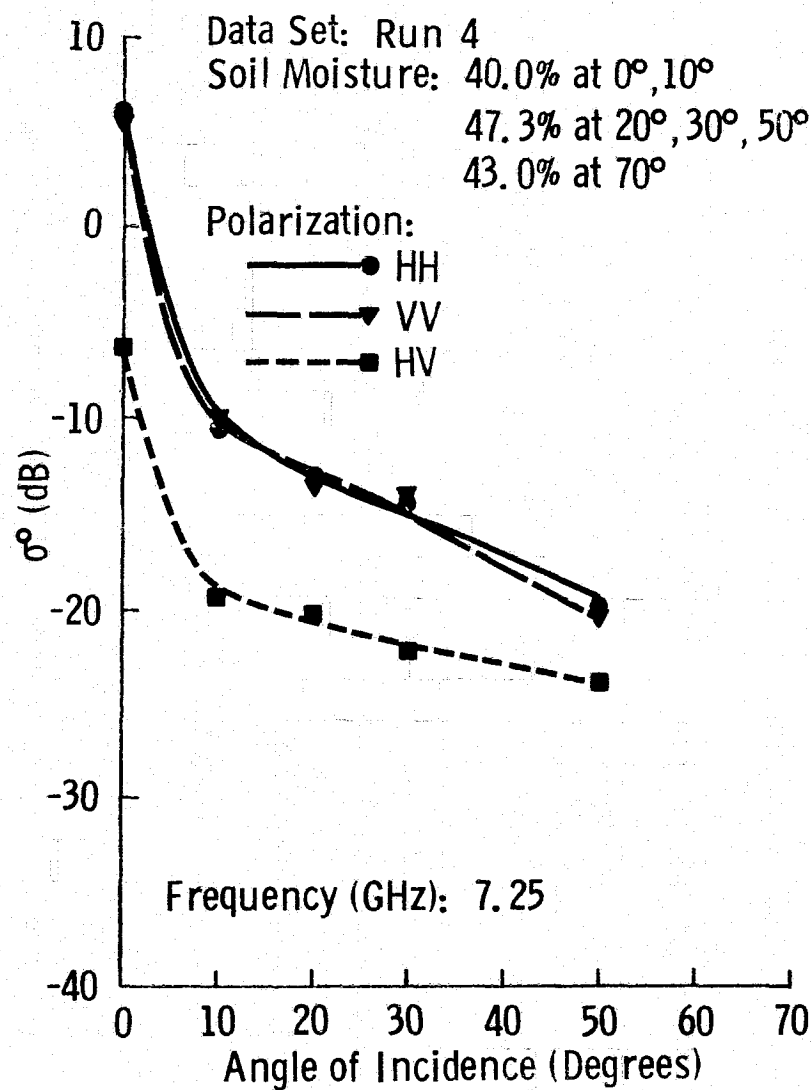
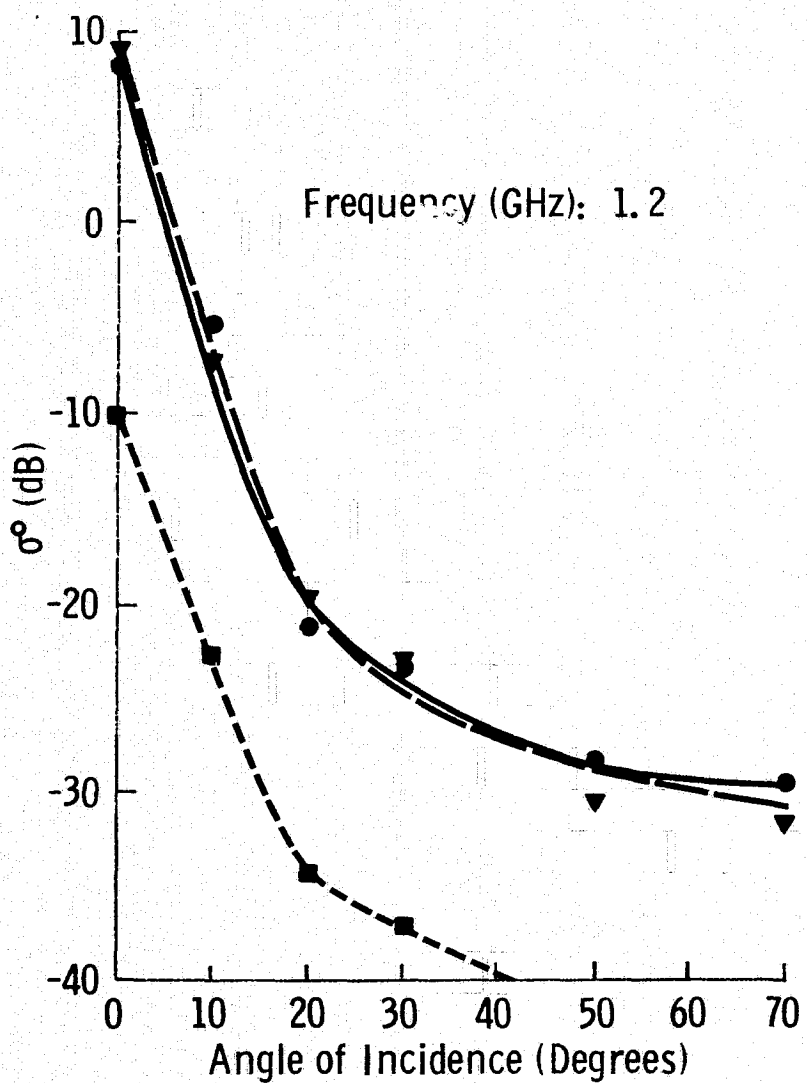


Figure 29. Polarization Response of σ_0 of Short Grass.

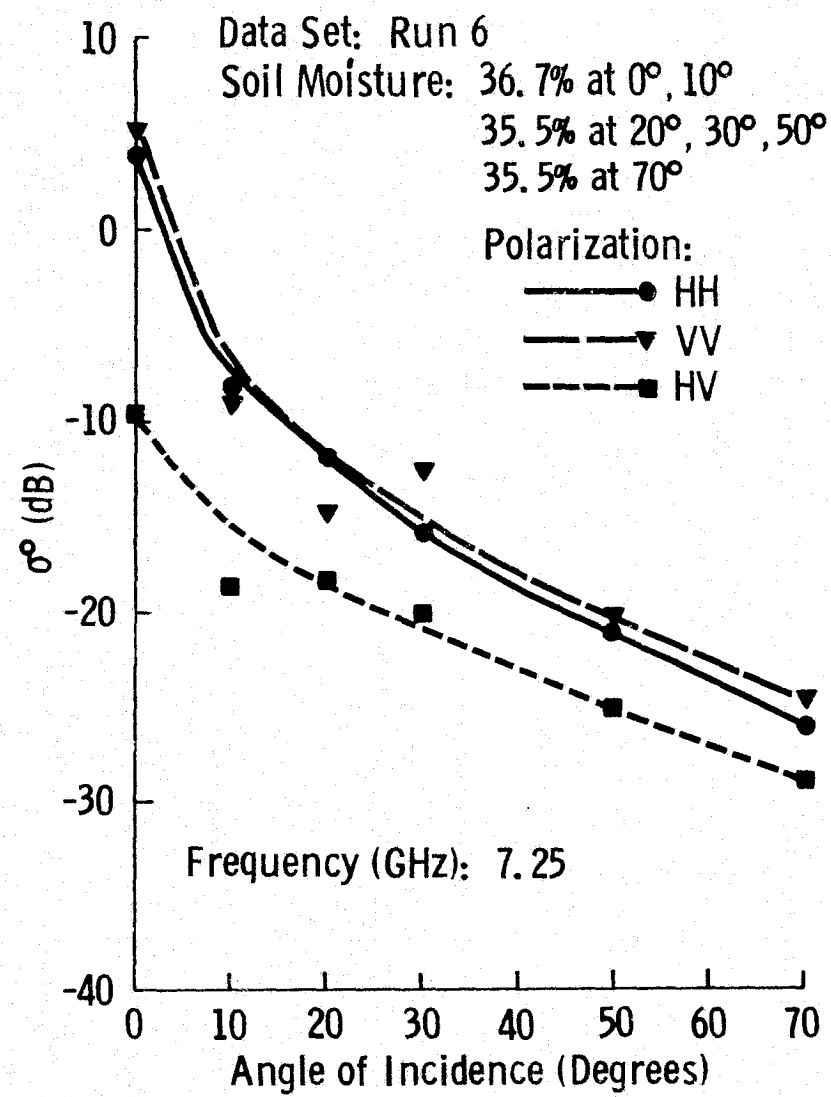
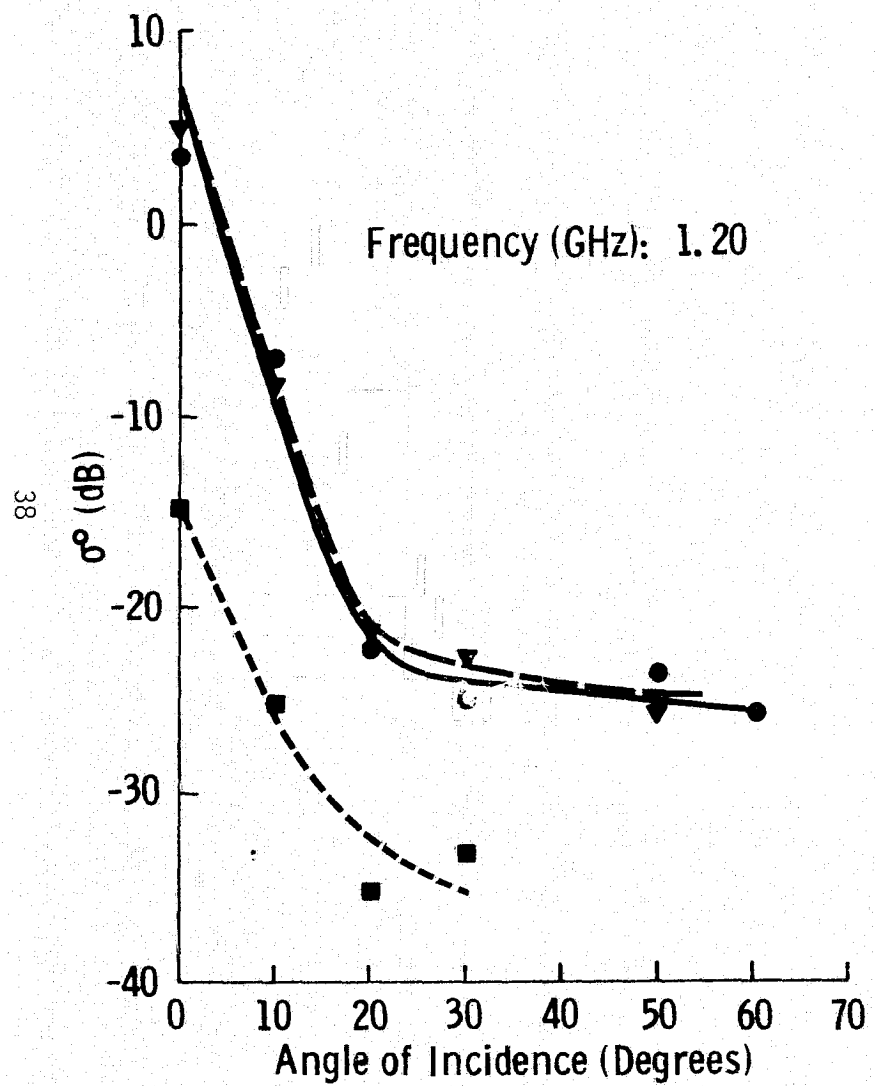


Figure 30. Polarization Response of σ^0 of Short Grass with 15 cm Dry Powder Snow Cover.

Data Set: Run 4

Polarization: HH

Soil Moisture: 40.0% at 0°, 10°

47.3% at 20°, 30°, 50°

43.0% at 70°

Angle of Incidence (Degrees):

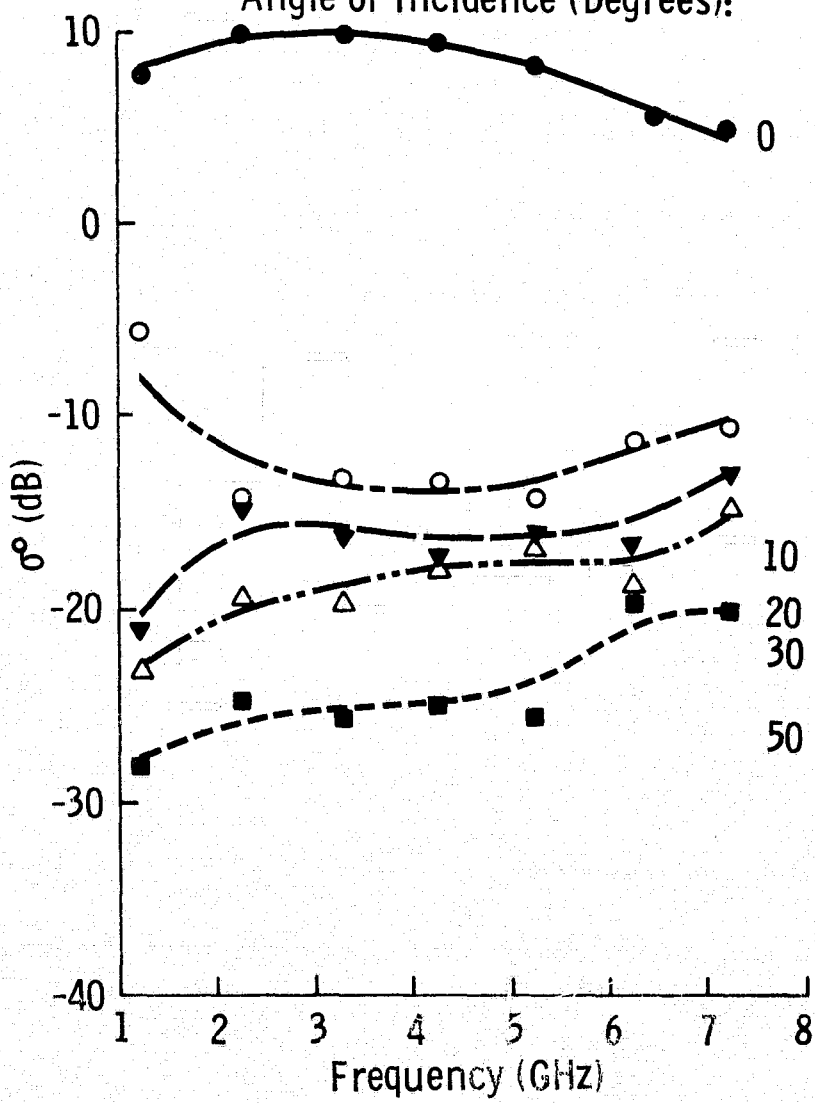


Figure 31. Spectral Response of σ^0 of Short Grass.

Data Set: Run 6
Polarization: HH
Soil Moisture: 36.7% at 0°, 10°
35.5% at 20°, 30°, 50°
35.5% at 70°

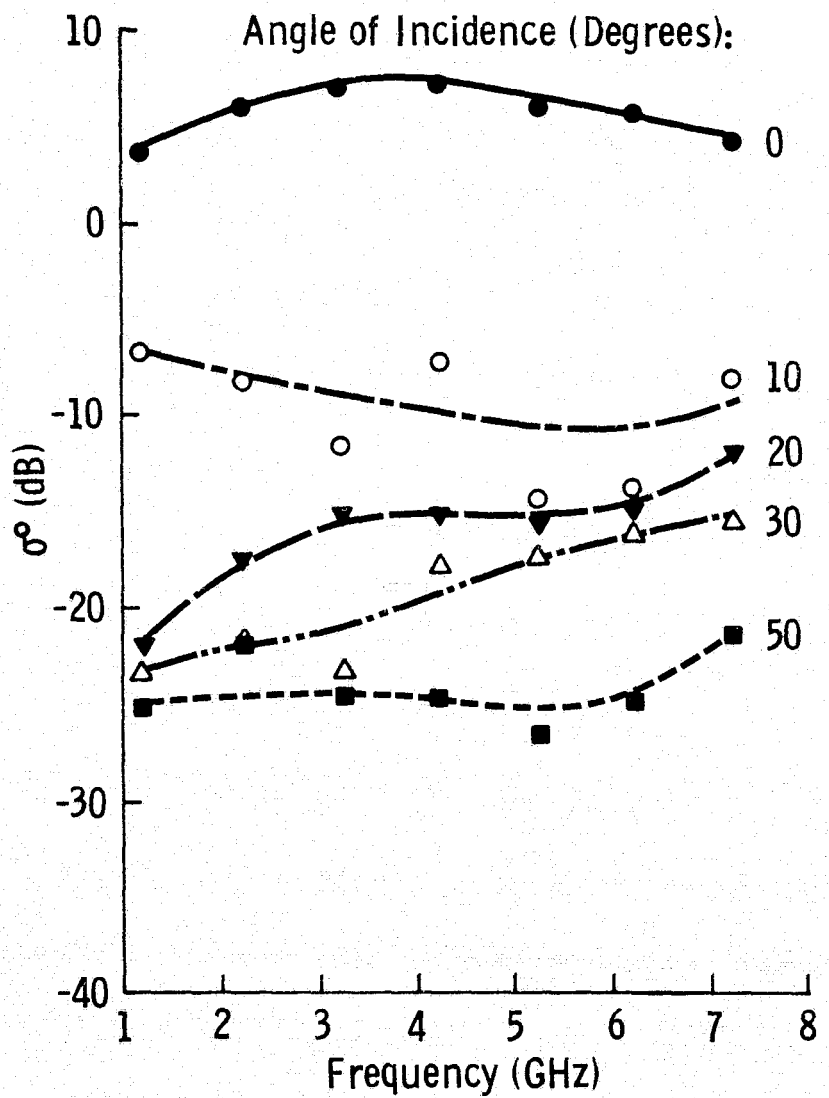


Figure 32. Spectral Response of σ_0 of Short Grass with Dry Powder Snow Cover.

Data Set: Run 9

Polarization: HH

Soil Moisture: 35.0% at 0°, 10°

34.0% at 20°, 30°, 50°

34.0% at 70°

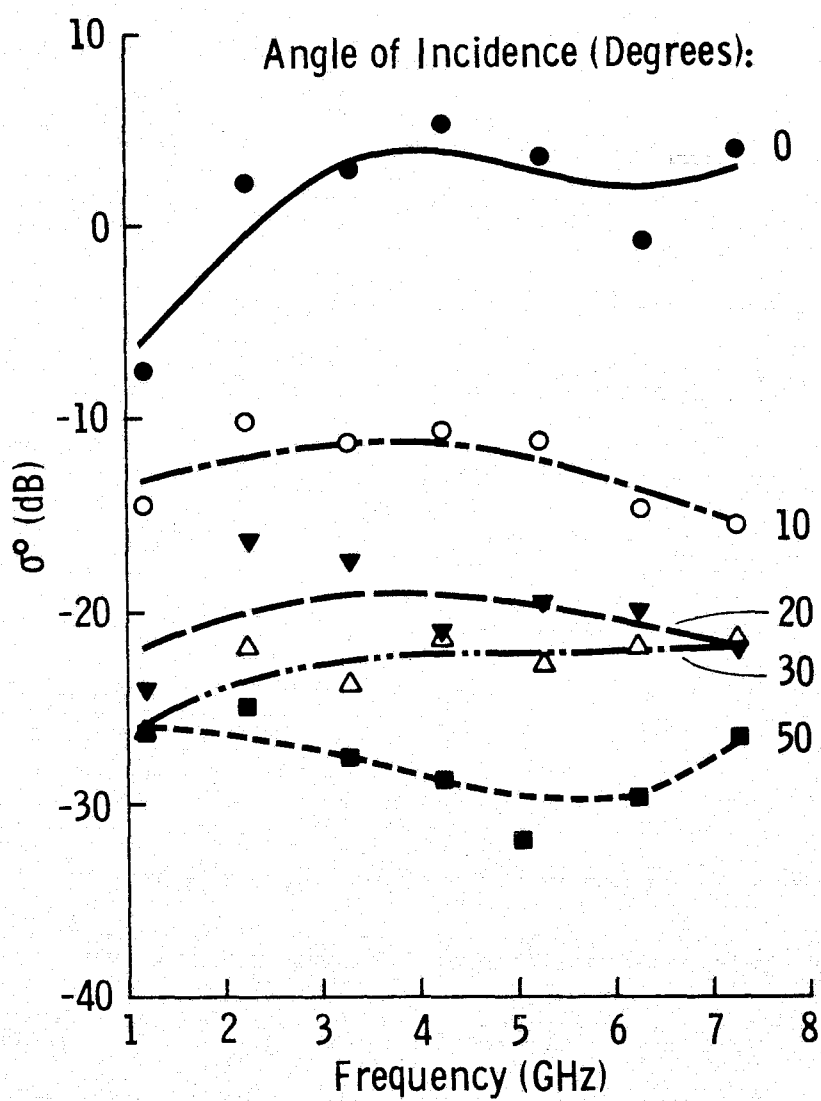


Figure 33. Spectral Response of σ^0 of Short Grass with 0.6 cm Ice Over 10.8 Snow Cover.

difference in the response at nadir for the powder snow (Run 6) and the snow with ice and snow cover (Run 9, Figure 33). Run 9 with 10.2 cm snow, but with a hard sleet layer at the air-snow interface shows an increase of about 12 dB between 1 and 4 GHz at nadir.

6.0 DATA ANALYSIS

6.1 Freeze-Thaw Effect

Due to conditions beyond the control of the experimenters, only one data set was taken when the ground was frozen. At that time, only the top 1 cm of the ground was frozen. Figure 34 shows the σ^0 spectral responses for Run 23 (frozen ground) and Run 24 (thawed ground). The return from the thawed ground is slightly higher at all incidence angles; however, it is more noticeable away from nadir. A possible explanation for the reduction in the backscatter due to the presence of the ice layer is that the ice layer serves to reduce the impedance mismatch between the air and the wet soil media.

6.2 Snow Effect

For dry snow, the skin depth is much greater than the 15 cm maximum snow depth encountered during the experiment. The effect of the dry snow cover is minor as demonstrated by Figure 35 showing the σ^0 response for Run 4 (no snow) and Run 6 (snow cover - 15 cm dry powder).

Immediately before Run 8 (snow cover - 12 cm) there was a fall of fine sleet. Although snow wetness could not be measured, the surface was damp. Figure 36 shows the σ^0 response of the control set, Run 4, and the wet snow cover set, Run 8. According to Linlor's data [16], the skin depth of "wet" snow at 1.0 GHz is 78 cm and the skin depth of foam with 8.5% water at 1.83 GHz is 43 cm (see Table 1). Hence at 1.2 GHz, the 12 cm wet snow (Run 8) in Figure 36 acts primarily as an attenuator of the backscatter from the underlying wet soil. At 7.25 GHz, on the other hand, the skin depth of the wet snow cover is probably comparable to or smaller than the 12 cm depth (see Table 1). Since two-way attenuation by one skin-depth is

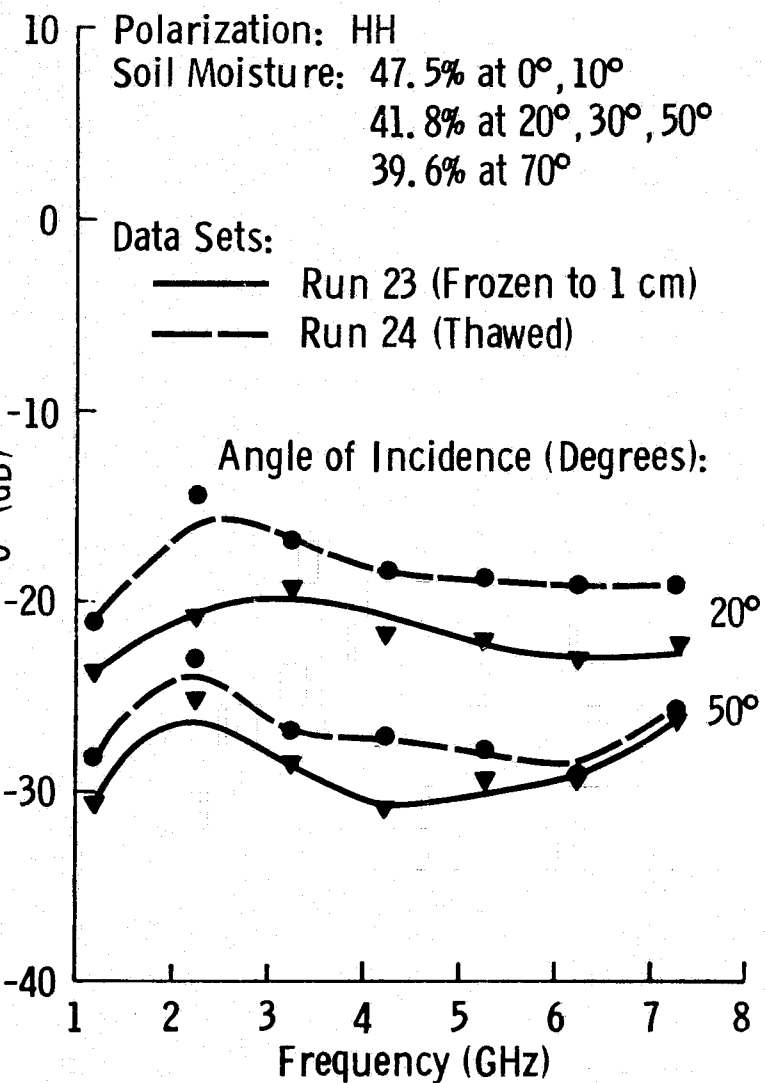
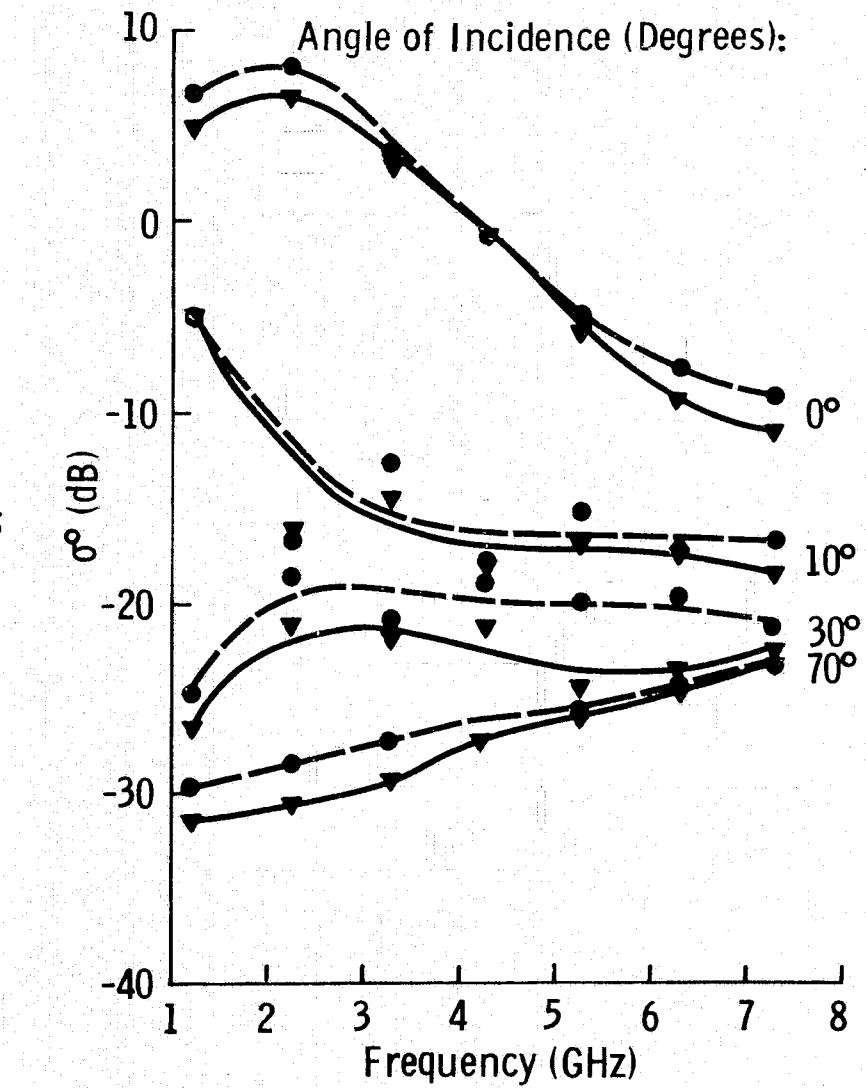


Figure 34. Spectral Response of σ^0 of Frozen (to 1 cm) and Thawed Ground with Short Grass Cover.

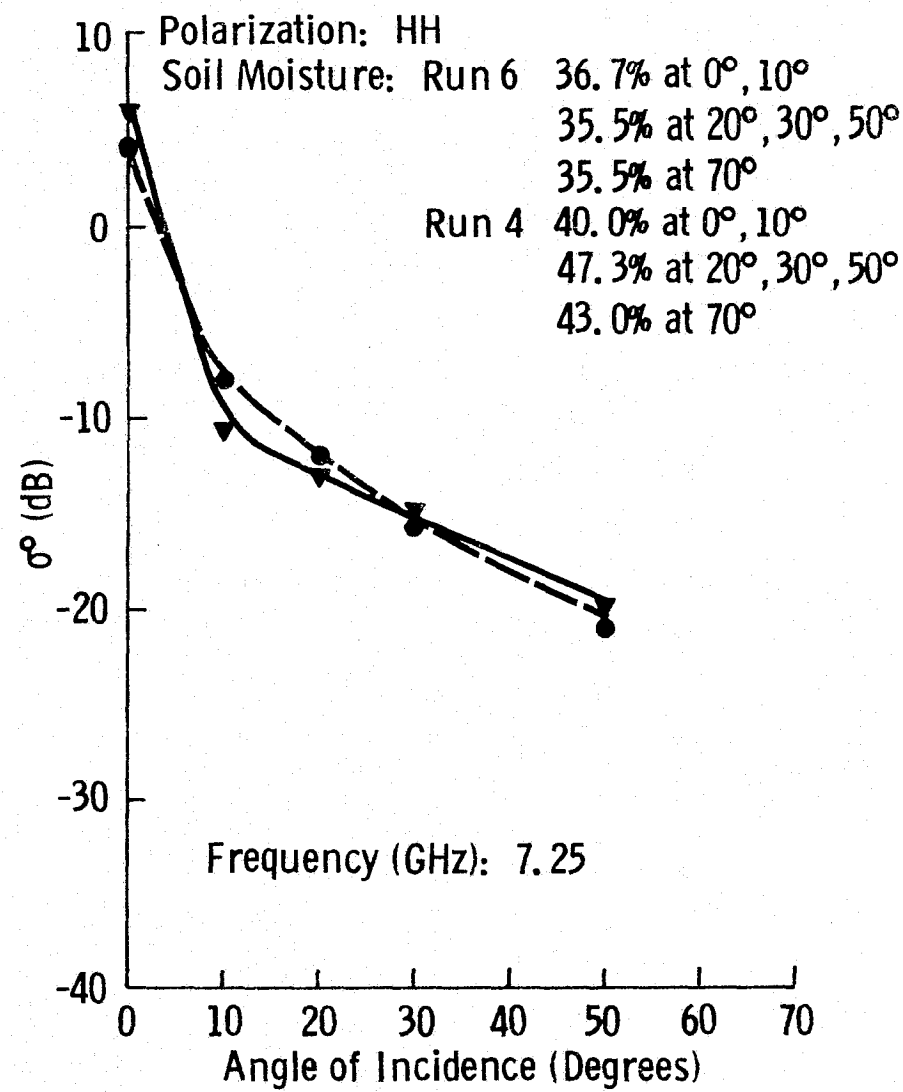
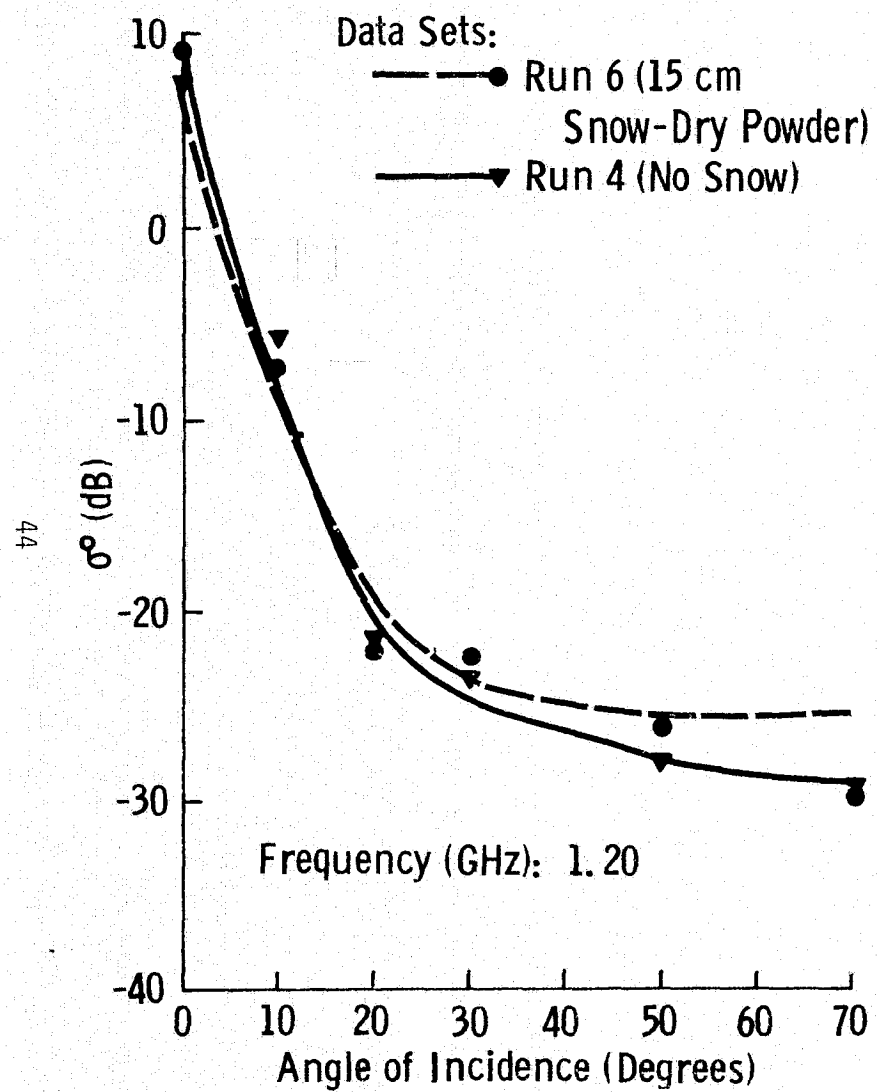


Figure 35. Angular Response of σ^0 of Short Grass and Short Grass with a 15 cm Dry Powder Snow Cover.

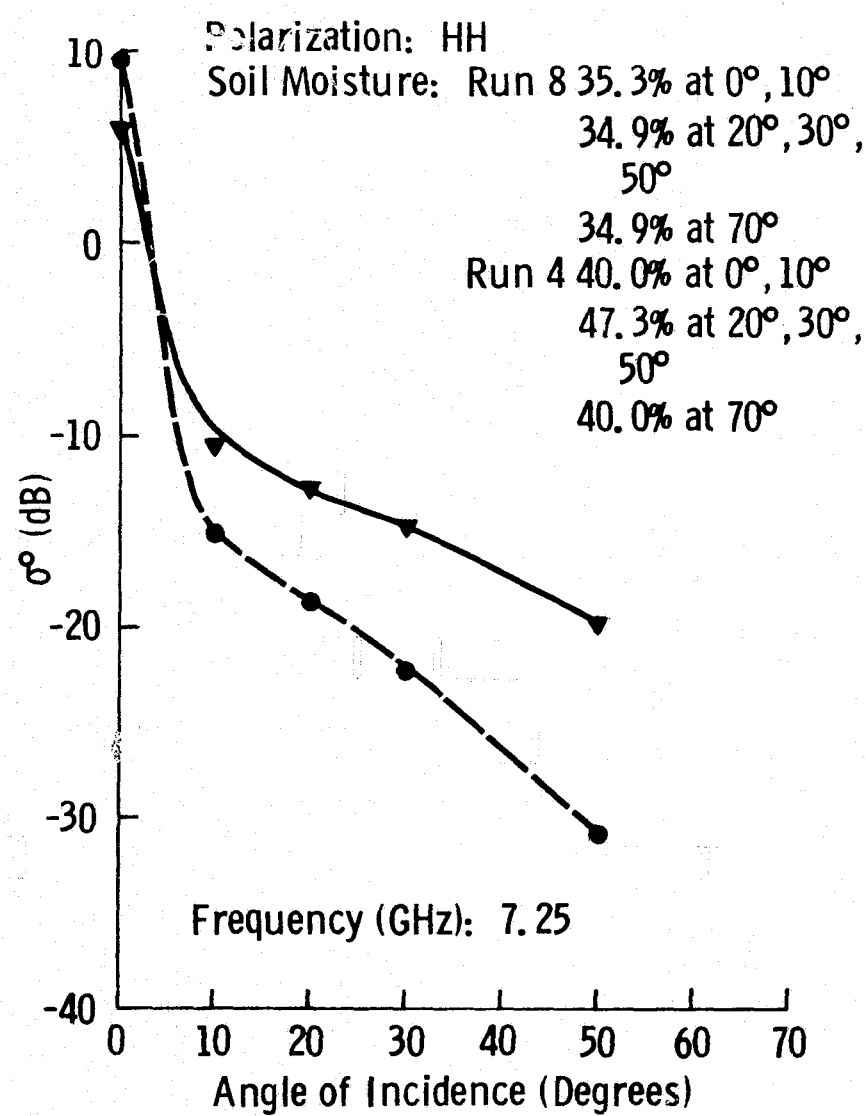
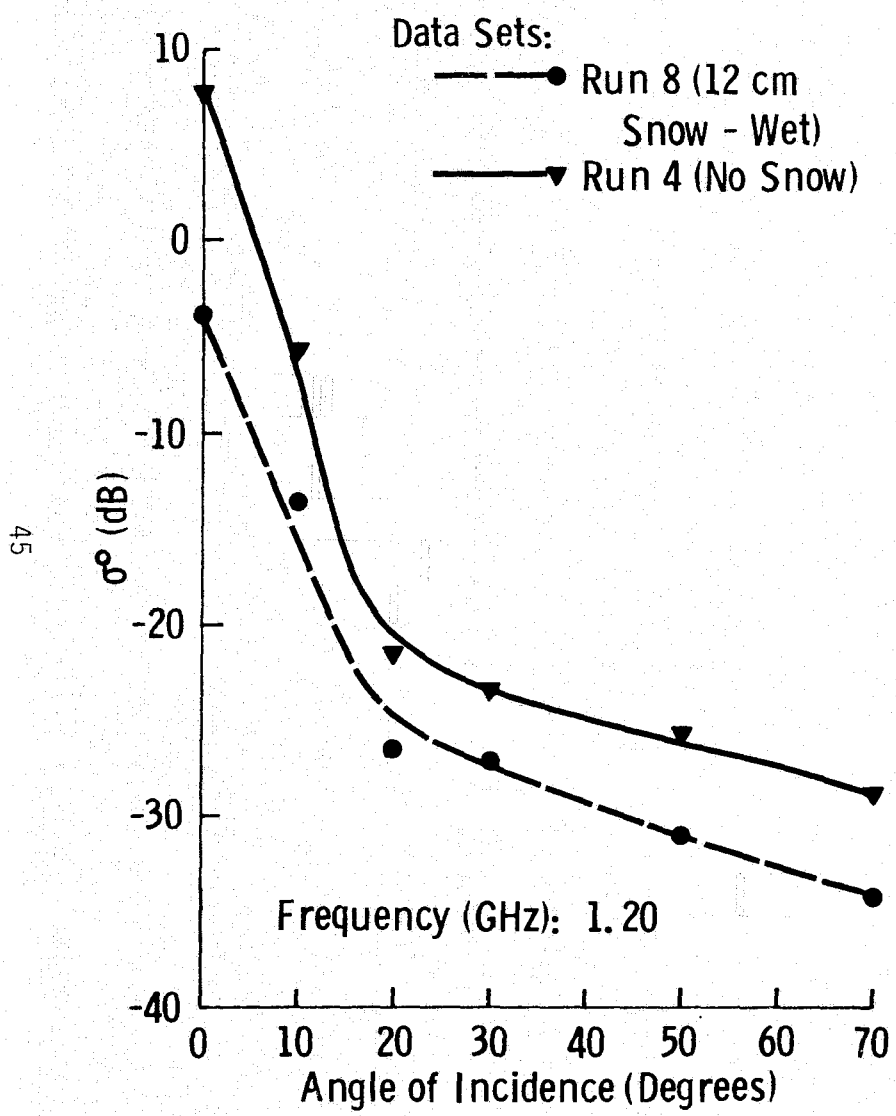


Figure 36. Angular Response of σ^0 of Short Grass and Short Grass with a 12 cm Wet Snow Cover.

approximately 20 dB, it is doubtful if any significant contribution to the 7.25 GHz response of Run 8 is due to the underlying soil. This conclusion is also supported by the distinct difference in the shape of the angular response curves of Runs 4 and 8.

The major conclusion to be drawn from the foregoing discussion is that the key snow parameter influencing the radar return is snow wetness (liquid water content); although the snow depth of Runs 6 and 8 were comparable, their σ^0 responses were drastically different.

For the group of data sets with snow cover, the response of σ^0 to all measured parameters was evaluated. The parameters investigated were temperature, snow depth, soil moisture, and total water content of the snow. In general, the σ^0 response showed a positive correlation with temperature; however, the sensitivity was low. The σ^0 response to snow depth demonstrated no consistent results. The σ^0 response to snow density also demonstrated no consistent results. The σ^0 response to soil moisture showed low correlation. This result, at first, seems to be inconsistent with the conclusions of Batlivala and Ulaby [5]. However, the soil moistures for this experiment were all greater than 30% by weight, which is close to the saturation point. Soil moistures greater than 50% are believed to be the result of standing water. Hence, the low correlation of σ^0 with moisture content is not surprising.

The σ^0 nadir (0°) response to m_t , the total snow water content per unit area, is illustrated in Figure 37 for 2.25 GHz, 4.24 GHz and 6.25 GHz. The response indicates a strong dependence on frequency as demonstrated by the large difference in sensitivity (slope) and correlation coefficient between 2.25 GHz and 6.25 GHz. Since the majority of the data points are clustered between the 1.0 g/cm^2 and 2.0 g/cm^2 range, the significance of the 0.5 g/cm^2 data point on the regression analysis was tested by generating linear regression equations with and without the 0.5 g/cm^2 data point at all frequencies in the 1-8 GHz region. The results are shown in Figure 38 which indicates that although the correlation coefficient is generally lower when the 0.5 g/cm^2 data point is excluded, the magnitude of the correlation coefficient is statistically significant for frequencies above 4 GHz. A similar conclusion was reached when the above test was applied to the data at the other angles of incidence.

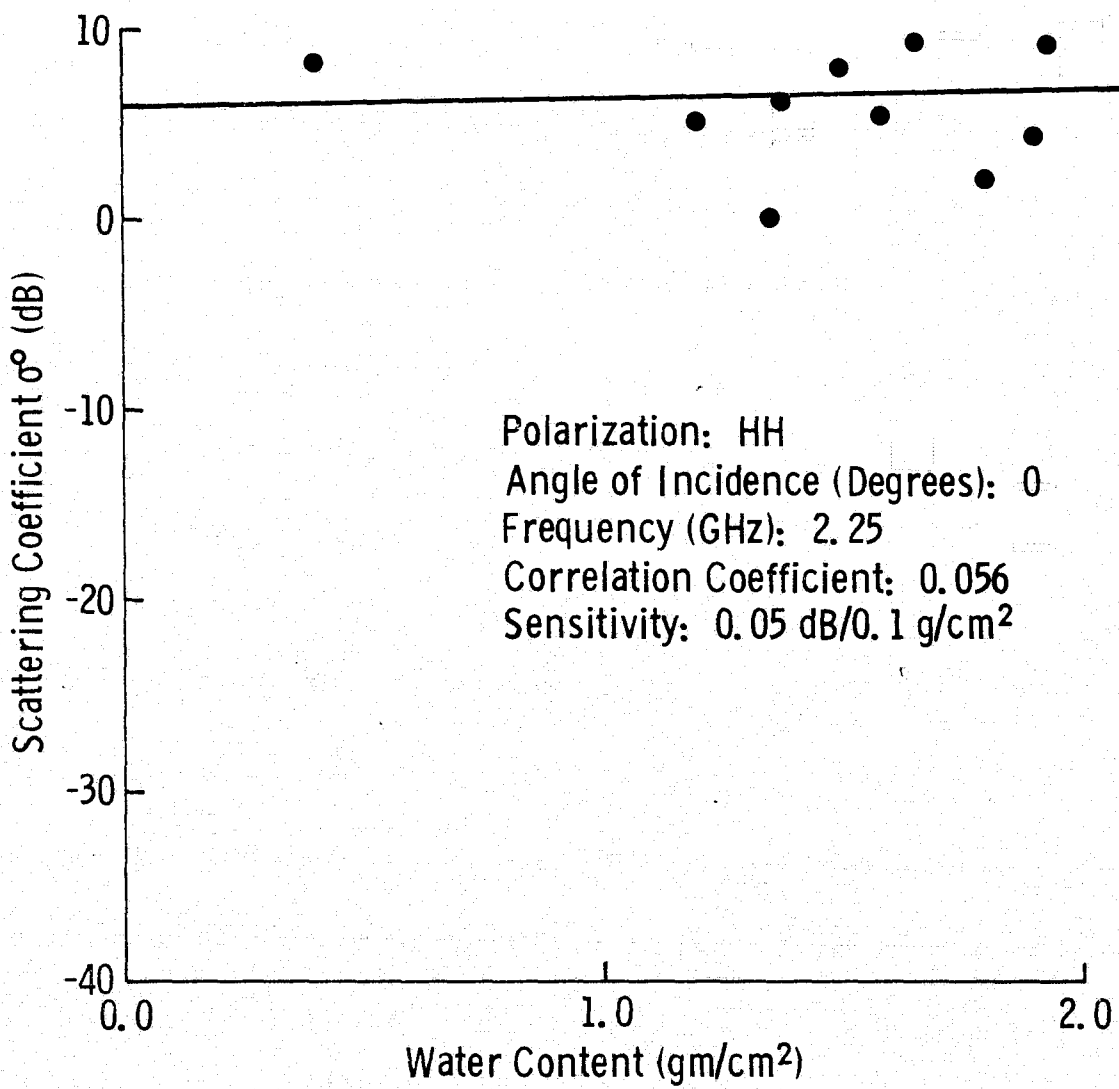


Figure 37a. Response of σ^0 to Total Snow Water Content per Unit Area.

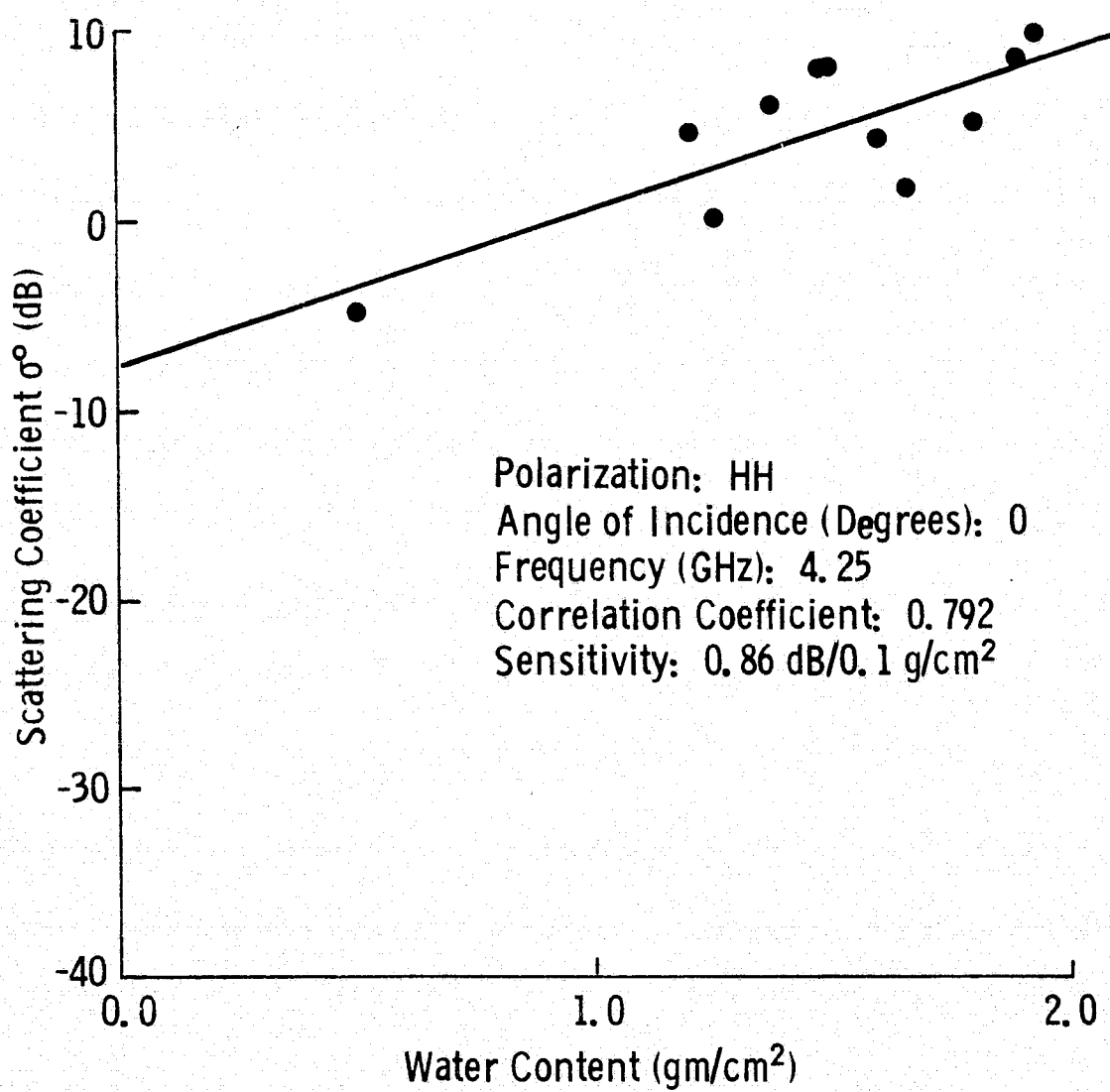


Figure 37b. Response of σ^0 to Total Snow Water Content per Unit Area.

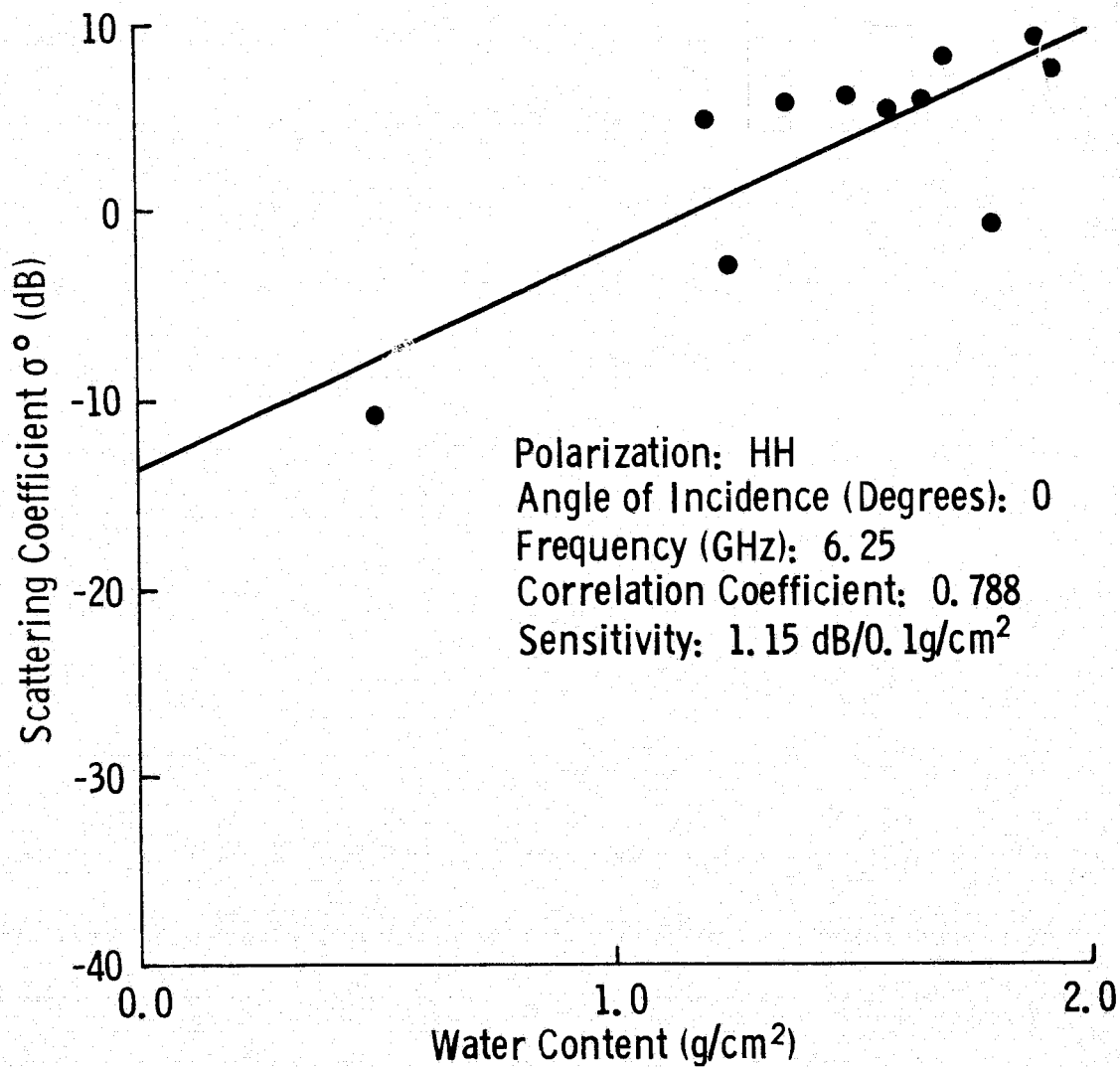


Figure 37c. Response of σ° to Total Snow Water Content per Unit Area.

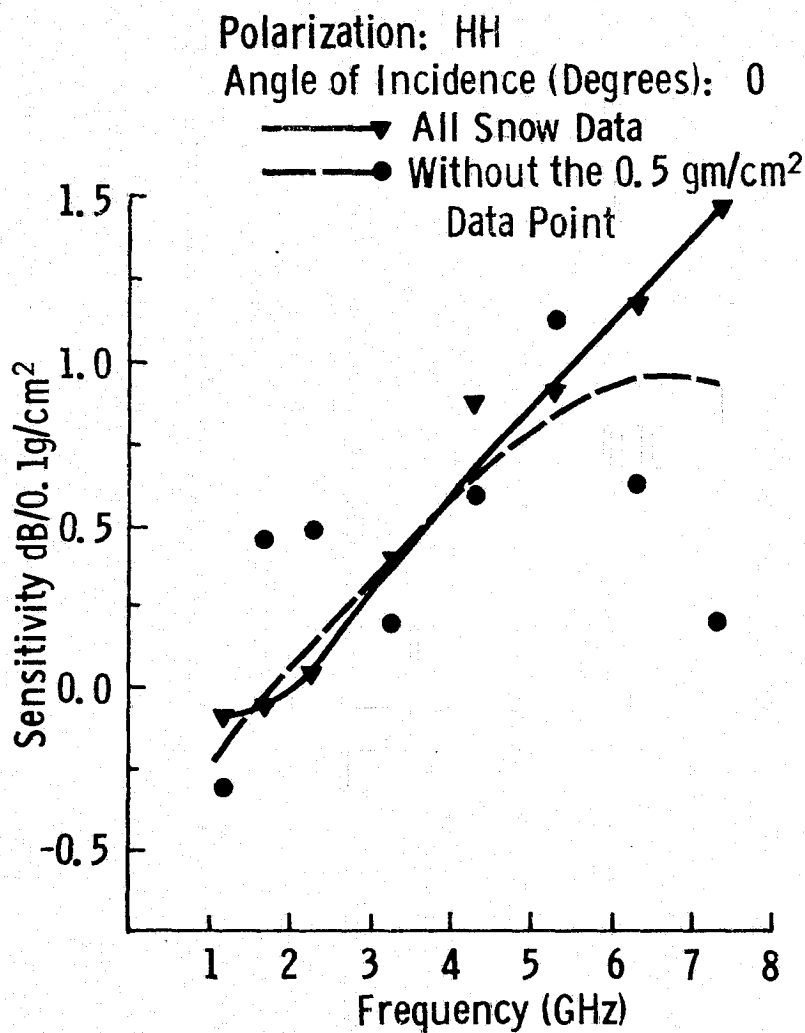
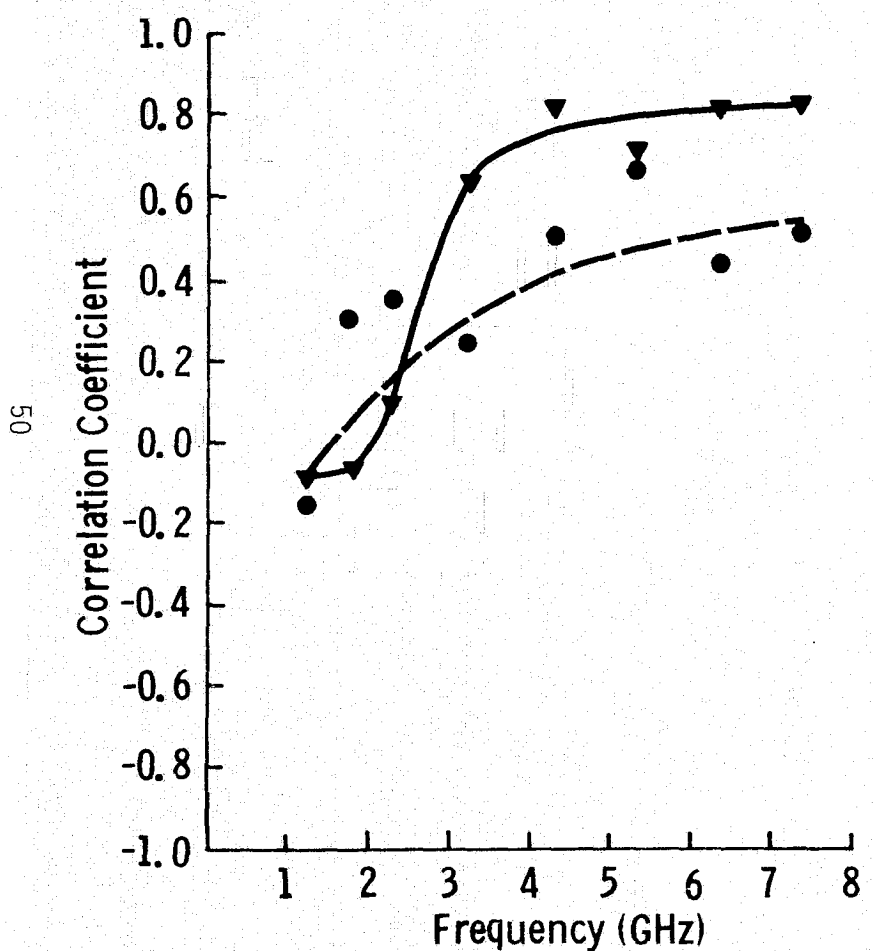


Figure 38. Correlation Coefficient and Sensitivity of σ^0 to Total Snow Water Content per Unit Area At 0° Angle of Incidence Versus Frequency, Both With and Without the 0.5 gm/cm^2 Snow Water Data Set.

To illustrate the radar response at the higher angle of incidence range, the 70° HH-polarized scattering coefficient data are plotted as a function of m_t in Figure 39. The slope is negative at all three frequencies and is less sensitive to frequency than the nadir case.

To summarize the σ^0 response to m_t , the calculated sensitivity (slope in dB/.1 g/cm²) and associated linear correlation coefficient are presented as a function of frequency at selected angles of incidence for HH, HV and VV polarizations in Figures 40-42 and as a function of angles of incidence at selected frequencies in Figures 43-45. Based on these families of curves, the following general remarks are made:

- a) Increasing frequency results in improved correlation coefficient and sensitivity of σ^0 to m_t .
- b) The sensitivity of σ^0 to m_t is almost angle independent for angles of incidence higher than 30°, particularly at the higher frequencies.
- c) Among the three polarizations, HH and VV show comparable σ^0 response to m_t , while HV is generally inferior in terms of sensitivity and correlation coefficient.

7.0 CONCLUSIONS AND RECOMMENDATIONS

Snow total water content, m_t , is one of the most important parameters in hydrological applications. The preliminary results of this study indicate that radar has the potential for mapping snow water content as evidenced by the observed sensitivity of σ^0 to m_t . Although the magnitude of the correlation coefficient between σ^0 and m_t seldom exceeded 0.8, the results are very encouraging if consideration is given to the inherent limitations of the experiment, which were: a) the limited number of snow data sets, b) the limited range of snow depth and total water content encountered and c) the unavailability of snow liquid water content data. It is recommended that:

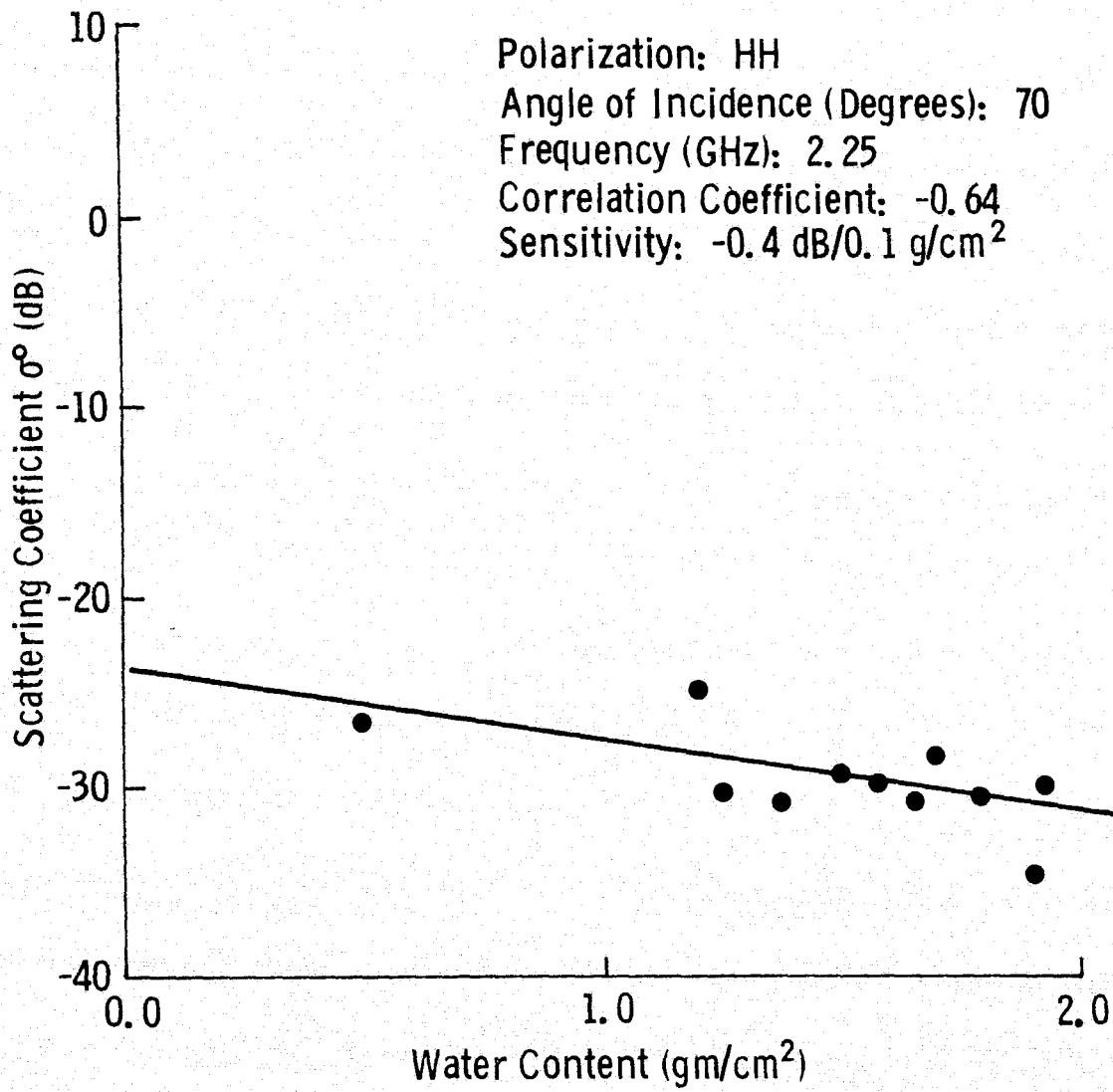


Figure 39a. Response of σ^0 to Total Snow Water Content per Unit Area.

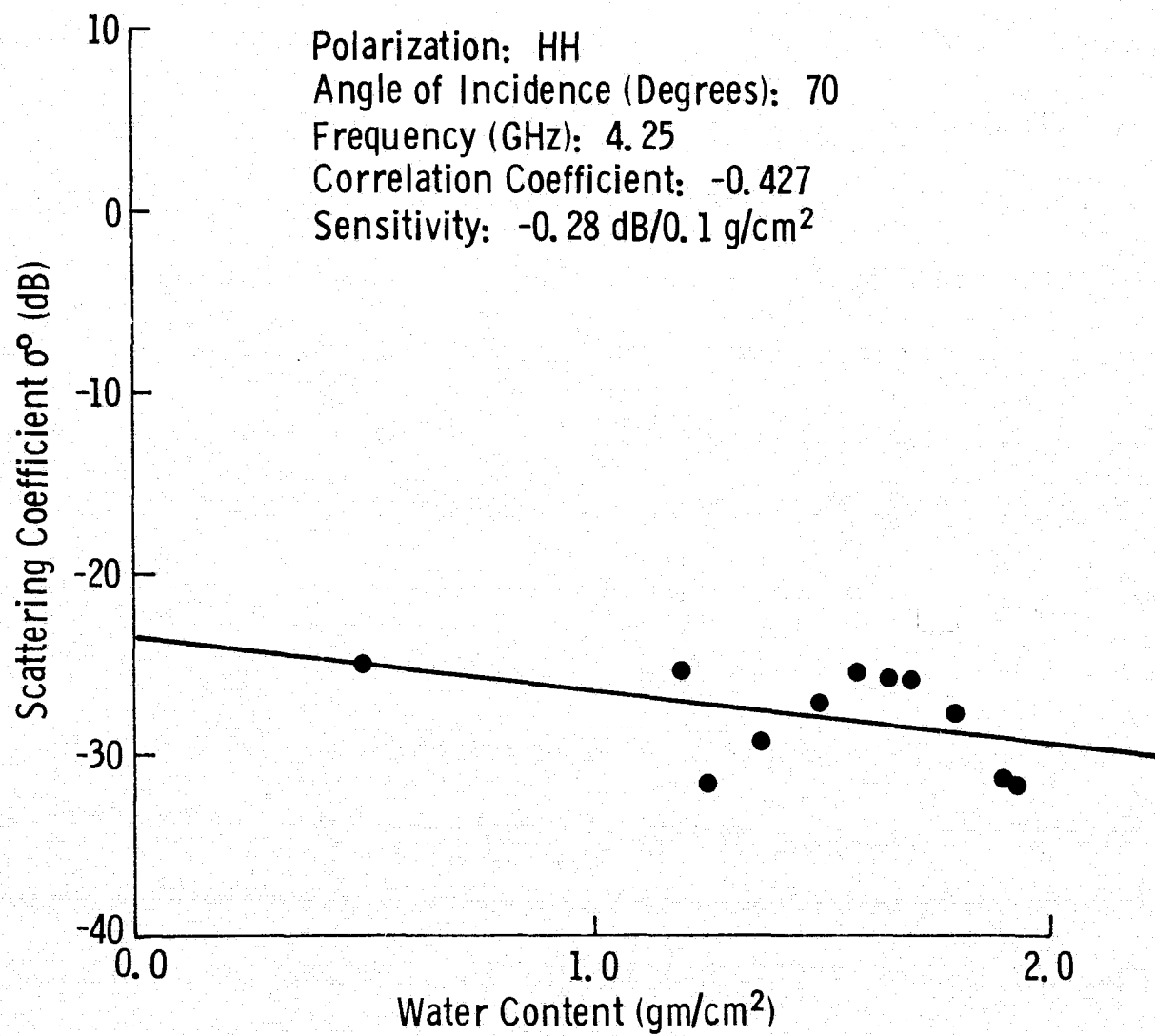


Figure 39b. Response of σ^0 to Total Snow Water Content per Unit Area.

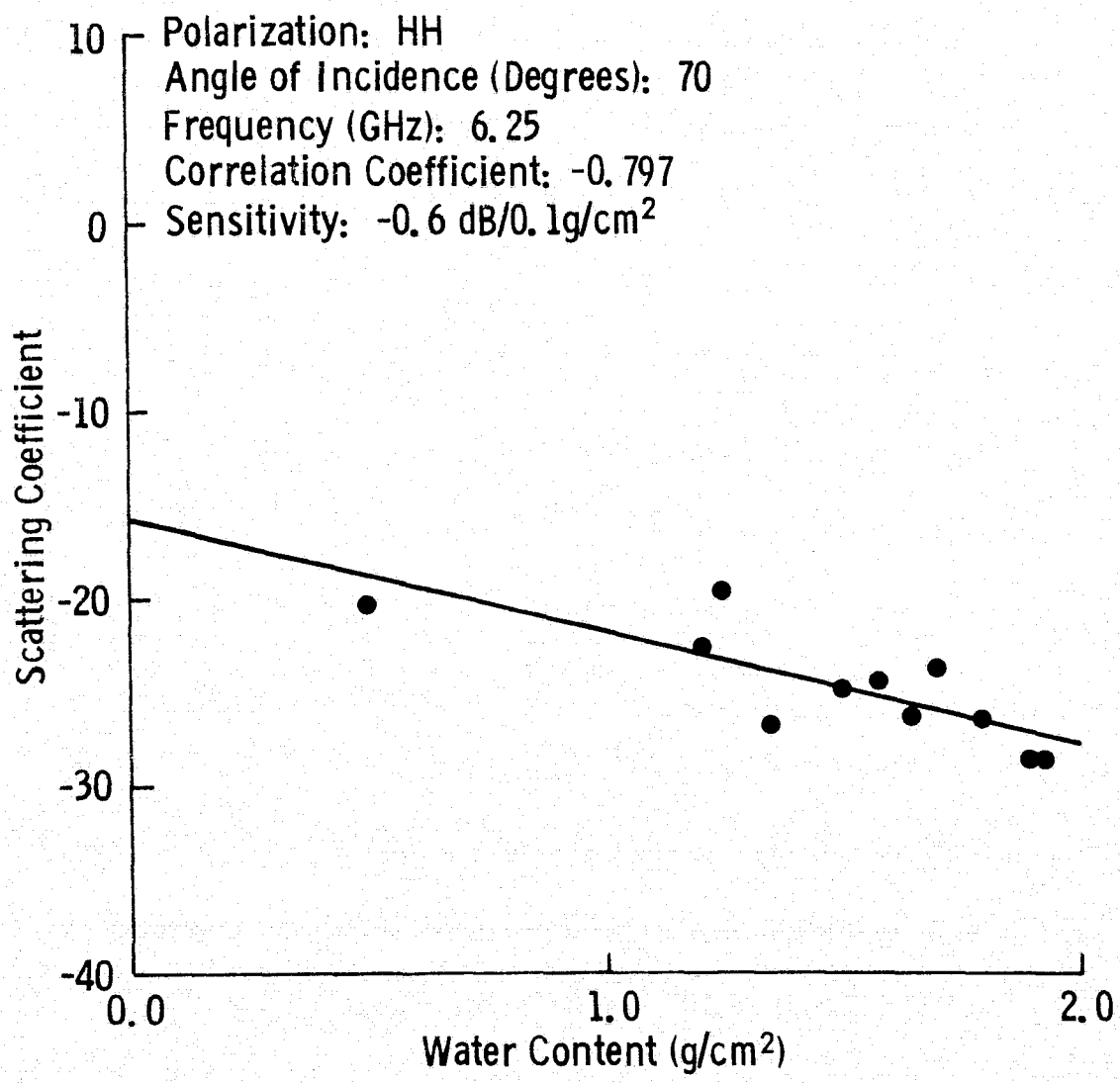


Figure 39c. Response of σ^0 to Total Snow Water Content per Unit Area.

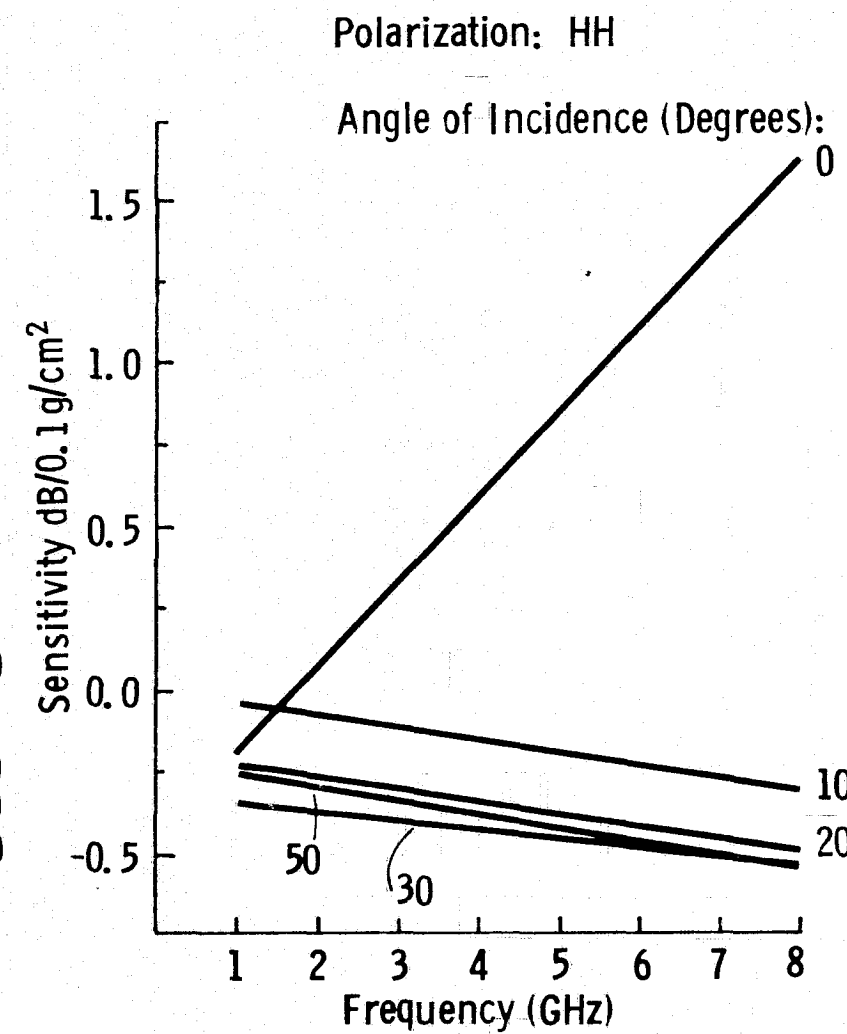
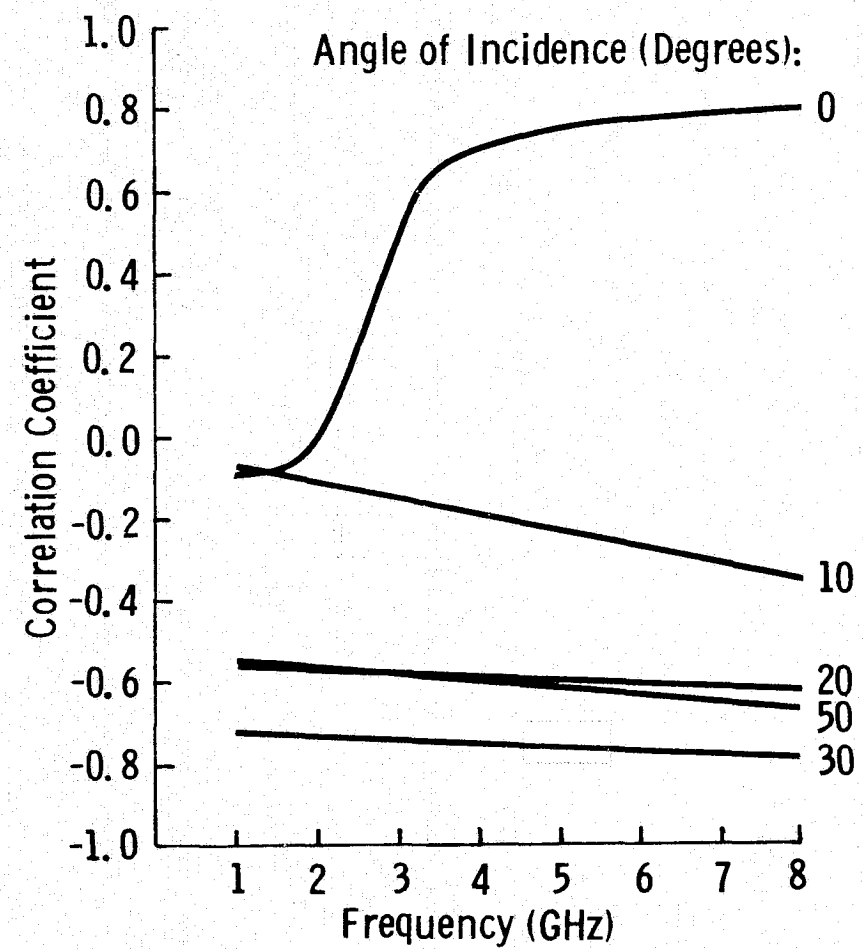


Figure 40. Correlation Coefficient and Sensitivity of σ^0 to Total Snow Water Content per Unit Area for HH Polarization versus Frequency.

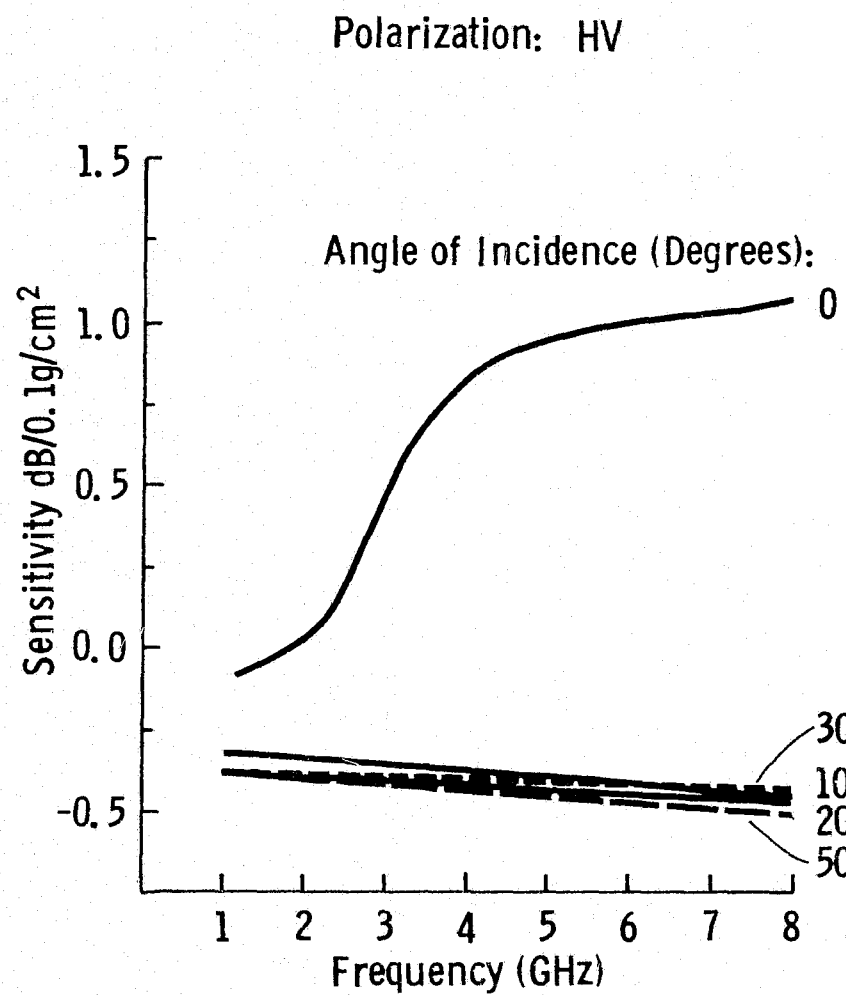
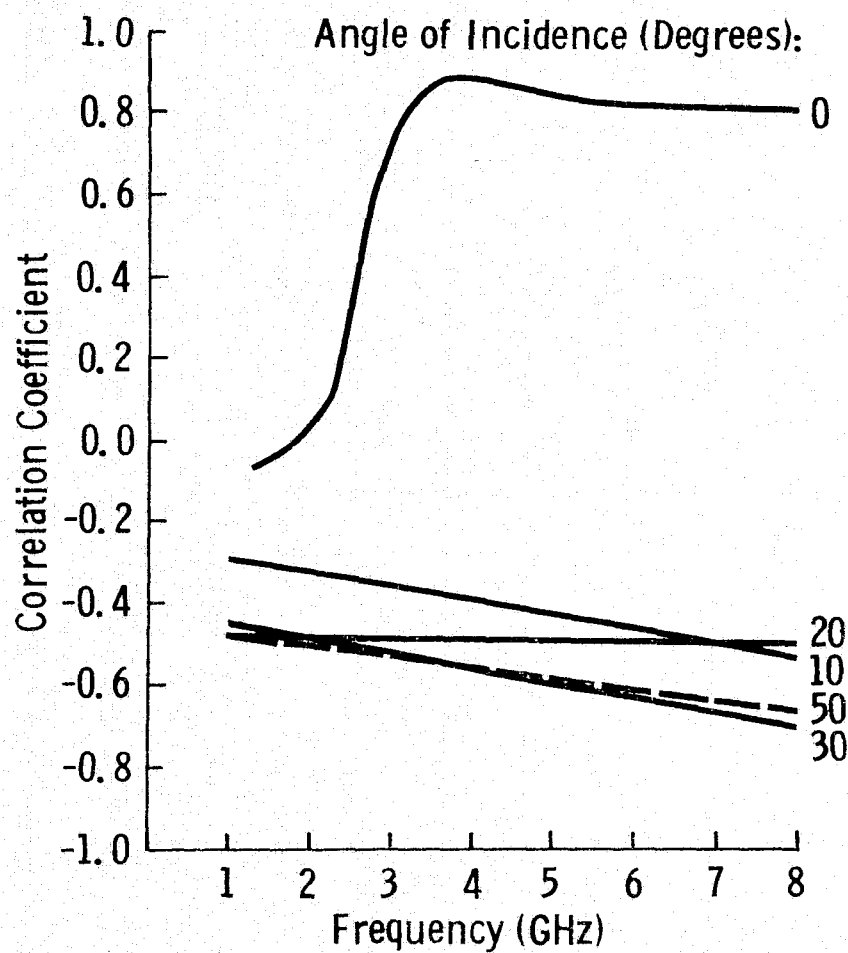


Figure 41. Correlation Coefficient and Sensitivity of σ^0 to Total Snow Water Content per Unit Area for HV Polarization versus Frequency.

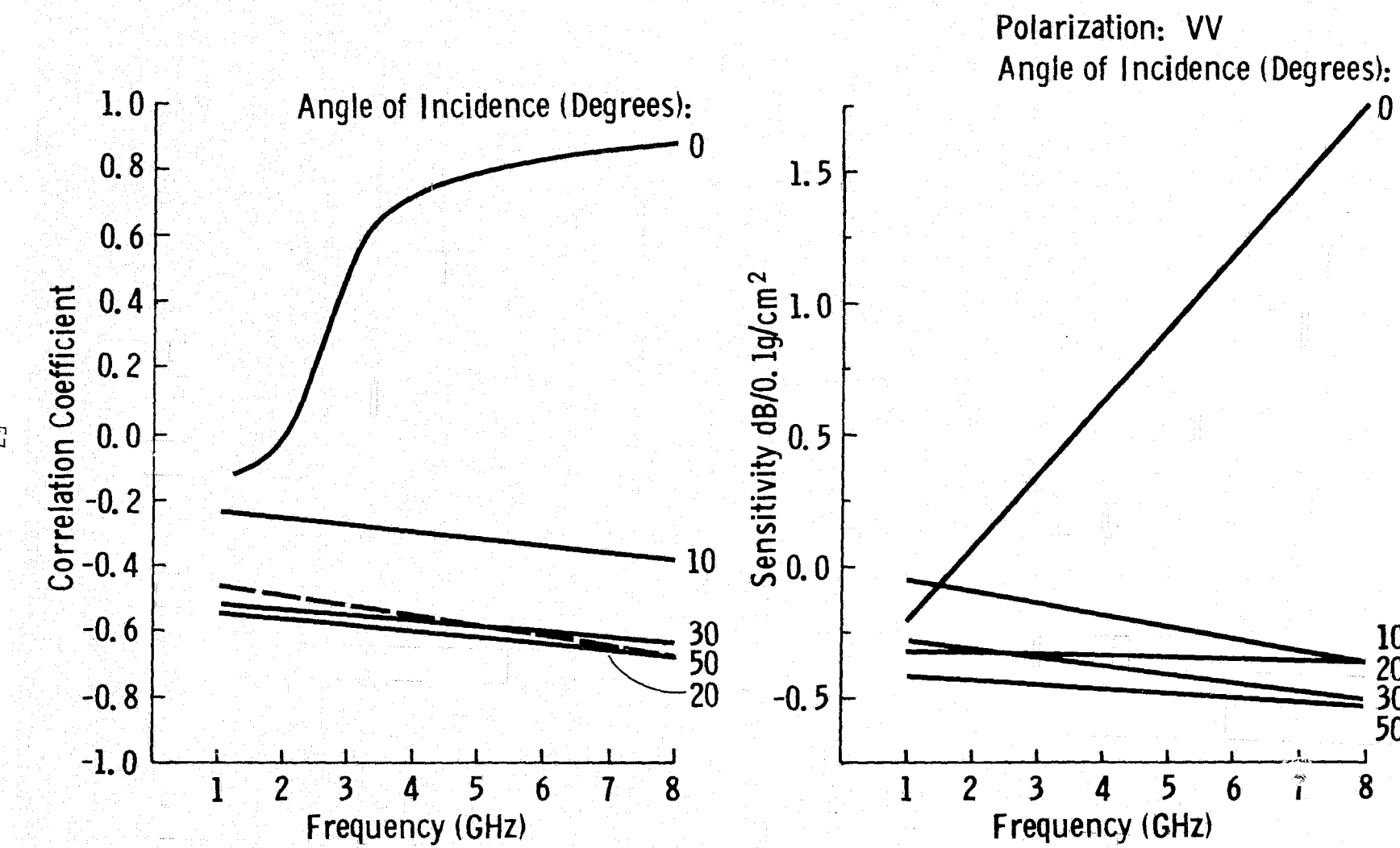


Figure 42. Correlation Coefficient and Sensitivity of 0° to Total Snow Water Content per Unit Area for VV Polarization versus Frequency.

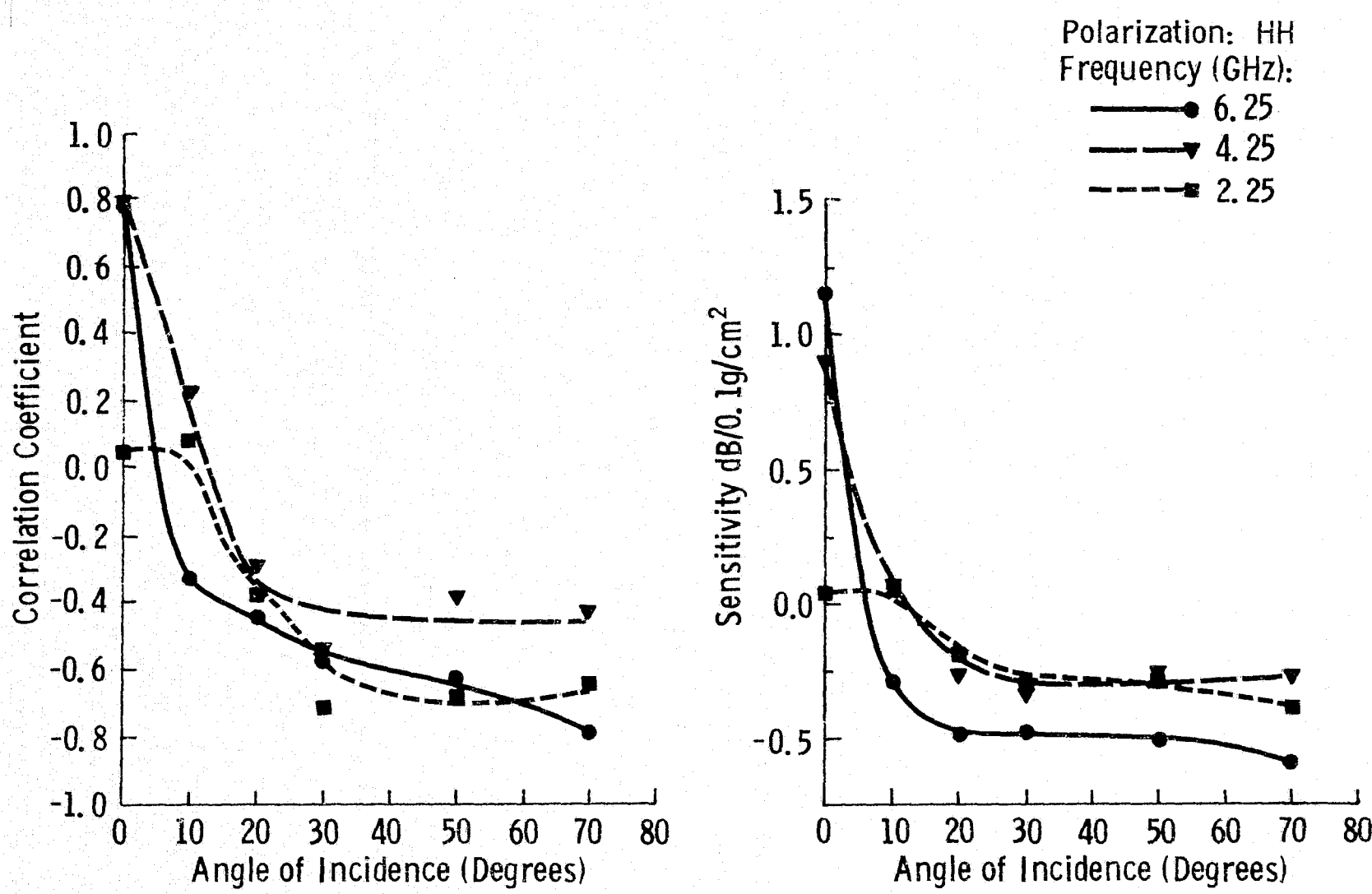


Figure 43. Correlation Coefficient and Sensitivity of 0° to Total Snow Water Content per Unit Area for HH Polarization versus Angle of Incidence.

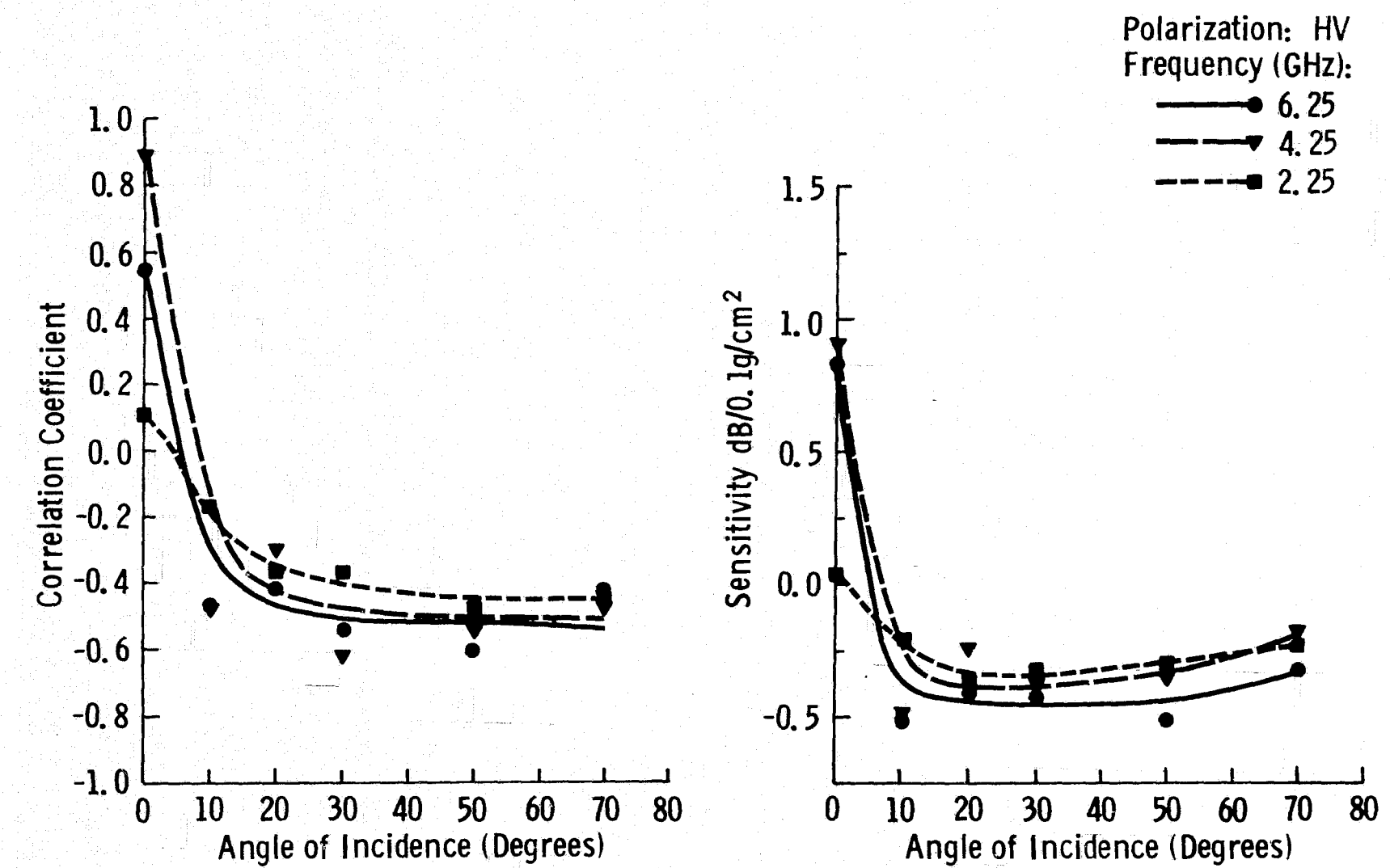


Figure 44. Correlation Coefficient and Sensitivity of σ^0 to Total Snow Water Content per Unit Area for HV Polarization versus Angle of Incidence.

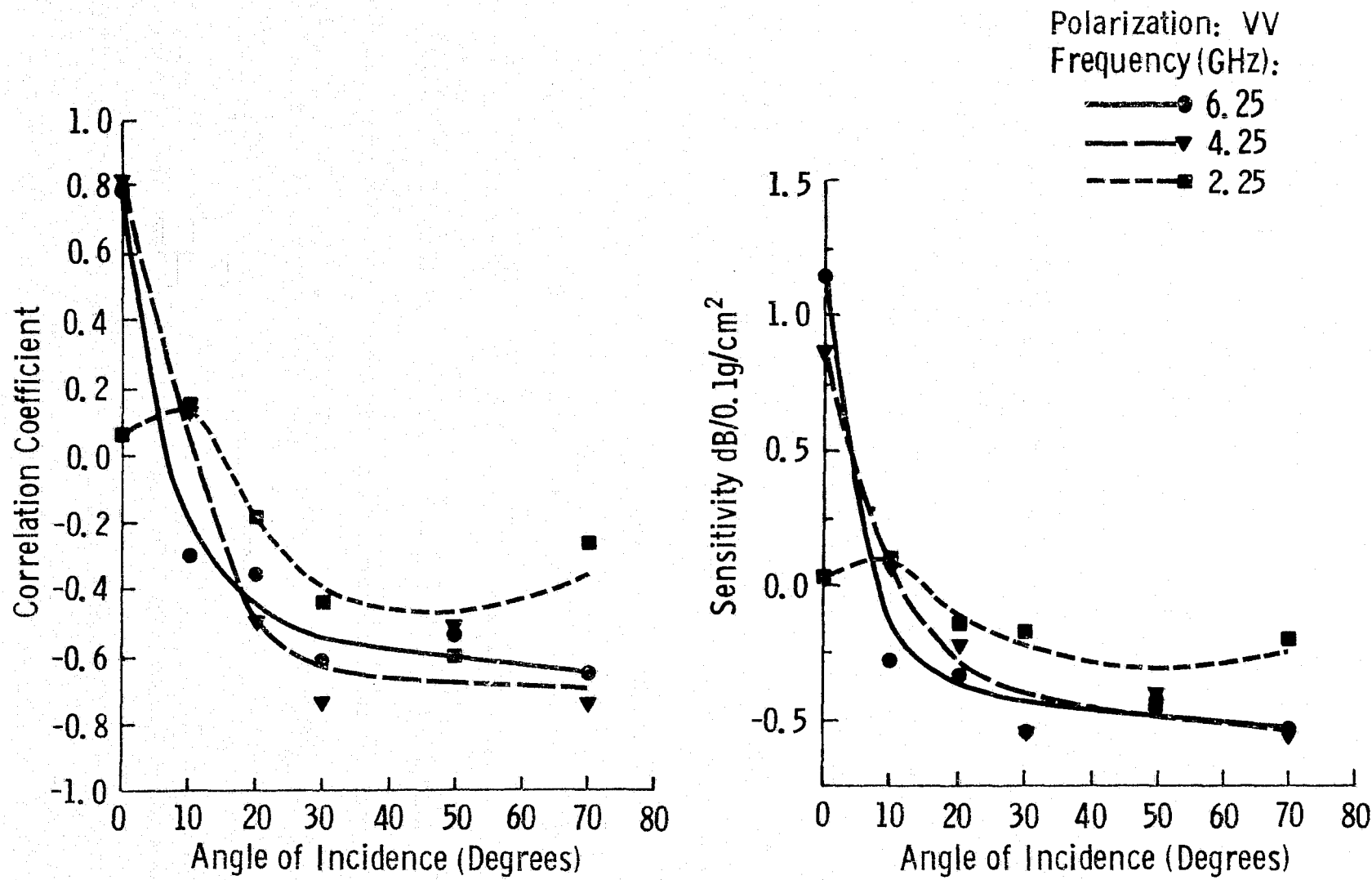


Figure 45. Correlation Coefficient and Sensitivity of σ^0 to Total Snow Water Content per Unit Area for VV Polarization versus Angle of Incidence.

- a) In future experiments, the test site should be chosen to guarantee heavy snow falls, long snow-cover periods and a wide range of snow depths.
- b) The 8-18 GHz MAS system be used since the sensitivity of σ^0 to m_t generally increases with frequency, as indicated by the present study.
- c) In addition to the ground-truth procedure employed by the present study, the snow liquid water content should also be measured.

REFERENCES

- [1] Linlor, W. I., F. D. Clapp, M. F. Meier and J. L. Smith, "Snow Wetness Measurements for Melt Forecasting," NASA Workshop, Operational Appl. of Satellite Snow Cover Observations, S. Lake Tahoe, Calif., 1975.
- [2] Chow, Ven Te, Editor, Handbook of Applied Hydrology, McGraw-Hill, New York, N.Y., 1964.
- [3] Lundien, J. R., "Terrain Analysis by Electromagnetic Means, Report 2, Radar Responses to Laboratory Prepared Soil Samples," U.S. Army Engineer Waterways Expt. Sta. Tech. Rept. 3-693, Vicksburg, Mississippi, pp. 1-55, September, 1966.
- [4] Batlivala, P. P. and F. T. Ulaby, "Effects of Roughness on the Radar Response to Soil Moisture of Bare Ground," RSL Technical Report 264-5, University of Kansas Center for Research, Inc., Lawrence, Kansas, September, 1975.
- [5] de Loor, G. P. and A. A. Jurriens, "The Radar Backscatter from Vegetation," AGARD Conf. Proc. No. 90 on Propagation Limitations on Remote Sensing, NATO, 1971.
- [6] Ulaby, F. T., "Radar Response to Vegetation," IEEE Trans. on Antennas and Propagation, v. AP-23, n. 1, pp. 36-45, January, 1975.
- [7] Cosgriff, R. L., W. H. Peake and R. C. Taylor, "Terrain Scattering Properties for Sensor System Design (Terrain Handbook II)," Ohio State University Experiment Station, 1960.
- [8] Vickers, R. S., "Airborne Profiling of Ice Thickness Using a Short Pulse Radar," NASA TM-X-71481.
- [9] Page, D. F., G. O. Venier and F. R. Cross, "Snow and Ice Depth Measurements by High Range Resolution Radar," Aeronautics and Space Journal, v. 19, n. 10, December, 1973.
- [10] Page, D. F., "Application of Radar Techniques to Ice and Snow Studies," Journal of Glaciology, v. 15, n. 75, 1975.
- [11] Parashar, S., "Investigation of Radar Discrimination of Sea Ice," RSL Technical Report 185-13, University of Kansas Center for Research, Inc., Lawrence, Kansas, November, 1973.
- [12] Sellmann, P. V., "use of Side Looking Airborne Radar to Determine Lake Depth on the Alaskan North Slope," Cold Regions Research and Engineering Laboratory, Report 230, May, 1975.
- [13] Bryan, M. L., "The Study of Fresh-Water Lake Ice Using Multiplexed Imaging Radar," Journal of Glaciology, v. 14, n. 72, 1975.

- [14] Vickers, R. S. and G. C. Rose, "High Resolution Measurements of Snowpack Stratigraphy Using a Short Pulse Radar," Proc. Eighth Intl. Symp. on Remote Sensing of Environment, University of Michigan, Ann Arbor, 1972.
- [15] Waite, W. P. and H. C. MacDonald, "Snowfield Mapping with K-band Radar," Remote Sensing of Environment, v. 1, pp. 143-150, 1970.
- [16] Linlor, W. I., "Snowpack Water Content by Remote Sensing," Intl. Symp. on Role of Snow and Ice in Hydrology, UNESCO-WMO, Banff, Canada, September, 6-20, 1972.
- [17] Edgerton, A T., A. Stogryn and G. Poe, "Microwave Radiometric Investigations of Snowpacks," Final Report for USGS, Aerojet General Corporation, El Monte, California, July, 1971.
- [18] Stogryn, A., "Equations for Calculating the Dielectric Constant of Saline Water," IEEE Trans. on Microwave Theory and Techniques, v. MTT-19, n. 8, August, 1971.
- [19] Cumming, W., "The Dielectric Properties of Ice and Snow at 3.2 Centimeters," Journal of Applied Physics, v. 23, 1952.
- [20] Evans, S., "Dielectric Properties of Ice and Snow, A Review," Journal of Glaciology, v. 5, p. 773, 1965.
- [21] Cihlar, J. and F. T. Ulaby, "Dielectric Properties of Soils as a Function of Soil Moisture Content," RSL Technical Report 177-47, University of Kansas Center for Research, Inc., Lawrence, Kansas, November, 1974.
- [22] Weiner, O., "Zur Theorie der Refraktionskonstanter, Berichte über die Verhandlungen der Königlich Sachsischen Gesellschaft der Wissenschaften zu Leipzig, Mathematisch-physikalische Klasse, Bd. 62, Ht. 5, pp. 256-268, 1910.
- [23] Ambach, W., "Zur Bestimmung des Schmelzwassergehaltes des Schnees durch dielektrische Messungen," Zeitschrift für Gletscherkunde und Glazialgeologie, Bd. 4, Ht. 1-2, pp. 1-8.
- [24] Linlor, W. I., J. L. Smith, M. F. Meier, F. C. Clapp and D. Angelakos, "Measurement of Snowpack Wetness," Proc. 43rd Annual Western Snow Conference, April 23-25, 1975, San Diego, California.

APPENDIX A: GROUND TRUTH DATA

The following discussion concerns the ground data taken for the freeze/thaw snow experiment from February 21 to April 23, 1975, in conjunction with measurements obtained during the same time period using the 1 GHz to 8 GHz microwave spectrometer.

The test plot for the experiment was located immediately north of the parking area on the west side of Nichols Hall. The areal extent of the test area was governed by system constraints, the initial (and minimal) size being approximately 30 feet wide by 60 feet long. This was later extended to 35 feet by approximately 180 feet.

The ground cover which has a considerable effect on the freeze/thaw rate of the underlying soil, consisted of maintained Little Blue Stem grass. Since the experiment was undertaken during the winter dormancy period, its height and physical condition remained constant throughout the data gathering period, except during the time period of April 4, Run #30 through April 23, Run #34, when grass height, physical condition, etc. were constantly changing parameters.

Another important parameter monitored was soil moisture. Soil samples were removed and analyzed in the lab for percent moisture by weight. An ice coring unit with a PVC plastic insert was utilized to remove a column of soil. The insert measured approximately 15 cm long by 4.4 cm in diameter; thus the maximum soil removed per sample consisted of a cylindrical plug of the above measurements. Metal soil sample containers were used to remove soil plugs at shallow depths. For samples at greater depths or for individual layer analysis within a given sample, a soil sampling tool was employed. The samples were removed, transported to the lab, weighed, dried 24 hours at 105° in the drying oven, reweighed and the percent water calculated from the formula:

$$\frac{S_w - S_d}{S_d} \times 100$$

where S_w is the weight of the wet soil and S_d is the weight of the dry soil.

Ground temperature was monitored electronically using buried thermistor-type thermometers spaced at 10 foot intervals (Figure 1a) and placed at varying depths beneath the ground's surface (Figure 1b). The temperature recording device consisted of a battery operated, solid-state recorder with multi-probe input capability and with an accuracy of 1°C. The recording range varies from a low of -22°F to a high of

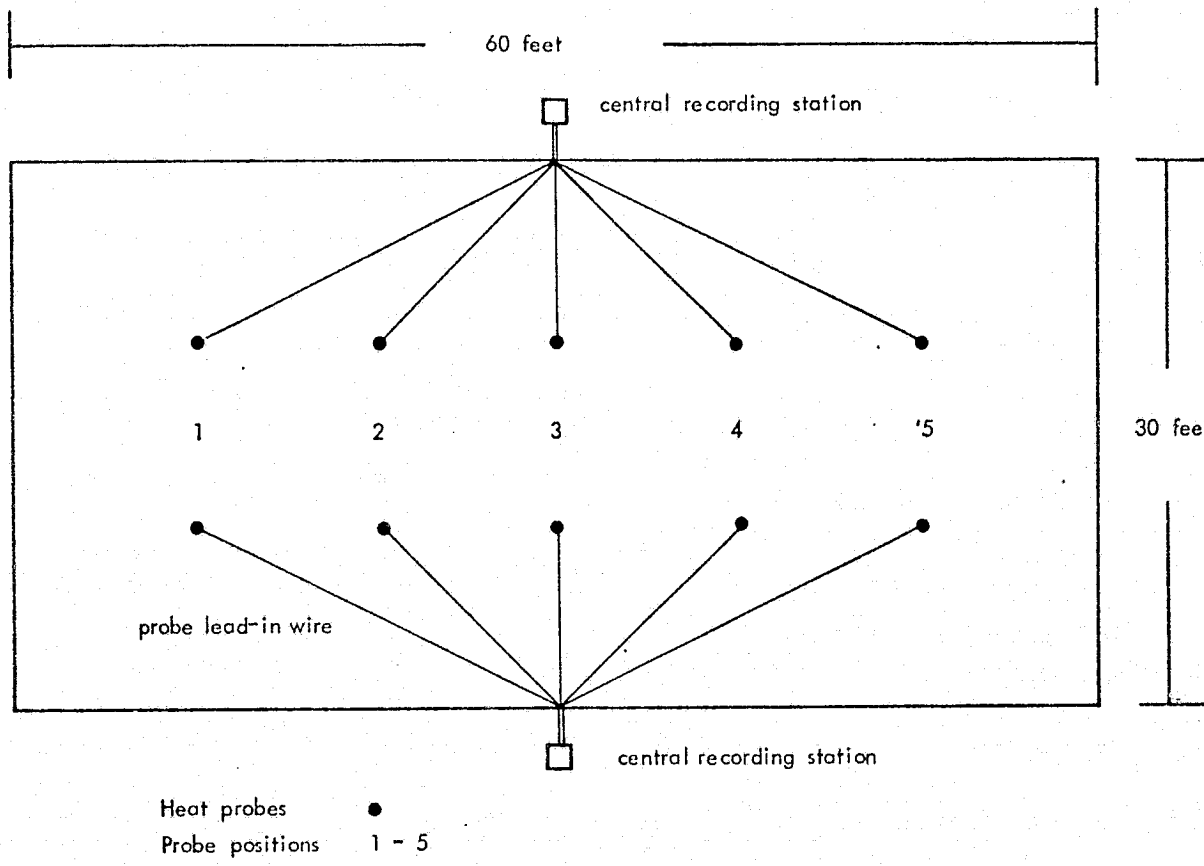


Figure 1a.

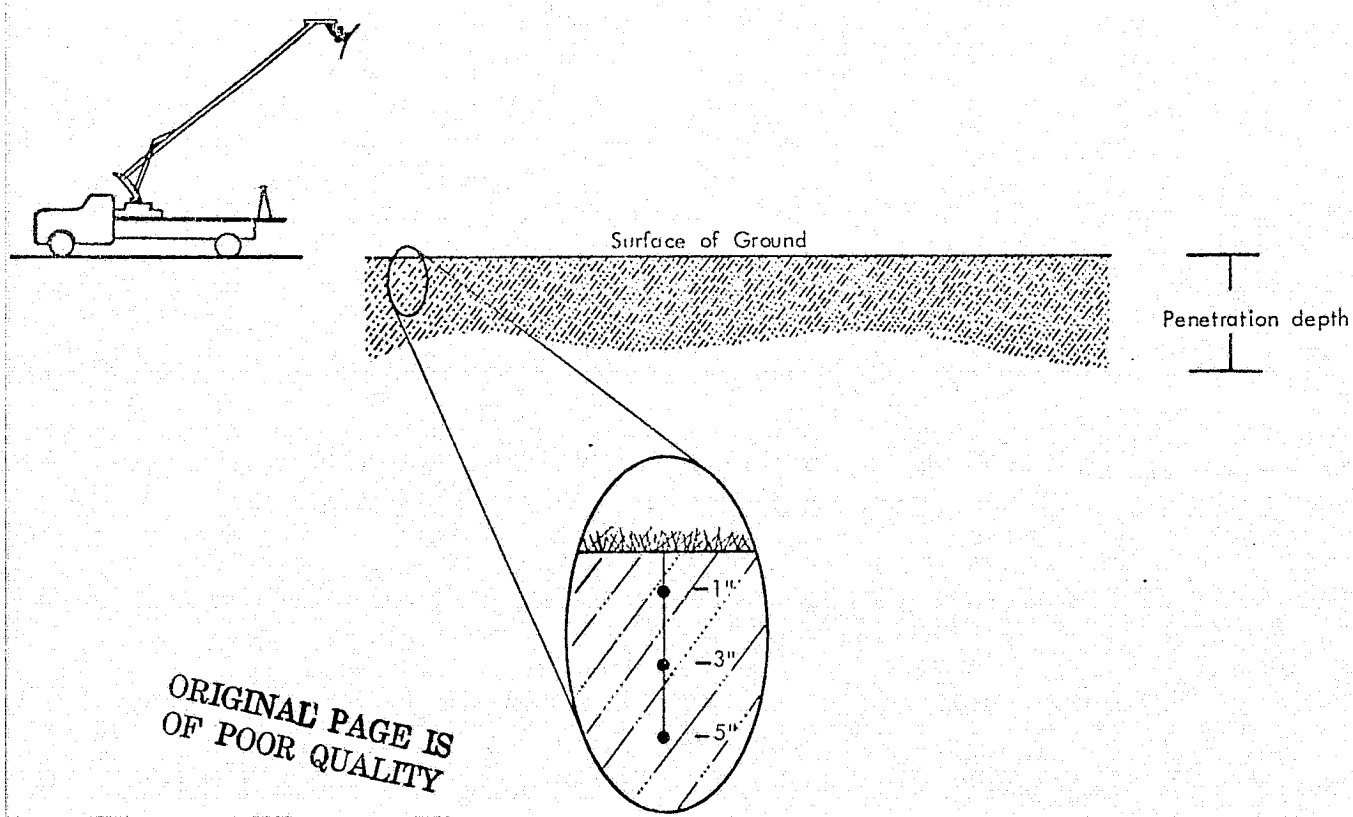


Figure 1b.

122° F with direct readings on either the Fahrenheit or the Centigrade scale. The temperature sensors are thermistor probes, 7/32" O.D., sealed in epoxy on the end of PVC coated leads. They are completely immersible and have a 7-second delay time for accurate readings.

The added capability of controlling the physical condition of the ground with respect to temperature was not put into operation since the weather conditions were such that the system was not needed.

During the brief periods in which snow covered the test plot, soil moisture and soil temperature were monitored plus snow characteristics such as its physical condition (grain structure, snowflake type, degree of layering/compaction), depth, plus the snow-water equivalency were calculated. The latter was determined by removing a given volume of snow, allowing it to melt, and measuring the resulting water. In addition to the above factors, the type of snowflake plus the history of the rainfall, and the degree of freezing and thawing were recorded.

Photographs, both 35 mm color slides and color prints, were utilized to augment the field notes. Field data including field notes recorded during each data set are listed in Table 1.

TABLE 1.

DATE	RUN	TIME	TEMP. soil	SOIL WATER CONTENT		COMMENTS	SNOW WATER EQUIV.	COMMENTS
				depth (cm)	percent			
3/3/75	03	0700	31.5	3.5	50.3	0°		
				3.5	49.2	10°		
				3.5	56.8	20°		
				3.5	50.0	40°		
				3.5	69.3	50°		
				3.5	65.4	60°		
				5.1	47.1	30°		
				1.3	90.3	30° Frozen layer		
				14.8	30.0	0° only		
				14.8	27.9	20°		
				14.8	27.8	30°		
				14.3	29.2	40°		
3/3/75	04	1500	36.0	3.5	42.0	0°		
				3.5	38.0	10°		
				3.5	43.5	20°		
				3.5	51.0	30°		
				3.5	40.1	40°		
				3.5	46.4	60°		
				15.0	30.4	30°		
3/4/75	05	0800	32.0	3.5	38.6	0°		
				3.5	39.5	10°		
				3.5	41.7	20°		
				3.5	43.6	40°		
				1.3	69.4	60° Frozen layer		
				12.7	33.3	20° only		
				12.7	33.1	40°		
				13.3	32.4	60°		
				3.5	36.7	0°	samples taken peripheral to test plot	1100 hrs 1300 hrs 1300 hrs 1330 hrs 1330 hrs
				3.5	34.3	30°		
				3.5	35.9	60°		
				14.0	33.0	40°		
3/11/75	07	0730	33.5	3.5	35.3	0°	12.7	10.2
				3.5	34.9	40°	12.7	9.5
				14.0	33.1	0°	11.43	10.8
				15.2	35.7	40°	11.43	10.9
3/11/75	08	1340	34.0	13.9	33.0	0°	11.43	14.5
				15.0	34.1	40°	12.70	14.1
							1.91	30.0
							1.91	25.0
							0.64	56.2
							1.27	31.1

• average

DATE	RUN	TIME	TEMP. soil	SOIL WATER CONTENT • depth (cm)	percent	COMMENTS	SNOW WATER EQUIV. • depth (cm)	percent	COMMENTS
3/12/75	09	1110	34.0	13.4	29.7	40°	0.64 10.80 1.27 11.11	66.4 12.6 34.8 11.8	1600 hrs; remaining distance
							0.64 8.89	74.5 16.1	Sleet layer; 1130 hrs Remaining snow; 1130 hrs Layer beneath sleet; 1400 hrs Snow; 1400 hrs
							0.64	65.0	Sleet; 1500 hrs
							0.96 8.89	42.4 14.7	Snow; 1500 hrs
3/13/75	10	0930	33.0	14.0	33.8	40°	0.64 8.89	54.9 14.1	Crust; 0930 hrs Remaining snow; 0930 hrs
							0.64 8.89	1200 hrs; Crust 1200 hrs; Snow	1200 hrs; Crust 1200 hrs; Snow
3/13/75	11	1600	33.5	12.7 13.4	35.2 35.6	0° 40°	0.96 10.80	40.2 11.1	Crust; 1600 hrs Snow; 1600 hrs
3/14/75	12	0900	31.5	14.6 14.6	33.8 38.7	0° 40°	0.80 8.90 0.64 7.62	49.1 15.3 54.2 17.3	Crust; 0930 hrs Snow; 0930 hrs Crust; 1215 hrs Snow; 1215 hrs
3/14/75	13	1430	32.5	14.6	31.6	40°	0.56 6.99	70.4 22.0	Crust; 1500 hrs Snow; 1500 hrs
3/15/75	14	0700	30.5	15.2	31.4	40°	0.56 6.35	41.8 20.0	Crust; 0900 hrs Snow; 0900 hrs
3/16/75	15	1300	33.5	13.9 14.6 15.2 3.5 3.5 3.5 3.5	44.7 39.2 39.3 64.7 55.7 47.7 55.2	0° 50° 70° 10° 40° 50° 70°	3.18	37.9	Snow; 1330 hrs
3/17/75	16	1000	33.5	3.5 3.5 3.5 3.5 3.5	56.7 52.8 49.6 51.2 47.6	10° 20° 30° 50° 70°			

* average

DATE	RUN	TIME	*TEMP. soil	SOIL WATER CONTENT		COMMENTS	SNOW WATER EQUIV.	COMMENTS
				* depth (cm)	* percent			
				1.91	69.0	70°, surface		No snow
				13.3	35.3	10°		
				15.8	33.9	20°		
				15.8	36.5	30°		
				15.8	36.0	50°		
				15.2	35.6	70°		
3/18/75	17	1330	45.0	3.5	41.3	10°		
				3.5	24.9	30°		
				3.5	67.7	60°		
				13.9	34.0	30°		
				15.2	38.6	60°		
				16.2	31.4	10°		
3/19/75	18	1500	50.0	3.5	45.1	10°		
				3.5	51.4	30°		
				3.5	46.4	60°		
				*14.0	33.7	10°		
				*14.0	34.2	30°		
				*14.0	35.0	60°		
3/20/75	19	1300	51.6	3.5	41.7	10°		
				3.5	45.7	20°		
				3.5	45.5	30°		
				13.9	39.9	10°		
				15.2	35.6			
				15.2	33.5	30°		
3/21/75	20	1400	Thawed	3.5	43.0	0°		
				3.5	41.0	30°		
				3.5	44.0	50°		
				15.2	34.5	0°		
				15.8	32.9	30°		
				15.2	35.2	50°		
3/24/75	21	1400	33.5	3.5	38.5	0°		
				3.5	36.4	30°		
				3.5	38.8	50°		
				15.5	33.6	0°		
				10.8	31.9	30°		
				15.2	30.4	50°		
3/28/75	22	1100	36.0	2.54	71.8	Surface zone		
				3.5	68.2	0°		
				3.5	54.8	30°		
				3.5	55.7	50°		
				3.5	45.9	70°		
				15.2	40.4	0°		
				15.8	35.1	30°		
				15.8	34.6	50°		
				16.5	39.0	70°		

* average

Snow intermit-
tent; no ac-
cumulation

DATE	RUN	TIME	TEMP. soil	SOIL WATER CONTENT * depth (cm)	* percent	COMMENTS	SNOW WATER EQUIV. * depth (cm)	COMMENTS
3/30/75	23	0800	31.5	3.5 3.5 3.5 3.5 3.5 3.5 14.6 15.2 14.6 15.2 14.9 14.6	74.0 38.6 83.2 83.3 70.7 68.5 37.4 35.0 37.0 38.9 20.7 56.4	0° 10° 20° 30° 50° 70° 0° 10° 20° 30° 50° 70°	Upper 1cm of ground frozen	
3/30/75	24	1700	40.0	2.54 2.54 2.54 2.54 2.54 2.54 2.54 --- --- --- --- ---	43.6 51.4 38.2 47.8 48.2 39.6 44.7 32.2 30.5 32.4 31.4 31.0	0° 10° 20° 30° 40° 50° 0° 0 cm -10.1 cm 0 cm -10.1 cm 0 cm -10.1 cm 0 cm -10.1 cm 0 cm -10.1 cm		No snow
4/1/75	25	1400	43.0	3.0 3.0 3.0 3.0 3.0 3.0 3.0 10.0 10.0 10.0 10.0 10.0 10.0 13.0 14.0 14.0	43.6 42.2 49.9 44.8 43.3 38.9 50.7 43.7 36.6 30.6 33.2 31.2 31.9 35.3 33.7 34.5 29.8	0° 10° 20° 30° 40° 50° 60° 70° 0° 10° 20° 30° 50° 70° 0° 30° 60°		
4/2/75	26	0830	34.0	3.0 3.0 3.0 13.0 14.0 14.0	51.5 53.1 54.4 42.1 35.3 34.9	0° 30° 60° 0° 30° 60°		Snow, sleet, freezing rain. No collection due to rapidly changing condi- tions

* average

DATE	RUN	TIME	TEMP. soil	SOIL WATER CONTENT		COMMENTS	SNOW WATER EQUIV.	COMMENTS
				depth (cm)	percent			
4/2/75	27	1415	34.0	3.0 3.0 3.0 13.0 14.0 14.0	51.7 53.6 54.3 42.6 35.4 34.8	0° 30° 60° 0° 30° 60°	2.0 24.9	At 1500 hrs conditions are rapidly changing.
4/3/75	28	0515	32.0	3.5 3.5 3.5 14.0 14.0 14.0	42.0 48.0 53.2 38.1 41.3 34.1	0° 30° 60° 0° 30° 60°	----No Data---	Snow depth about 5 cm.
4/3/75	29	1445	35.0	3.0 3.0 3.0 12.0 12.0 15.0 V A R I A B L E	50.8 54.0 53.6 42.8 46.7 41.7 39.0 30.8 29.8 36.1 36.8	0° 30° 60° 0° 30° 60° 3.0-9.0 9.0-16.0 16.0-23.0 23.0-30.0 30.0-44.0	30°	Snow very patchy; 1.5 cm in depth.
4/4/75	30	1300	43.5	3.3 3.3 3.3 3.3 3.3-17.0 3.3-18.0 3.3-18.5 3.3-17.0 18.5-34.5 34.5-41.5 3.0-9.0 9.0-20.0 20.0-31.0 17.0-34.5	52.8 38.1 47.8 42.5 34.8 32.2 32.8 34.1 34.8 34.2 34.9 32.6 33.3 29.9	0° 30° 50° 70° 0° 30° 50° 70° 50° 50° 30° 30° 30° 70°		No snow
4/11/75	31	UNK.	UNK.	0-5.0 5.0-9.5 9.5-14.5 14.5-19.5	31.3 24.0 28.4 26.7	0°		No snow

* average

DATE	RUN	TIME	TEMP. soil	SOIL WATER CONTENT * depth * percent (cm)	COMMENTS	SNOW WATER EQUIV. * depth * percent (cm)	COMMENTS
				0-5.0 30.0 5.0-10.0 25.7 10.0-15.5 26.1 15.5-21.5 24.1	40°		No snow
				0-3.0 32.5 3.0-6.0 26.5 6.0-10.0 23.7 10.0-14.0 21.8	70°		
4/15/75	32	1500	Thawed	0-3.0 39.6 3.0-9.0 27.6 0-3.0 41.6 2.0-9.0 30.3 0-3.0 43.3 3.0-9.0 30.8 0-11.0 35.4 11.0-22.0 31.5	0° 30° 60° 40°		No snow
4/21/75	33	1540	Thawed	0-3.0 30.4 3.0-9.0 27.9 0-3.0 25.7 3.0-9.0 25.0 9.0-19.0 27.5	0° 30°		No snow
4/23/75	34	UNK.	Thawed	0-3.0 38.6 3.0-9.0 27.8 0-3.0 57.9 3.0-9.0 45.5 0-3.0 38.9 3.0-9.0 27.1 9.0-20.0 26.5	0° 30° 60°		No snow
END OF	DATA	SETS					

* average

Run 03

3/3/75

Overnight low of 18.0°F.

Run 04

3/3/75

Began data set at 1500 hours; began sampling at 1600 hours.

Run 05

3/4/75

Began data collection of 0800 hours; samples 584, 597, and 575 are voided--
core unit broken.

Run 06

3/10/75

Began data set at 1200 hours; light powdery snow approximately 15 cm deep--
measured at B-box local, the type locale. Took B & W/color slide depicting depth
at 1100 hours with scale; at 1330 hours, snow still 15 cm thick at type area.

Run 07

3/11/75

Began data set at 0800 hours; air temperature, A(t), 27.0°F. Snow depth at type
area is 12.7 cm. At 0730 hours, cloudy and overcast; few dry snowflakes. Snow
depth 12.7 cm overall with approximately 0.95 cm light fluff with 11.75 cm
moderately packed; slides. Overall snow conditions, dry and powdery. Sublimation
is quite rapid this am; about 0.64 cm lost between 0700 and 0830 hours.

About 3.18 cm void space between soil surface and the bottom of the snow. 0830
hours, still about 0.95 cm dry fluff with 11.75 cm dry packed, no flurries, light
wind, overcast. Extremely light mist at 0900 hours.

Run 08

3/11/75

Began data set at 1340 hours. Approximately 5 minutes of rain then turning to sleet; #5-#10 photos. Sleet began at 1330 and became intense almost immediately; at 1440 sleet reverted to fine rain. Up to this point, sleet crystals had built up to approximately 0.64 cm over the snow layer; are distinct crystals coated with water. Sleet layer formed was welded quite solidly over moist (not soggy) snow layer of about 10.8 cm thick. Outside temperature at 1445 hours was about 33°F. At 1500 hours approximately 1.27 cm sleet and water covering had accumulated. At 1600 still light drizzle with sleet crystals still present and layer buildup to about 1.27 cm to 1.91 cm thick; below this layer remaining snow still relatively dry. Completed data at 1607 hours; at 1700 snow depth (total) at type area approximately 10.8 cm.

Run 09

3/12/75

Began data set at 1110 hours. Overnight low of 30°F, no rain, sleet, or snow during the night. Partly cloudy and $A(t)$ of 34°F; still hard sleet layer composed of well defined crystals, layer is dry; no observable moisture on the surface. Overall snow depth at type area is 10.16 cm; therefore lost depth due to compaction. Sleet layer still approximately 0.64 cm with 1.27 cm layer of snow immediately underneath possessing a slightly higher water content than the remaining cover though such a distinction may not be true. NW wind gusting to 25 mph. At 1345 hours took #2 and #3 (120 format) of snow depth--pictures attached. At 1400 hours, overcast, 34°F, wind gusts to about 20 mph, no precipitation, sleet layer shows no visible signs of free water coating the surface, snow depth at type area about 9.53 cm. Upon examination, sleet layer exhibits an undulating bottom surface with thicknesses ranging from 0.64 cm to 1.27 cm. Finished data set at 1415 hours.

Run 10

3/13/75

Began data set at 0915 hours. Overnight low of 13°F, clear skies, dry light NW wind (less than 5 mph). Snow depth (all measurements as to snow depth are assumed to be made at the type area unless otherwise indicated) approximately 8.89 cm; slide #22. Snow beneath frozen layer is very dry and powdery--not wet and sticky as yesterday pm.

Wind velocity at 1930 hours increased to about 10 mph (wind chill of -5°F). Frozen sleet layer same thickness, 0.64 cm to 1.27 cm thick with undulating bottom surface; no free water at surface of layer. At 0945 hours, wind speed increased to 15 mph. At 1200 hours, snow depth still 8.89 cm; snow still powdery in nature.

Run 11

3/13/75

Began data set at 1456 hours. Snow depth at 1515 is 8.89 cm of light powder beneath frozen sleet layer; no observable free surface water on the latter. At 1700 hours, wind speed approximately 15 mph from NW, clear skies, high of 38°F for the day.

Run 12

3/14/75

Began data set at 0900 hours. Overnight low on hill was 0°F ; temperature at 0830 was 2.5°F . Wind less than 5 mph. Snow condition, 8.89 cm deep; sleet layer about 0.64 cm to 0.95 cm thick with no visible signs of free surface water; underlying snow layer very dry--a loose powder. Obtained slides of snow surface depicting crenulated surface (#17-24). Skies are clear. At 0930 hours, very difficult to obtain samples (snow); values of dubious precision. Note: Sleet layer no longer distinct circular nodules; are small "snowflake structures" stuck vertically at the surface (#23). 1-2 oscillator problems at 1030 hours; resumed data accumulation at 1100 hours. 1215 hours, temperature of snow beneath the crust (at snow-crust interface) is 32° . Snow no longer a powder, increasing water content. Crustal layer not as brittle as this am though no free water visible at the surface. Layer consists of smoothed, reworked circular ice crystals with perhaps a very thin layer of free surface water though the latter is difficult to ascertain. The frozen crust at 1215 hours does not exhibit the fine, delicate "snowflake" tree-like structure of this am. Finished data set at 1245 hours.

Run 13

3/14/75

Began data set at 1430 hours. **Outside** temperature is 38° , snow depth is 7.75 cm. Snow condition, frozen layer 0.48 cm to 0.64 cm with visible amounts of free surface water

filling in the crenulations thus tending to smooth the ice sheet. Fine delicate structure has disappeared as already indicated this am due to surface melting leaving a somewhat smooth, yet undulating surface with second order roughness at the surface (#24, 25). Underlying snow appears wetter than at 1200 hours today but not saturated. Excellent snowball quality. Skies are clear with NW wind less than 5 mph. Outside temperature has had its effect on the snow cover. Temperature at crust-snow interface is 32.5°F.

Run 14

3/15/75

Began data set at 0700, skies cloudy, wind is calm with slight movement from the south. Overnight low on hill was 22°. Snow condition is 6.99 cm deep. Surficial structure of crust is identical to yesterday pm, run 13; no free surface water visible. Snow beneath crystal layer different from yesterday; is totally metamorphosed into firn. Very friable with the once dry powder recrystallized into small, brittle ice pods (#31, 32). Crust is glazed ice, no longer distinct sleet nodules but now are totally reconstituted into a rough (lumpy) layer (#26-30, #30 shows physical characteristics of bottom side of crust). Firm layer extends to ground level. #33 shows snow geese. Slide #3, 4 with 2-1/4" format, covers overall area. Note: firn is dry, not wet; this condition will not last long due to climbing temperatures expected today. The frozen layer-snow interface (#30) is very irregular with firn cemented to this crustal layer in irregular, vertical, stringy clumps. Skies cleared and sun shown at 0930. Completed data at 0945 hours, conditions within snow remained same throughout the data set.

Run 15

3/16/75

Began 1215 hours. Slide #5 (120 format) shows nature of surface. Skies overcast, low of 37°. No rain or snow since run #14. Snow condition, wet to soggy and very patchy. Ground condition, surface has large patches of standing water (snow melt) up to 3 cm deep in many places. Completed data set at 1420 hours (#6, 120 format).

Run 16

3/17/75

Began data set at 0926. No snow on ground whatsoever. Over night low of 30°. Morning is overcast, light frost but gone by 0800. Wind calm. Skies clearing to east. Slide #7 (120 format) depicts test plot conditions. Soil conditions are very soggy (super-saturated) but NO standing water. Slide #8 (120 format) shows condition of grass cover (matted down).

Run 17

3/18/75

Overnight low of 40°. Began data set at 1330 hours. Skies are partly cloudy, south wind 15-20 mph. Slide #9 (120 format) taken at same locale as run 16. Soil no longer super-saturated at surface.

Run 18

3/19/75

Began data set at 1353 hours. Overnight low of 38°, ground thawed, no snow.

Run 19

3/20/75

Began data set at 1300 hours. Are taking only 0°-30°. Slide #11 (120 format) shows grass condition, soil surface layer drying out.

Run 20

3/21/75

Began data set at 1400 hours. Slide #12 (120 format) shows ground condition, soil progressively drying out since snow melted.

Run 21

3/25/75

Began data set at 0730 hours. Overnight low of 17°. No rain since snow melted, wind about 15 mph from NW. Wind-chill temperature equivalent to -9°F. Slide #3,4 (120 format, roll 2). Note: Frozen soil layer of 0.6 cm in patches, full extent of this condition impossible to pinpoint.

Run 22

3/28/75

Began data set at 1000 hours. Overnight low of 28°F. Light snow falling at 1030 hours. Had considerable precipitation on 3/27/75. Begin roll #2, 35 mm (36 exposures). Slides #2,3 taken at 1145 hours. Ground not frozen, very wet at surface, but no standing water. Snow patchy in clumps of grass (#2); snow not a wet flake but more rounded sleet-type of flake. All snow, no rain mixed in. As of 1200 hours, snow not really accumulating. Grass beginning to green. Finished taking data samples at 1145 hours, data set completed at 1300 hours.

Run 23

3/30/75

Began data set at 0710. Overnight low of 17°. No overnight precipitation. Wind calm, skies clear, frost on grass (#4-8). Grass clear of frost by 0920 hours (#9). Grass frozen (stiff) until about 0900 hours. Data set completed at 0920 hours.

Run 24

3/30/75

Began data set at 1700. #10 taken at 1700 hours, ground thawed, air temperature 46°.

Run 25

4/1/75

Began data set at 1407. Overnight low of 30°, ground thawed, NW winds at 15 mph, present temperature 48°. Skies overcast. #12 shows the grass condition (metric scale for first time).

Run 26

4/2/75

Began data set at 0825. Overnight low of 24°. On 4/1/75 at 2230 hours, it began to rain; at about 2330 it began to sleet (very rough, jagged balls, not the smooth type as before) with an average size of 5 mm. It then rained lightly the remaining part of the night. At 0600 on 4/2/75, began to snow (very dry, crystalline type). At 0830 snow began falling very heavy with northerly winds about 20 mph; ground condition unknown due to frozen sensor connectors. Rain that fell most of early morning hours inflicted an ice coating on the grass blades of about 8 mm diameter (#17,18). Some standing water between A and B-box as snow began to accumulate. #13,14,15 show grass condition before heavy snow started. #16 shows overall view of plot from west end. Snow that is falling has moderate flakes (about 3-4 mm). Snow is not the wet, soggy variety or the dry, crystalline variety. Will continue the data set until finished even though ground conditions are rapidly changing with respect to the snow cover. Very difficult to obtain soil moisture samples due to the nature of the ice covered surface. Snow ceased at 0910 hours, began falling at 0930 hours. At 1100 hours, still snowing. Air temperature is 20°, ground temperature is 33° (average) wind chill is -10°F. #20 shows grass and snow, taken about 3 feet west of B-box, #21 shows overall condition from west end of plot. #22 is closeup of grass taken from SE corner of plot (looking NW). #23 is closeup (withscale) looking SE from B-box at about 30 foot marker. #24 is SE (without tape) at 40 foot marker. There is free water standing between the ground-ice and soil surface interface. End data set at 1145 hours.

Run 27

4/2/75

Began data set at 1415. Outside temperature is 27°F. NW winds. #25 shows grass condition. #26 looking SE from B-box, #27 looking E from west end of plot, #28 VOID, #29 is extreme closeup of B-box. Snowing lightly with small, dry, rounded flakes. Overall snow depth varies but generally about 3.5 cm above soil surface. Snow falling moderately as of 1530 hours. Note: For runs 26 and 27, an ice layer about 1 cm thick exists beneath the overlying snow layer(at the snow-soil interface). Beneath the ice

layer, the upper 3 cm of soil is super-saturated, though no free standing water. #30 shows the nature of the soil condition beneath the ice layer. Completed data set at 1615 hours, still snowing.

Run 28

4/3/75

Began data set at 0515; early morning hours were necessary to insure that ground conditions would remain constant throughout the data set. Overnight low of +9°, present temperature is 12°. Skies clear, winds calm. Snow powdery; snow temperature is 14.5°, depth is about 5 cm. Same general description on snow and ground and grass cover holds as 4/2/75 pm including the ice layer (1 cm thick) at snow-soil interface. #35 shows SE look at sunrise showing grass condition. Slide #36 is closeup of grass cover. Completed data set at 0710, temperature now +9°F, winds calm.

Run 29

4/3/75

Began data set at 1445. #14 (roll 3) is closeup of grass; #15, 16 show overall condition of plot from west end. Snow cover patchy and very wet (soggy); snow depth is about 1 cm. Free standing water in patches of about 1.5 cm. Slide #17 shows closeup of snow-grass relationship. Slide #18 depicts the EW rows of grass as they were planted and the snow present in the intervening furrows highlight this. #18 was taken at 1500 hours, #2 (120 format, roll 4) taken at 1530 with 60 cm scale; #19 (roll 3, 35mm) taken at 30° from TV tube to show distribution on ground. Ground is super-saturated with depths up to 3 cm but average depth of about 2 cm, this free standing water is present throughout the test plot. Note: When the data set began, the 1 cm ice layer at the snow-soil interface had melted, was absent throughout the test area. #3,4 (set 4, 120 format) taken at 1615 and 1630 respectively.

Run 30

4/4/75

Began data set at about 1300. Overnight low of 33 degrees, skies are clear with present temperature of 60 degrees. #5,6 show ground condition; is soggy at surface but no free standing water is present. Snow completely melted, grass beginning to green, #7 of boom and microwave system.

Run 31

4/11/75

Taken while in Oklahoma, D. Petrie took samples and weight, no photographs.

Run 32

4/15/75

Began at 1500 hours. Ground thawed, no precipitation within 24 hours, overnight low of 37°. Present temperature of 63°, skies clear with S winds about 5-10 mph; Grass is green and about 10 cm high. No photographs.

Run 33

4/21/75

Began data set at 1540 hours. #5,6,7 (roll 5); grass about 14 cm high, has not been cut since fall of 1974. Rained past weekend, SW winds 5-15 mph, 71° presently. Can no longer see white, incidence angle, marker tubes. #7 is rule stick total of 25 cm above ground surface; not sure of scale for #5.

Run 34

4/23/75

Rain last night, temperature presently 80°. Very humid. #9 (roll 5) is of grass height-- tape is 25 cm above ground. #10,11 taken from east end; #12,13 looking from west end of plot. SW winds 15-20 mph. Grass an average of 17 cm high.

End of data sets for freeze/thaw winter experiments.

APPENDIX B: TABULATED SCATTERING COEFFICIENTS

AVERAGED SIGNAC SET 4 FREEZE

ANTENNA ANGLE 0

FREQ	1.2	1.7	2.3	3.3	4.3	5.3	6.3	7.3
POL HH	7.8	5.9	10.8	10.7	10.2	8.3	5.6	6.1
POL HV	-10.1	-12.5	-12.0	-14.0	-14.3	-8.2	-7.1	-6.6
POL VV	8.9	7.5	11.3	10.0	9.7	8.5	5.4	5.9

ANTENNA ANGLE 10

FREQ	1.2	1.7	2.3	3.3	4.3	5.3	6.3	7.3
POL HH	-5.5	-15.5	-14.1	-13.1	-13.3	-14.1	-11.2	-10.4
POL HV	-22.7	-30.8	-27.8	-29.1	-27.9	-26.1	-22.0	-19.5
POL VV	-7.5	-14.7	-12.8	-12.3	-13.1	-13.0	-10.2	-9.7

ANTENNA ANGLE 20

FREQ	1.2	1.7	2.3	3.3	4.3	5.3	6.3	7.3
POL HH	-21.1	-24.7	-14.6	-16.2	-17.0	-16.1	-16.5	-12.9
POL HV	-34.2	-38.1	-31.5	-30.0	-26.5	-24.8	-21.9	-20.3
POL VV	-19.4	-24.4	-15.3	-16.1	-18.6	-14.5	-15.8	-13.4

ANTENNA ANGLE 30

FREQ	1.2	1.7	2.3	3.3	4.3	5.3	6.3	7.3
POL HH	-23.2	-25.1	-19.4	-19.6	-17.8	-17.1	-18.5	-14.6
POL HV	-36.8	-39.2	-33.7	-29.7	-27.0	-25.5	-23.6	-22.3
POL VV	-22.6	-24.7	-21.2	-19.1	-17.4	-18.4	-20.4	-14.0

ANTENNA ANGLE 50

FREQ	1.2	1.7	2.3	3.3	4.3	5.3	6.3	7.3
POL HH	-28.1	-27.0	-24.6	-25.5	-24.9	-25.4	-19.6	-20.0
POL HV	-42.6	-41.9	-37.2	-35.6	-29.7	-28.9	-26.0	-23.7
POL VV	-33.5	-32.4	-30.0	-27.3	-25.0	-23.5	-23.3	-20.1

ANTENNA ANGLE 70

FREQ	1.2	1.7	2.3	3.3	4.3	5.3	6.3	7.3
POL HH	-29.2	-32.1	-30.1	-31.2	-28.5	-28.6	-23.2	-28.4
POL HV	100.0	-43.6	-41.6	-39.4	-33.2	38.9	-31.8	-31.5
POL VV	-34.1	-37.8	-35.6	-32.6	-29.2	-27.1	-27.1	-27.7

AVERAGED SIGMA0 SET 6 FREEZE

ANTENNA ANGLE 0

FREQ	1.2	1.7	2.3	3.3	4.3	5.3	6.3	7.3
POL HH	3.6	-4.5	6.2	7.0	7.7	6.1	6.0	4.2
POL HV	-15.0	-22.3	-17.4	-18.2	-15.9	-12.2	-6.9	-9.3
POL VV	5.0	-3.1	6.8	7.3	6.9	6.7	6.6	5.3

ANTENNA ANGLE 10

FREQ	1.2	1.7	2.3	3.3	4.3	5.3	6.3	7.3
POL HH	-7.0	-20.3	-8.2	-11.7	-7.2	-14.4	-13.7	-8.0
POL HV	-25.0	-32.9	-21.9	-24.7	-20.6	-21.3	-17.1	-18.4
POL VV	-8.4	-20.3	-9.5	-13.0	-8.8	-13.0	-11.7	-8.7

ANTENNA ANGLE 20

FREQ	1.2	1.7	2.3	3.3	4.3	5.3	6.3	7.3
POL HH	-22.2	-27.5	-17.4	-15.1	-15.2	-15.7	-14.9	-11.7
POL HV	-35.3	-36.7	-25.6	-26.7	-23.4	-22.4	-21.1	-18.1
POL VV	-21.5	-25.2	-14.7	-17.1	-14.6	-15.6	-13.7	-14.6

ANTENNA ANGLE 30

FREQ	1.2	1.7	2.3	3.3	4.3	5.3	6.3	7.3
POL HH	-25.1	-30.4	-21.6	-23.1	-17.7	-17.3	-16.2	-15.5
POL HV	-33.0	-39.5	-27.1	-28.0	-27.3	-24.0	-22.0	-20.0
POL VV	-22.7	-26.7	-18.7	-20.4	-20.3	-17.6	-13.8	-12.2

ANTENNA ANGLE 50

FREQ	1.2	1.7	2.3	3.3	4.3	5.3	6.3	7.3
POL HH	-23.6	-30.3	-21.7	-24.5	-24.5	-26.6	-24.7	-21.2
POL HV	100.0	-44.1	-30.2	-32.9	-31.8	-29.5	-29.3	-25.1
POL VV	-25.7	-30.1	-21.3	-22.0	-23.4	-24.2	-23.5	-20.1

ANTENNA ANGLE 70

FREQ	1.2	1.7	2.3	3.3	4.3	5.3	6.3	7.3
POL HH	-26.3	-38.5	-30.6	-29.9	-29.0	-28.5	-26.7	-26.0
POL HV	100.0	-47.9	-38.1	-37.8	-35.4	-31.8	-32.0	-28.8
POL VV	-99.7	-39.8	-28.5	-28.3	-28.7	-27.9	-26.0	-24.5

AVERAGED SIGNAC SET 7 FREEZE

ANTENNA ANGLE 0

FREQ	1.2	1.7	2.3	3.3	4.3	5.3	6.3	7.3
POL HH	-4.4	-9.3	-0.2	5.5	0.4	-9.3	-2.8	10.1
POL HV	-23.4	-23.2	-20.4	-20.1	-23.0	-21.1	3.3	-8.5
POL VV	-2.8	-7.2	0.5	5.7	-0.3	-8.5	-1.6	4.0

ANTENNA ANGLE 10

FREQ	1.2	1.7	2.3	3.3	4.3	5.3	6.3	7.3
POL HH	-15.0	-21.0	-12.7	-7.6	-15.2	-11.1	-13.3	-13.4
POL HV	-30.5	-22.2	35.2	34.7	-23.0	-26.2	-21.4	-20.7
POL VV	-17.2	-22.0	-13.6	-7.2	-17.0	-11.2	4.6	-9.3

ANTENNA ANGLE 20

FREQ	1.2	1.7	2.3	3.3	4.3	5.3	6.3	7.3
POL HH	-25.7	-26.2	-18.6	-18.0	-19.7	-16.9	-15.5	-13.3
POL HV	-34.4	-38.0	-25.8	-27.2	-27.3	-25.3	-20.3	-17.8
POL VV	-23.9	-23.8	-16.9	-17.2	-18.2	-16.7	-13.9	9.8

ANTENNA ANGLE 30

FREQ	1.2	1.7	2.3	3.3	4.3	5.3	6.3	7.3
POL HH	-26.3	-30.2	-22.6	-20.8	-23.7	-20.5	-16.2	-19.2
POL HV	-36.5	-39.3	-30.1	-28.9	-25.3	-27.1	9.8	-24.1
POL VV	-24.9	-25.9	-22.4	-20.4	-19.0	-20.0	-15.2	-16.0

ANTENNA ANGLE 50

FREQ	1.2	1.7	2.3	3.3	4.3	5.3	6.3	7.3
POL HH	-28.8	-31.2	-24.4	-25.6	-23.5	-32.5	-25.5	-21.8
POL HV	-41.9	-42.4	-33.5	-34.6	-33.0	-32.2	-32.0	-27.6
POL VV	-28.2	-29.6	-22.0	-24.4	-23.3	-27.6	-26.9	-19.3

ANTENNA ANGLE 70

FREQ	1.2	1.7	2.3	3.3	4.3	5.3	6.3	7.3
POL HH	-31.3	-38.5	-30.3	-30.6	-31.4	-31.3	-19.5	31.2
POL HV	100.0	-48.9	-41.4	-40.2	-35.7	-35.6	-36.0	-33.4
POL VV	-36.5	-39.8	-32.2	-31.3	-24.5	-28.1	-29.0	-32.0

ORIGINAL PAGE IS
OF POOR QUALITY

AVERAGED SIGMAD SET 8 FREEZE

ANTENNA ANGLE

0

FREQ	1.2	1.7	2.3	3.3	4.3	5.3	6.3	7.3
POL HH	-3.6	-3.9	4.4	7.4	8.9	8.6	9.1	9.3
POL HV	-20.1	-20.9	-16.3	-15.2	-12.8	-9.0	-5.6	-3.7
POL VV	-2.6	-2.2	5.4	7.9	9.3	9.5	9.3	9.9

ANTENNA ANGLE

10

FREQ	1.2	1.7	2.3	3.3	4.3	5.3	6.3	7.3
POL HH	-13.7	-17.6	-10.2	-11.2	-14.7	-15.8	-17.6	-15.3
POL HV	-29.9	-33.3	-26.5	-29.4	-31.4	-26.0	-26.2	-22.9
POL VV	-15.1	-18.3	-9.5	-12.5	-15.2	-15.1	-17.7	-17.2

ANTENNA ANGLE

20

FREQ	1.2	1.7	2.3	3.3	4.3	5.3	6.3	7.3
POL HH	-26.5	-26.6	-18.8	-19.2	-22.3	-24.7	-19.6	-18.6
POL HV	-34.0	-38.5	-30.0	-31.4	-28.5	-30.5	-28.8	-26.9
POL VV	-23.4	-24.9	-16.4	-19.0	-18.9	-22.8	-20.7	-19.5

ANTENNA ANGLE

30

FREQ	1.2	1.7	2.3	3.3	4.3	5.3	6.3	7.3
POL HH	-27.1	-28.7	-22.9	-24.4	-20.8	-23.6	-22.8	-22.3
POL HV	-37.3	-37.5	-29.9	-31.2	-31.2	-30.0	-31.1	-26.9
POL VV	-25.3	-27.1	-22.1	-22.8	-21.8	-23.4	-23.3	-20.8

ANTENNA ANGLE

50

FREQ	1.2	1.7	2.3	3.3	4.3	5.3	6.3	7.3
POL HH	-31.4	-35.6	-25.8	-30.3	-29.4	-31.8	-32.4	-31.0
POL HV	-41.9	-44.7	-36.3	-38.5	-38.9	-36.9	-36.2	-34.7
POL VV	-30.5	-34.0	-28.2	-27.9	-32.6	-33.7	-32.9	-30.5

ANTENNA ANGLE

70

FREQ	1.2	1.7	2.3	3.3	4.3	5.3	6.3	7.3
POL HH	-34.5	-35.9	-34.7	-32.8	-31.1	-30.3	-28.7	-27.3
POL HV	100.0	-50.4	-41.3	-41.4	-36.1	-36.1	-35.8	-30.1
POL VV	-38.6	-33.3	-35.1	-34.9	-33.0	-33.6	-32.6	-28.9

AVERAGED SIGMA0 SET 9 FREEZE

ANTENNA ANGLE		0						
FREQ	1.2	1.7	2.3	3.3	4.3	5.3	6.3	7.3
POL HH	-7.3	-6.7	2.3	3.7	5.4	3.7	-0.8	4.2
POL HV	-24.9	-24.1	-18.6	-17.3	-15.2	-14.2	-12.1	-7.3
POL VV	-6.8	-5.1	2.6	2.9	4.9	3.5	-0.6	3.4
ANTENNA ANGLE		10						
FREQ	1.2	1.7	2.3	3.3	4.3	5.3	6.3	7.3
POL HH	-14.4	-17.7	-10.2	-11.1	-10.6	-11.2	-14.8	-15.5
POL HV	-29.9	-33.6	-25.5	-26.4	-25.8	-25.7	-25.3	-23.3
POL VV	-15.4	-17.9	-10.9	-12.0	-12.8	-10.9	-13.8	-13.3
ANTENNA ANGLE		20						
FREQ	1.2	1.7	2.3	3.3	4.3	5.3	6.3	7.3
POL HH	-24.0	-25.7	-16.4	-17.5	-21.5	-19.8	-20.2	-22.2
POL HV	-33.5	-37.8	-29.8	-28.6	-27.6	-27.9	-29.4	-23.6
POL VV	-23.1	-23.9	-13.2	-20.6	-18.5	-20.1	-20.4	-20.1
ANTENNA ANGLE		30						
FREQ	1.2	1.7	2.3	3.3	4.3	5.3	6.3	7.3
POL HH	-26.2	-29.0	-21.8	-23.6	-21.3	-22.9	-21.6	-21.5
POL HV	-35.9	-36.9	-27.3	-29.0	-30.3	-29.7	-28.5	-27.9
POL VV	-24.7	-25.3	-20.3	-21.6	-21.7	-23.1	-21.4	-21.2
ANTENNA ANGLE		50						
FREQ	1.2	1.7	2.3	3.3	4.3	5.3	6.3	7.3
POL HH	-26.1	-31.8	-24.9	-27.9	-28.8	-31.8	-29.6	-26.5
POL HV	-38.4	-42.4	-33.6	-36.2	-35.7	-37.0	-35.9	-32.9
POL VV	-24.6	-29.5	-22.0	-26.5	-27.1	-30.1	-31.0	-25.9
ANTENNA ANGLE		70						
FREQ	1.2	1.7	2.3	3.3	4.3	5.3	6.3	7.3
POL HH	-29.6	-36.8	-30.4	-28.5	-27.5	-28.0	-26.7	-25.6
POL HV	100.0	-45.7	-39.5	-37.3	-33.0	-33.8	-31.0	-29.7
POL VV	-30.8	-35.4	-29.5	-27.7	-26.6	-28.5	-27.5	-25.7

ORIGINAL PAGE IS
OF POOR QUALITY

AVERAGED SIGMAO SET 10 FREEZE

ANTENNA ANGLE 0

FREQ	1.2	1.7	2.3	3.3	4.3	5.3	6.3	7.3
POL HH	5.6	-0.6	9.4	6.5	2.0	5.7	5.8	5.7
POL HV	-12.1	-19.4	-14.2	-16.3	-16.0	-9.6	-6.2	-4.7
POL VV	6.8	0.5	10.0	7.1	3.1	7.0	6.7	6.8

ANTENNA ANGLE 10

FREQ	1.2	1.7	2.3	3.3	4.3	5.3	6.3	7.3
POL HH	-6.4	-19.6	-15.0	-18.4	-13.8	-18.0	-22.4	-17.5
POL HV	-25.0	-37.1	-33.7	-31.1	-26.7	-28.9	-29.8	-25.8
POL VV	-8.7	-20.4	-14.1	-15.7	-11.9	-18.3	-21.0	-18.7

ANTENNA ANGLE 20

FREQ	1.2	1.7	2.3	3.3	4.3	5.3	6.3	7.3
POL HH	-24.8	-27.9	-19.2	-22.7	-17.9	-25.5	-28.0	-21.3
POL HV	-38.0	-42.3	-35.4	-34.5	-31.3	-28.4	-31.9	-28.3
POL VV	-22.5	-27.6	-20.2	-20.6	-16	-25.0	-24.1	-20.6

ANTENNA ANGLE 30

FREQ	1.2	1.7	2.3	3.3	4.3	5.3	6.3	7.3
POL HH	-26.5	-29.9	-20.7	-25.8	-21.6	-22.6	-24.9	-23.4
POL HV	-39.3	-43.2	-35.5	-32.8	-30.5	-29.5	-27.5	-27.2
POL VV	-26.4	-30.7	-22.0	-22.7	-22.3	-21.2	-23.1	-23.8

ANTENNA ANGLE 50

FREQ	1.2	1.7	2.3	3.3	4.3	5.3	6.3	7.3
POL HH	-27.3	-32.7	-25.4	-29.5	-28.8	-28.1	-28.9	-27.9
POL HV	-43.0	-47.8	-37.4	-39.0	-35.8	-36.4	-37.5	-32.0
POL VV	-32.2	-36.4	-24.4	-29.8	-30.5	-28.8	-31.3	-27.5

ANTENNA ANGLE 70

FREQ	1.2	1.7	2.3	3.3	4.3	5.3	6.3	7.3
POL HH	-28.5	-38.7	-30.7	-32.2	-25.7	-28.6	-26.1	-27.7
POL HV	-38.3	-49.4	-39.3	-39.4	-34.6	-34.5	-32.6	-30.0
POL VV	-35.0	-41.3	-31.6	-32.6	-29.0	-27.3	-28.4	-28.4

AVERAGED SIGMA0 SET 11 FREEZE

ANTENNA ANGLE 0

FREQ	1.2	1.7	2.3	3.3	4.3	5.3	6.3	7.3
POL HH	1.1	-6.4	5.6	6.1	8.0	3.6	5.5	6.1
POL HV	-16.4	-25.1	-18.3	-16.7	-16.9	-11.6	-6.7	-3.5
POL VV	2.1	-5.2	6.0	5.5	7.3	4.4	4.5	3.9

ANTENNA ANGLE 10

FREQ	1.2	1.7	2.3	3.3	4.3	5.3	6.3	7.3
POL HH	-8.7	-19.0	-12.4	-13.2	-10.0	-14.8	-17.0	-13.1
POL HV	-27.0	-35.5	-24.7	-28.6	-22.7	-26.7	-21.1	-19.9
POL VV	-10.7	-20.1	-13.8	-11.7	-10.7	-15.5	-14.0	-9.5

ANTENNA ANGLE 20

FREQ	1.2	1.7	2.3	3.3	4.3	5.3	6.3	7.3
POL HH	-26.1	-28.8	-20.1	-19.9	-19.1	-16.6	-16.7	-18.1
POL HV	-41.4	-39.6	-28.6	-32.6	-27.1	-25.9	-25.9	-23.1
POL VV	-25.5	-28.1	-19.7	-20.3	-18.5	-17.3	-18.5	-18.2

ANTENNA ANGLE 30

FREQ	1.2	1.7	2.3	3.3	4.3	5.3	6.3	7.3
POL HH	-27.9	-32.1	-21.6	-25.2	-19.9	-22.8	-21.4	-21.8
POL HV	-42.0	-42.0	-27.7	-31.4	-29.2	-28.3	-27.1	-25.0
POL VV	-29.7	-31.2	-20.6	-20.8	-26.0	-20.4	-20.2	-18.5

ANTENNA ANGLE 50

FREQ	1.2	1.7	2.3	3.3	4.3	5.3	6.3	7.3
POL HH	-26.3	-35.3	-26.5	-29.0	-27.7	-29.3	-30.1	-27.0
POL HV	-77.1	-48.2	-32.9	-34.5	-34.4	-34.3	-32.7	-28.9
POL VV	-75.5	-37.4	-27.4	-26.6	-28.1	-30.5	-26.3	-25.3

ANTENNA ANGLE 70

FREQ	1.2	1.7	2.3	3.3	4.3	5.3	6.3	7.3
POL HH	-26.5	-38.4	-29.8	-28.7	-25.4	-26.4	-24.4	-22.5
POL HV	-76.3	-47.1	-37.9	-38.0	-34.2	-32.5	-29.1	-26.6
POL VV	-74.6	-39.9	-27.7	-31.4	-28.0	-27.0	-25.4	-23.1

ORIGINAL PAGE IS
OF POOR QUALITY

AVERAGED SIGMAO SET 12 FREEZE

ANTENNA ANGLE 0

FREQ	1.2	1.7	2.3	3.3	4.3	5.3	6.3	7.3
POL HH	5.9	1.4	12.2	9.2	4.9	5.2	8.1	10.0
POL HV	-10.6	-16.5	-11.9	-15.2	-12.8	-8.6	-4.0	-0.5
POL VV	8.3	2.5	12.8	9.6	4.4	6.1	9.1	11.8

ANTENNA ANGLE 10

FREQ	1.2	1.7	2.3	3.3	4.3	5.3	6.3	7.3
POL HH	-3.5	-12.5	-12.3	-19.3	-12.9	-16.7	-17.7	-14.0
POL HV	-22.8	-31.6	-28.5	-31.9	-30.0	-27.5	-25.6	-22.5
POL VV	-6.4	-14.3	-11.6	-17.1	-11.5	-18.0	-15.5	-17.5

ANTENNA ANGLE 20

FREQ	1.2	1.7	2.3	3.3	4.3	5.3	6.3	7.3
POL HH	-20.9	-29.7	-17.2	-23.5	-18.0	-24.3	-22.6	-18.1
POL HV	-78.9	-42.3	-33.6	-34.7	-31.8	-28.7	-29.9	-26.3
POL VV	-19.9	-26.6	-18.3	-19.6	-18.2	-21.6	-20.7	-18.4

ANTENNA ANGLE 30

FREQ	1.2	1.7	2.3	3.3	4.3	5.3	6.3	7.3
POL HH	-25.0	-30.9	-21.5	-25.5	-22.8	-21.6	-22.5	-20.1
POL HV	-78.5	-43.7	-33.3	-33.5	-31.7	-28.1	-27.3	-25.1
POL VV	-77.1	-30.4	-22.2	-22.3	-25.6	-19.7	-22.4	-18.9

ANTENNA ANGLE 50

FREQ	1.2	1.7	2.3	3.3	4.3	5.3	6.3	7.3
POL HH	-26.0	-33.6	-24.4	-30.7	-28.1	-28.6	-27.2	-24.5
POL HV	-99.6	-48.9	-34.0	-37.7	-36.2	-34.0	-35.0	-27.6
POL VV	-36.0	-37.6	-25.4	-30.3	-30.6	-28.8	-27.3	-25.6

ANTENNA ANGLE 70

FREQ	1.2	1.7	2.3	3.3	4.3	5.3	6.3	7.3
POL HH	-95.1	-37.0	-28.4	-29.4	-25.6	-26.9	-23.7	-20.7
POL HV	-94.9	-46.6	-37.4	-38.9	-34.5	-33.2	-29.6	-24.6
POL VV	-93.2	-38.9	-27.5	-29.6	-28.9	-26.6	-25.6	-21.5

AVERAGED SIGMA0 SET 13 FREEZE

ANTENNA ANGLE 0

FREQ	1.2	1.7	2.3	3.3	4.3	5.3	6.3	7.3
POL HH	3.7	1.2	9.1	9.9	10.0	6.1	7.5	8.9
POL HV	-14.6	-16.0	-15.3	-12.8	-10.3	-12.6	-6.6	-5.3
POL VV	4.0	2.2	10.0	10.6	9.7	7.8	8.4	11.2

ANTENNA ANGLE 10

FREQ	1.2	1.7	2.3	3.3	4.3	5.3	6.3	7.3
POL HH	-7.5	-14.8	-10.5	-16.1	-13.1	-18.8	-21.6	-15.7
POL HV	-30.3	-31.9	-28.2	-31.7	-30.5	-30.7	-29.9	-24.7
POL VV	-9.4	-17.1	-10.0	-17.1	-12.2	-18.5	-21.1	-14.9

ANTENNA ANGLE 20

FREQ	1.2	1.7	2.3	3.3	4.3	5.3	6.3	7.3
POL HH	-23.3	-30.2	-18.4	-20.5	-23.0	-27.9	-22.9	-21.3
POL HV	-78.3	-41.9	-31.7	-32.9	-30.8	-31.3	-30.6	-26.6
POL VV	-26.1	-27.5	-18.3	-20.9	-21.4	-25.1	-23.5	-19.9

ANTENNA ANGLE 30

FREQ	1.2	1.7	2.3	3.3	4.3	5.3	6.3	7.3
POL HH	-30.9	-31.6	-28.1	-26.0	-25.8	-25.9	-26.6	-24.0
POL HV	-78.0	-43.3	-32.9	-34.7	-32.9	-33.1	-32.8	-26.3
POL VV	-76.5	-29.6	-20.8	-22.7	-26.4	-25.4	-25.2	-22.9

ANTENNA ANGLE 50

FREQ	1.2	1.7	2.3	3.3	4.3	5.3	6.3	7.3
POL HH	-28.7	-36.5	-25.5	-29.6	-33.2	-34.3	-35.7	-27.6
POL HV	-99.8	-47.4	-34.3	-38.6	-39.8	-38.4	-38.7	-29.3
POL VV	-98.2	-36.5	-26.3	-26.7	-32.6	-33.2	-32.8	-26.9

ANTENNA ANGLE 70

FREQ	1.2	1.7	2.3	3.3	4.3	5.3	6.3	7.3
POL HH	-96.0	-39.1	-29.7	-29.1	-31.5	-31.1	-28.7	-23.3
POL HV	-95.8	-45.6	-38.2	-38.0	-36.5	-34.6	-32.9	-24.5
POL VV	-94.9	-39.7	-27.8	-28.8	-33.8	-30.5	-27.7	-23.1

AVERAGED SIGMA0 SET 14 FREEZE

ANTENNA ANGLE 0

FREQ	1.2	1.7	2.3	3.3	4.3	5.3	6.3	7.3
POL HH	7.6	2.6	8.0	9.2	8.6	1.7	6.3	5.3
POL HV	-12.8	-15.0	-17.0	-16.4	-14.5	-13.7	-8.7	-8.9
POL VV	6.4	4.3	8.6	9.2	7.8	1.8	5.5	4.6

ANTENNA ANGLE 10

FREQ	1.2	1.7	2.3	3.3	4.3	5.3	6.3	7.3
POL HH	-5.8	-13.7	-15.0	-18.6	-14.7	-19.7	-20.6	-14.4
POL HV	-16.2	-31.9	-34.1	-31.0	-32.2	-29.9	-29.2	-25.3
POL VV	-7.6	-14.7	-14.4	-16.8	-13.8	-17.6	-19.8	-17.6

ANTENNA ANGLE 20

FREQ	1.2	1.7	2.3	3.3	4.3	5.3	6.3	7.3
POL HH	-24.1	-30.0	-17.2	-22.8	-17.0	-23.0	-25.3	-20.1
POL HV	-37.9	-42.6	-35.9	-34.9	-30.6	-28.4	-30.0	-26.1
POL VV	-21.8	-28.0	-18.3	-20.4	-17.1	-19.7	-24.5	-19.2

ANTENNA ANGLE 30

FREQ	1.2	1.7	2.3	3.3	4.3	5.3	6.3	7.3
POL HH	-27.6	-30.2	-21.6	-25.4	-21.6	-22.3	-23.2	-20.6
POL HV	-42.9	-44.4	-35.4	-35.1	-33.0	-27.3	-28.2	-26.0
POL VV	-29.9	-31.2	-21.4	-22.9	-23.0	-20.4	-22.2	-19.1

ANTENNA ANGLE 50

FREQ	1.2	1.7	2.3	3.3	4.3	5.3	6.3	7.3
POL HH	-29.6	-34.6	-25.1	-29.2	-27.5	-30.6	-29.1	-25.9
POL HV	-46.0	-50.7	-37.9	-38.5	-33.9	-34.9	-34.5	-29.3
POL VV	-33.1	-37.4	-27.2	-31.0	-25.9	-29.2	-29.1	-27.8

ANTENNA ANGLE 70

FREQ	1.2	1.7	2.3	3.3	4.3	5.3	6.3	7.3
POL HH	-33.2	-38.5	-29.4	-29.2	-26.9	-28.8	-24.9	-20.8
POL HV	100.0	-46.9	-38.6	-37.6	-36.2	-32.2	-31.0	-26.9
POL VV	-34.3	-37.2	-28.7	-30.0	-30.7	-28.9	-25.7	-24.0

AVERAGED SIGMA0 SET 15 FREEZE

ANTENNA ANGLE		0						
FREQ	1.2	1.7	2.3	3.3	4.3	5.3	6.3	7.3
POL HH	3.8	-2.1	5.3	6.3	4.7	2.2	4.9	6.2
POL HV	-13.5	-19.5	-16.3	-16.7	-17.6	-17.3	-11.1	-8.2
POL VV	5.5	-0.4	6.0	6.7	5.0	3.0	4.9	6.7
ANTENNA ANGLE		10						
FREQ	1.2	1.7	2.3	3.3	4.3	5.3	6.3	7.3
POL HH	-10.2	-13.8	-7.2	-8.9	-10.7	-10.6	-10.7	-5.9
POL HV	-27.0	-27.8	-19.0	-22.8	-20.3	-21.2	-19.3	-16.1
POL VV	-12.0	-12.3	-6.2	-8.7	-10.6	-10.3	-9.2	-4.3
ANTENNA ANGLE		20						
FREQ	1.2	1.7	2.3	3.3	4.3	5.3	6.3	7.3
POL HH	-18.9	-23.1	-9.9	-11.3	-14.2	-16.4	-14.9	-14.0
POL HV	-29.5	-32.5	-24.3	-25.9	-21.0	-20.9	-22.5	-17.3
POL VV	-18.0	-20.5	-7.5	-12.6	-14.7	-16.9	-14.1	-12.1
ANTENNA ANGLE		30						
FREQ	1.2	1.7	2.3	3.3	4.3	5.3	6.3	7.3
POL HH	-23.2	-24.2	-17.4	-20.5	-16.8	-17.5	-17.8	-13.2
POL HV	-34.5	-35.3	-24.6	-27.6	-26.6	-26.9	-22.5	-20.2
POL VV	-22.2	-22.3	-17.3	-18.2	-19.0	-17.7	-17.2	-13.6
ANTENNA ANGLE		50						
FREQ	1.2	1.7	2.3	3.3	4.3	5.3	6.3	7.3
POL HH	-27.5	-29.8	-20.5	-23.7	-25.6	-28.1	-25.9	-23.4
POL HV	-36.8	-37.7	-31.2	-29.4	-31.6	-29.9	-27.1	-24.6
POL VV	-26.9	-26.3	-18.6	-23.5	-23.4	-27.2	-24.1	-19.8
ANTENNA ANGLE		70						
FREQ	1.2	1.7	2.3	3.3	4.3	5.3	6.3	7.3
POL HH	-32.0	-34.7	-24.9	-25.6	-25.1	-23.7	-22.5	-16.4
POL HV	-41.3	-42.6	-34.2	-33.1	-30.9	-28.4	-25.6	-21.5
POL VV	-33.6	-32.6	-25.0	-28.8	-25.3	-23.1	-19.6	-14.0

AVERAGED SIGMA0 SET 23 FREEZE

ANTENNA ANGLE 0

FREQ	1.2	1.7	2.3	3.3	4.3	5.3	6.3	7.3
POL HH	4.9	1.2	6.5	2.6	-0.9	-5.9	-9.7	-11.0
POL HV	-11.8	-16.5	-16.5	-22.3	-21.7	-23.3	-21.2	-21.0
POL VV	6.2	2.4	6.8	2.5	-0.6	-5.6	-9.1	-11.3

ANTENNA ANGLE 10

FREQ	1.2	1.7	2.3	3.3	4.3	5.3	6.3	7.3
POL HH	-4.9	-13.7	-16.2	-14.3	-18.6	-16.7	-17.4	-18.5
POL HV	-23.3	-33.0	-32.9	-31.2	-28.3	-28.5	-26.7	-25.6
POL VV	-7.1	-14.8	-16.0	-14.1	-17.2	-16.1	-16.7	-17.9

ANTENNA ANGLE 20

FREQ	1.2	1.7	2.3	3.3	4.3	5.3	6.3	7.3
POL HH	-23.8	-28.7	-20.7	-19.4	-21.7	-22.1	-23.6	-22.5
POL HV	-34.5	-41.0	-35.0	-33.9	-30.2	-32.9	-32.6	-27.5
POL VV	-21.0	-26.6	-20.5	-19.0	-19.1	-20.5	-22.8	-21.7

ANTENNA ANGLE 30

FREQ	1.2	1.7	2.3	3.3	4.3	5.3	6.3	7.3
POL HH	-26.4	-29.5	-21.1	-21.9	-21.6	-24.4	-23.3	-22.5
POL HV	-39.9	-42.3	-35.1	-33.0	-30.5	-29.5	-29.8	-27.1
POL VV	-26.3	-29.2	-21.6	-21.8	-19.3	-22.9	-23.2	-22.3

ANTENNA ANGLE 50

FREQ	1.2	1.7	2.3	3.3	4.3	5.3	6.3	7.3
POL HH	-30.7	-33.6	-25.2	-28.9	-30.9	-29.5	-29.4	-26.8
POL HV	-41.2	-44.2	-35.2	-36.2	-35.5	-34.9	-35.7	-30.6
POL VV	-33.1	-32.2	-23.7	-26.9	-27.3	-28.8	-29.2	-27.0

ANTENNA ANGLE 70

FREQ	1.2	1.7	2.3	3.3	4.3	5.3	6.3	7.3
POL HH	-31.5	-36.1	-30.5	-29.5	-27.3	-26.1	-24.6	-22.8
POL HV	-40.7	-44.1	-39.8	-37.7	-33.0	-31.6	-30.4	-27.4
POL VV	-37.1	-36.7	-29.1	-29.3	-27.3	-26.9	-25.8	-25.4

AVERAGED SIGMA0 SET 24 FREEZE

ANTENNA ANGLE 0

FREQ	1.2	1.7	2.3	3.3	4.3	5.3	6.3	7.3
POL HH	6.8	2.8	8.3	3.5	-0.9	-5.3	-7.7	-8.5
POL HV	-10.9	-15.1	-16.4	-23.0	-23.4	-23.2	-20.6	-19.2
POL VV	8.0	4.3	8.8	3.6	-0.8	-5.0	-7.5	-7.3

ANTENNA ANGLE 10

FREQ	1.2	1.7	2.3	3.3	4.3	5.3	6.3	7.3
POL HH	-4.8	-15.4	-16.3	-12.6	-18.0	-15.1	-17.2	-16.3
POL HV	-22.4	-30.5	-25.8	-25.4	-22.7	-25.5	-24.8	-22.7
POL VV	-6.9	-14.6	-14.2	-12.4	-16.1	-14.1	-18.1	-14.7

ANTENNA ANGLE 20

FREQ	1.2	1.7	2.3	3.3	4.3	5.3	6.3	7.3
POL HH	-21.0	-26.0	-14.3	-16.8	-18.5	-18.7	-19.4	-19.0
POL HV	-31.6	-36.6	-28.9	-27.6	-25.9	-26.8	-26.9	-24.1
POL VV	-18.6	-24.1	-13.7	-15.6	-15.3	-16.4	-20.0	-18.3

ANTENNA ANGLE 30

FREQ	1.2	1.7	2.3	3.3	4.3	5.3	6.3	7.3
POL HH	-24.6	-26.7	-18.4	-20.8	-18.7	-19.9	-19.7	-21.3
POL HV	-36.3	-37.6	-30.3	-28.0	-24.5	-25.7	-25.8	-23.2
POL VV	-23.5	-27.1	-19.6	-17.4	-17.4	-17.8	-18.8	-18.9

ANTENNA ANGLE 50

FREQ	1.2	1.7	2.3	3.3	4.3	5.3	6.3	7.3
POL HH	-28.2	-32.1	-23.0	-26.8	-27.0	-27.8	-29.2	-26.0
POL HV	-41.2	-43.2	-32.7	-31.2	-32.1	-32.0	-32.1	-31.8
POL VV	-32.5	-32.0	-22.0	-23.3	-25.6	-24.4	-27.4	-24.6

ANTENNA ANGLE 70

FREQ	1.2	1.7	2.3	3.3	4.3	5.3	6.3	7.3
POL HH	-29.4	-34.8	-28.5	-27.3	-23.3	-26.1	-24.1	-23.5
POL HV	-38.4	-43.8	-36.9	-35.7	-30.6	-30.4	-27.9	-27.9
POL VV	-37.8	-40.4	-30.2	-27.2	-26.0	-24.1	-23.9	-23.8

ORIGINAL PAGE IS
OF POOR QUALITY

B-13

AVERAGE SIGMA0 SET 27 FREEZE

ANTENNA ANGLE 0

FREQ	1.2	1.7	2.3	3.3	4.3	5.3	6.3	7.3
POL HH	1.3	1.0	8.3	1.6	-4.9	-4.2	-10.9	-16.1
POL HV	-15.6	-17.2	-15.4	-23.6	-24.6	-22.8	-22.3	-22.6
POL VV	2.4	2.2	8.7	2.1	-4.9	-6.0	-10.6	-14.1

ANTENNA ANGLE 10

FREQ	1.2	1.7	2.3	3.3	4.3	5.3	6.3	7.3
POL HH	-6.4	-11.3	-13.3	-13.4	-16.4	-14.9	-17.7	-13.8
POL HV	-24.7	-28.7	-25.4	-24.6	-25.4	-27.1	-23.6	-20.0
POL VV	-7.8	-12.0	-13.5	-12.4	-14.2	-14.9	-16.8	-12.6

ANTENNA ANGLE 20

FREQ	1.2	1.7	2.3	3.3	4.3	5.3	6.3	7.3
POL HH	-20.0	-24.2	-17.1	-19.6	-19.7	-20.1	-17.8	-16.8
POL HV	-30.4	-35.5	-29.3	-27.1	-29.2	-27.4	-29.3	-21.2
POL VV	-18.3	-22.1	-17.4	-18.7	-17.3	-21.0	-20.1	-17.9

ANTENNA ANGLE 30

FREQ	1.2	1.7	2.3	3.3	4.3	5.3	6.3	7.3
POL HH	-22.7	-24.6	-17.9	-20.8	-18.4	-19.5	-20.0	-16.0
POL HV	-33.5	-35.2	-28.2	-28.7	-28.3	-25.9	-26.9	-22.3
POL VV	-21.3	-23.8	-19.7	-21.2	-17.7	-20.6	-18.8	-17.2

ANTENNA ANGLE 50

FREQ	1.2	1.7	2.3	3.3	4.3	5.3	6.3	7.3
POL HH	-28.7	-31.7	-22.1	-25.9	-29.2	-27.6	-27.1	-21.4
POL HV	-38.6	-40.8	-31.9	-31.1	-35.3	-34.0	-32.7	-26.7
POL VV	-26.3	-30.2	-21.5	-25.4	-28.3	-25.2	-28.2	-22.6

ANTENNA ANGLE 70

FREQ	1.2	1.7	2.3	3.3	4.3	5.3	6.3	7.3
POL HH	-32.0	-35.5	-26.3	-28.7	-24.7	-24.1	-20.3	-16.4
POL HV	-40.7	-41.3	-36.6	-34.7	-33.0	-30.0	-28.6	-23.8
POL VV	-28.8	-33.2	-28.5	-28.1	-24.6	-25.3	-22.1	-18.0

AVERAGED SIGMAC SET 28 FREEZE

ANTENNA ANGLE 0

FREQ	1.2	1.7	2.3	3.3	4.3	5.3	6.3	7.3
POL HH	5.8	3.1	9.6	8.3	2.7	1.5	-2.1	-0.4
POL HV	-11.8	-15.3	-14.2	-16.5	-19.0	-17.1	-14.5	-11.4
POL VV	6.8	4.4	9.6	8.3	3.1	2.1	-1.8	0.1

ANTENNA ANGLE 10

FREQ	1.2	1.7	2.3	3.3	4.3	5.3	6.3	7.3
POL HH	-4.9	-11.8	-10.8	-11.4	-11.0	-15.0	-9.5	-8.9
POL HV	-23.2	-29.8	-29.1	-27.8	-26.0	-25.3	-20.9	-17.8
POL VV	-6.7	-12.3	-11.3	-10.8	-11.5	-12.4	-10.2	-10.4

ANTENNA ANGLE 20

FREQ	1.2	1.7	2.3	3.3	4.3	5.3	6.3	7.3
POL HH	-21.9	-25.0	-15.7	-14.2	-17.0	-15.9	-16.8	-14.5
POL HV	-32.7	-36.3	-31.7	-28.3	-27.4	-25.0	-26.4	-22.6
POL VV	-18.7	-23.0	-16.0	-14.4	-16.7	-16.5	-18.5	-13.9

ANTENNA ANGLE 30

FREQ	1.2	1.7	2.3	3.3	4.3	5.3	6.3	7.3
POL HH	-24.0	-25.8	-19.1	-18.5	-19.6	-18.1	-16.8	-16.0
POL HV	-36.9	-38.6	-31.2	-31.0	-27.8	-27.1	-25.6	-22.0
POL VV	-22.4	-24.4	-19.7	-18.8	-19.1	-16.6	-15.8	-15.2

ANTENNA ANGLE 50

FREQ	1.2	1.7	2.3	3.3	4.3	5.3	6.3	7.3
POL HH	-29.0	-33.0	-20.6	-27.1	-24.8	-25.7	-26.4	-21.2
POL HV	-43.3	-45.0	-37.6	-34.3	-32.1	-32.8	-31.9	-26.6
POL VV	-28.7	-30.9	-21.2	-26.5	-22.2	-24.1	-25.2	-18.4

ANTENNA ANGLE 70

FREQ	1.2	1.7	2.3	3.3	4.3	5.3	6.3	7.3
POL HH	-31.5	-36.0	-26.2	-26.7	-24.3	-23.3	-23.1	-15.6
POL HV	-40.7	-43.6	-39.1	-36.9	-31.6	-31.1	-29.2	-21.9
POL VV	-30.6	-32.9	-26.7	-29.2	-19.9	-22.2	-21.6	-16.7

AVERAGED SIGMA0 SET 29 FREEZE

ANTENNA ANGLE 0

FREQ	1.2	1.7	2.3	3.3
POL HH	5.4	0.3	3.4	-1.1
POL HV	-12.5	-18.7	-18.5	-22.4
POL VV	6.5	1.7	3.2	-1.4

ANTENNA ANGLE 10

FREQ	1.2	1.7	2.3	3.3
POL HH	-5.4	-16.3	-10.3	-12.0
POL HV	-23.4	-30.7	-22.9	-21.3
POL VV	-7.6	-15.6	-8.3	-12.1

ANTENNA ANGLE 20

FREQ	1.2	1.7	2.3	3.3
POL HH	-19.0	-21.6	-9.2	-15.5
POL HV	-30.3	-33.4	-23.9	-24.2
POL VV	-17.1	-19.9	-6.4	-15.0

ANTENNA ANGLE 30

FREQ	1.2	1.7	2.3	3.3
POL HH	-22.1	-22.4	-17.7	-17.3
POL HV	-32.9	-32.8	-25.4	-26.7
POL VV	-20.0	-21.0	-15.8	-17.0

ANTENNA ANGLE 50

FREQ	1.2	1.7	2.3	3.3
POL HH	-27.3	-29.0	-19.6	-24.0
POL HV	-36.7	-38.3	-29.0	-28.0
POL VV	-26.1	-25.2	-15.9	-23.8

ANTENNA ANGLE 70

FREQ	1.2	1.7	2.3	3.3
POL HH	-29.0	-33.9	-25.8	-26.0
POL HV	-40.7	-43.3	-32.9	-32.8
POL VV	-33.4	-32.8	-24.1	-26.7